

BRL MR 2118

BRL

AD

AD 729775

MEMORANDUM REPORT NO. 2118

AIR SHOCK LOADING OF EXTERIOR WALLS OF SHELTER MODELS

by

George A. Coufter

August 1971

DDC
RECEIVED
SEP 20 1971
C

Approved for public release; distribution unlimited.

U.S. ARMY ABERDEEN RESEARCH AND DEVELOPMENT CENTER
BALLISTIC RESEARCH LABORATORIES
ABERDEEN PROVING GROUND, MARYLAND

Reproduced by
NATIONAL TECHNICAL
INFORMATION SERVICE
Springfield, Va. 22157

124

Unclassified
Security Classification

DOCUMENT CONTROL DATA - R & D

(Security classification of title, body of abstract and indexing annotation must be entered when the overall report is classified)

1. ORIGINATING ACTIVITY (Corporate author) U.S. Army Aberdeen Research and Development Center Ballistic Research Laboratories Aberdeen Proving Ground, Maryland 21005		2a. REPORT SECURITY CLASSIFICATION Unclassified	
2b. GROUP			
3. REPORT TITLE AIR SHOCK LOADING OF EXTERIOR WALLS OF SHELTER MODELS			
4. DESCRIPTIVE NOTES (Type of report and inclusive dates)			
5. AUTHOR(S) (First name, middle initial, last name) George A. Coulter			
6. REPORT DATE August 1971	7a. TOTAL NO. OF PAGES 139	7b. NO. OF REFS 7	
8a. CONTRACT OR GRANT NO.	8b. ORIGINATOR'S REPORT NUMBER(S) Memorandum Report No. 2118		
a. PROJECT NO.	8c. OTHER REPORT NO(S) (Any other numbers that may be assigned this report)		
c. OCD DAHC-20-70-W-0310			
d.			
10. DISTRIBUTION STATEMENT Approved for public release; distribution unlimited.			
11. SUPPLEMENTARY NOTES		12. SPONSORING MILITARY ACTIVITY Office of Civil Defense Office of Secretary of the Army Washington, D.C. 20310	
13. ABSTRACT Experimental results for input shock overpressure of 5 psi are shown for differential loading on the exterior walls of a shelter model with a single front entrance. Further results are shown for a basement shelter model, where it is assumed that the top floor structure is blown away and the blast wave enters the basement from above. Air velocities and dynamic pressures are given for the interior of the model. /			

Details of illustrations in
this document may be better
studied on microfiche

DD FORM 1473
NOV 68

REPLACES DD FORM 1473, 1 JAN 64, WHICH IS OBSOLETE FOR ARMY USE.

Unclassified
Security Classification

Destroy this report when it is no longer needed.
Do not return it to the originator.

Secondary distribution of this report by originating or
sponsoring activity is prohibited.

Additional copies of this report may be purchased from
the U.S. Department of Commerce, National Technical
Information Service, Springfield, Virginia 22151

ACCESSION NO.	
ADPT	WHITE SECTION <input checked="" type="checkbox"/>
DDC	DEF SECTION <input type="checkbox"/>
ORAMPORES	<input type="checkbox"/>
PUBLICATION	
BY	
DISTR. SECTION/AVAILABILITY CODES	
DIST.	AVAIL. 200/07 SPECIAL
A	

The findings in this report are not to be construed as
an official Department of the Army position, unless
so designated by other authorized documents.

*The use of trade names or manufacturers' names in this report
does not constitute indorsement of any commercial product.*

14. KEY WORDS	LINK A		LINK B		LINK C	
	ROLE	WT	ROLE	WT	ROLE	WT
Chamber Filling Blast Loading Transient Flows						

BALLISTIC RESEARCH LABORATORIES

MEMORANDUM REPORT NO. 2118

AUGUST 1971

AIR SHOCK LOADING OF EXTERIOR WALLS OF SHELTER MODELS

George A. Coulter

Terminal Ballistics Laboratory

Details of illustrations in
this document may be better
studied on microfiche

Approved for public release; distribution unlimited.

This work was supported by Office of Civil Defense, Work Order
Number DAHC-20-70-W-0310 (OCD Work Unit Number 1123C)

ABERDEEN PROVING GROUND, MARYLAND

SUMMARY

A. Introduction

The results are presented from a study to determine the differential pressure loading across the exterior walls of a shelter structure when it has been exposed to a blast wave. Experimental pressure-time records obtained from opposite sides of the walls and the algebraic subtraction of the two records are shown for an input shock over pressure of 5 psi.

Preliminary results are shown for a basement type shelter model in which it is assumed that the upper floors of the structure containing the shelter are blown away by the blast wave. High speed photography was used to record the motion of the shock wave as it entered through a top entrance into a two-dimensional model. A smoke grid tracer method was used to follow the shock created air flow within the model.

B. Experiments

Two- and three-dimensional models were exposed to step shock waves produced in the Ballistic Research Laboratories (BRL) shock tubes. As was noted above, photography was used to monitor the two-dimensional experiments. Pressure transducers placed in the walls of the three-dimensional loading model were used with a tape recorder system to acquire the pressure-time loading data.

C. Results and Conclusions

The Appendixes of the report contain pressure-time records, a computer program to predict the loading on the outside of the front wall with a single opening exposed to a step shock wave, photographs, and tables of flow calculations.

Comparison is made of the experimental loading results with the prediction methods given by the Army design manual, TMS-856-1.

The following conclusions are believed to be valid over the test pressure range of 5 to 10 psi.

1. The clearing time which is the time required to reduce the front wall to stagnation pressure, is apparently proportional to the

smaller of the half-width or the height, and not proportional to a weighted sum of the wall opening-edge dimension as indicated in the design manual. This is probably true because reflections from the entrance walls do not allow the faster predicted clearing time to occur.

2. Internal side wall reflections cause a higher internal front wall loading than is predicted by the manual. Also, some type of oscillating loading function should probably be used in any prediction method devised.

3. The area influenced by the edge vortices may be limited to that within a few inches of the edge. For full size structure walls, this region might be neglected if the major vortex effects still occur in the first few inches from the edge.

4. The basement shelter results are quite preliminary, but they appear to show a strong flow towards the floor from the overhead entrance, and not at a shallow angle into the model, as it previously was thought to occur.

BALLISTIC RESEARCH LABORATORIES

MEMORANDUM REPORT NO. 2118

GACoulter/mew
Aberdeen Proving Ground, Md.
August 1971

AIR SHOCK LOADING OF EXTERIOR WALLS OF SHELTER MODELS

ABSTRACT

Experimental results for input shock overpressure of 5 psi are shown for differential loading on the exterior walls of a shelter model with a single front entrance. Further results are shown for a basement shelter model, where it is assumed that the top floor structure is blown away and the blast wave enters the basement from above. Air velocities and dynamic pressures are given for the interior of the model.

Preceding page blank

TABLE OF CONTENTS

	Page
ABSTRACT.	3
LIST OF ILLUSTRATIONS	7
LIST OF TABLES.	9
LIST OF SYMBOLS	11
I. INTRODUCTION.	13
II. EXPERIMENTS	14
A. Three-Dimensional Experiment.	14
B. Two-Dimensional Smoke Grid Experiment	18
III. RESULTS	18
A. Differential Loading.	18
B. Flows in the Basement Model	32
IV. COMPARISONS OF RESULTS WITH THEORY.	34
A. Front Wall.	34
B. Side Wall	44
C. Back Wall	47
V. SUMMARY AND CONCLUSIONS	50
REFERENCES.	52
APPENDIXES.	53
A - PRESSURE-TIME RECORDS.	53
B - COMPUTER PROGRAM	81
C - HIGH SPEED PHOTOGRAPHS - MODEL 39.	89
D - AIR FLOW TABLES AND VECTOR PLOTS	101
E - APPLICATION TO A FULL-SIZE ROOM	127
DISTRIBUTION LIST	135

Preceding page blank

LIST OF ILLUSTRATIONS

Figure	Page
1. Model 37 - Differential Loading Experiment	16
2. Model 38 - Two-Dimensional Loading Experiment.	17
3. Model 39 - Air Flow Experiment	19
4. Pressure-Time Records - Front Wall of Model 37	20
5. Pressure-Time Records - Side Wall of Model 37.	21
6. Pressure-Time Records - Back Wall of Model 37.	22
7. Pressure-Time Records - Model 38	23
8. A Shock Wave Entering the Front of a Model	29
9. A Shock Wave Entering Model of Basement Shelter.	33
10. Notation and Equations for Computer Program - Loading of Outside Front Wall.	36
11. Sketch of Model 38(A), No Openings	37
12. Loading for Front Wall of Model 38(A).	38
13. Loading for Outside of Front Wall - Model 37	39
14. Average Transmitted Peak Pressure on Inside of Front Wall	43
15. Comparison of Pressure-Time Records with the Predicted Average Loading Curves on the Front Wall	45
16. Comparison of Records with the Average Predicted Loading on the Side Wall	46
17. Comparison of Records with the Average Predicted Loading on the Back Wall	48
A-1. Records from Front Wall - Model 37	55
A-2. Records from Side Wall - Model 37.	59
A-3. Records from Rear Wall - Model 37.	68

Preceding page blank

LIST OF ILLUSTRATIONS (Continued)

Figure		Page
A-4.	Records from Model 38.	74
A-5.	Upstream Input Records	78
C-1.	Shadowgraphs of a Shock Wave Entering Model of Basement Shelter - $P_s = 5$ psi.	91
C-2.	Shadowgraph of a Shock Wave Entering Model of Basement Shelter - $P_s = 10$ psi	94
C-3.	Smoke Grid Flow Patterns	97
D-1.	Flow Vectors from Model 39 - Shot 359.	125
D-2.	Flow Vectors from Model 39 - Shot 363.	126
E-1.	Full-Size Room	132
E-2.	Records from Model 37.	133
E-3.	Records for Model 37 Scaled to a Full Size Room.	134

LIST OF TABLES

Table		Page
I.	Model Data	15
II.	Summary of Results	24
III.	Example of Machine Program Output.	40
D-I.	Flow Calculations - Shot 359	105
D-II.	Flow Calculations - Shot 363	113

LIST OF SYMBOLS

A	Area of entrance to model, in. ²
A _F	Area of outside front wall of model, in. ²
A _{IN}	Area of inside front wall of model, in. ²
A ₁	Ambient sound speed, ft/sec
L	Length of model, in.
P _{max}	Largest positive or negative pressure, psi
P _{ref}	Reflected overpressure, psi
P _S	Side-on overpressure of external input shockwave, psi
P _{stag}	Stagnation overpressure, psi
Q	Dynamic pressure, $1/2 \rho u^2$, lb/ft ²
V	Internal volume of model, in. ³
W	Width of basement entrance, in.
X	Distance along model, measured from the inside front wall
ρ	Density of air, slug/ft ³
\bar{u}	Average velocity of air flow, ft/sec
θ	Angle of air flow measured from horizontal, deg
γ	Distance perpendicular to axis of model, measured from inside bottom of model, in.

1. INTRODUCTION

The purpose of this study is to determine the differential loading across the exterior walls of a shelter structure when it is exposed to a blast wave. A secondary goal of the study is to determine the internal air flow inside of a basement type shelter if the upper floors have been destroyed by the blast wave. In this case, the blast wave is free to enter through the overhead interior stairwell. The problems of structure removal and the debris are not considered. The internal flow study will continue into the next work period and initial results are reported here. The work is sponsored by the Office of Civil Defense (OCD) under a contract (Work Order Number DAHC-20-70-W-0310 with the Ballistic Research Laboratories (PRL).

The differential loading part of the study was done with a three-dimensional model exposed to top shock waves produced in the 5.5 ft BRL shock tube. Pressure transducers were used to measure the pressure as a function of time at locations on each of the shelter walls. The differential load was recorded by electronically combining the outputs from each pair of transducers inside and outside.

The study of internal flow was begun with a two-dimensional model exposed to air shock waves in the photographic section of the 4 x 15 in. shock tube. The shock induced air flow within the model was photographically monitored with smoke grid tracers.

Data from each experiment are placed in the Appendixes. Appendix A shows the several pressure-time histories recorded during the diffraction loading experiments. Appendix B lists a computer program for calculating the air shock loading parameters on the outside of a front wall of a shelter structure with an opening. Appendix C shows the photographs from the flow experiment with the two-dimensional basement model. Appendix D contains the air flow tables and vector plots calculated from motion of the smoke grids.

11. EXPERIMENTS

In order for existing structures which are used for shelters (References 1, 2, and 3)* to be evaluated for strength correctly, the differential loading caused by blast waves needs to be better defined. Accordingly, experiments are being carried out at the BRL Shock Tube Facility to acquire this type of information. Part A below describes one such experiment at the 5.5 ft diameter shock tube.

If one assumes that the upper floors of a protective structure are removed by a blast wave, the problem then becomes one of flow into the basement through the interior overhead entrance. A two-dimensional experiment described in Part B below, was designed to visualize the internal air flow associated with this type of filling process.

Table I summarizes the pertinent model data.

A. Three-Dimensional Experiment

This experiment consisted of instrumenting the interior and exterior walls of a model of a single room structure with one entrance. The model was then exposed face-on to step shock waves of a nominal 5.5 psi overpressure inside the 5.5 ft shock tube. Figure 1 shows a sketch of this model (Model 37) with the transducer locations.

The pressure transducers used were a ceramic piezoelectric type (Susquehanna Instruments ST2) coupled to a source follower (Piezotronics PCB 402A), and the voltage output (pressure-time history) was recorded by a tape recorder (Bell and Howell VR 3300). The FM recorder had a frequency response of near DC to 20 KHz.

The same instrumentation was used to determine the loading for the two-dimensional wall - Model 38. A sketch of this model with transducer locations is shown as Figure 2. This model was two-dimensional early in time only, until reflections or rarefactions returned from other edges.

*References are listed on page 52.

Table I. Model Data

Model	Size	Type of Filling	Input Pressure, psi	A/AF, %	V/A, ft	Remarks
<u>Models for 5.5 ft Shock Tube</u>						
37	10x15x25 in.	Front	5.5	17	6	6 1/2x8 in. entrance
38	2 3/4x13 1/2 in.	Front	5.6	-	-	two-dimensional wall
38-A	4.18x8.375x3 in.	-	5.0	No Opening		
<u>Model for 4 x 15-in. Shock Tube</u>						
39	2 1/2 x 4 in.	Top	5, 10	-	0.83	two-dimensional 1 x 4 in. entrance at top

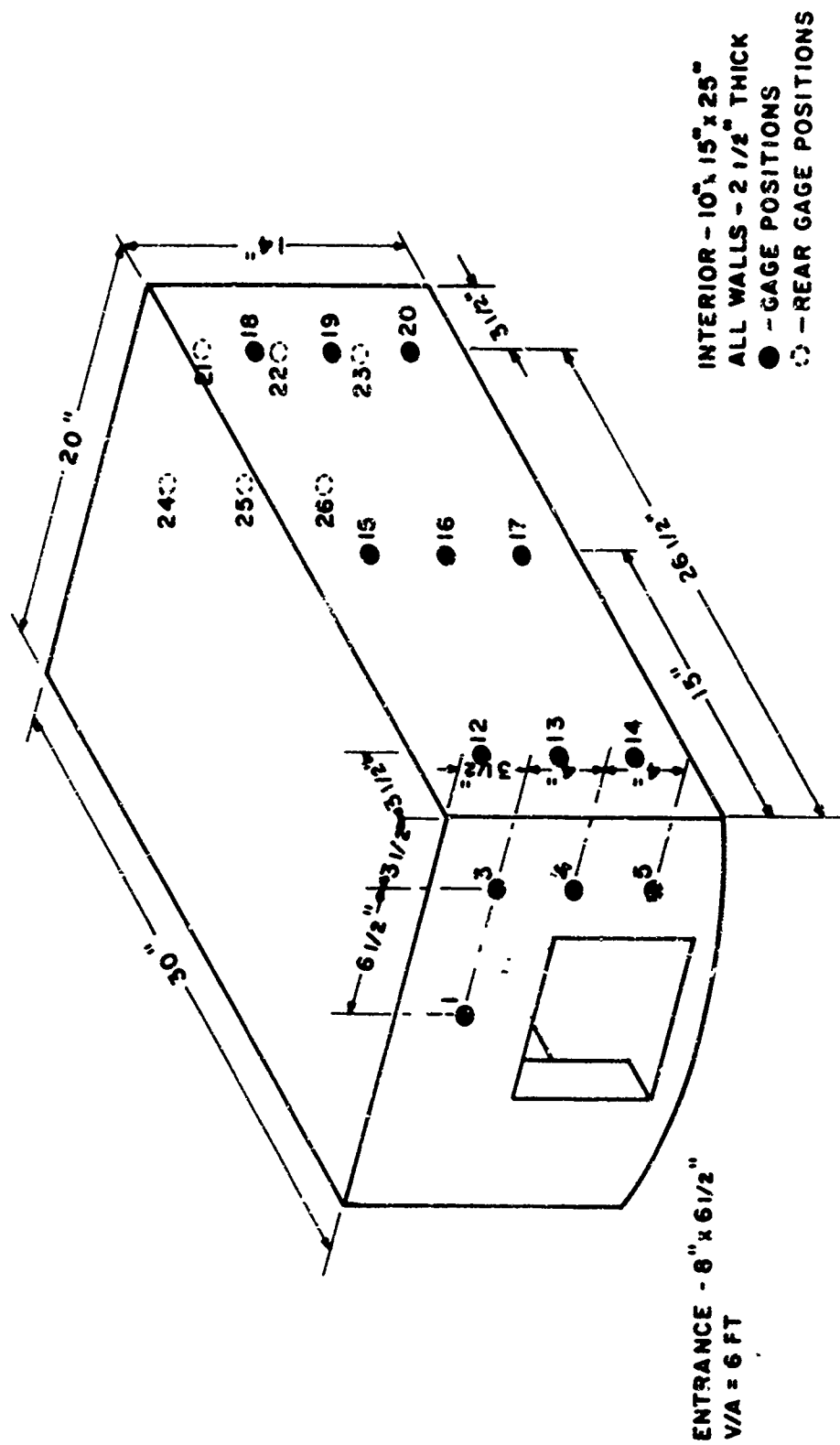


Figure 1. Model 37 - Differential Loading Experiment

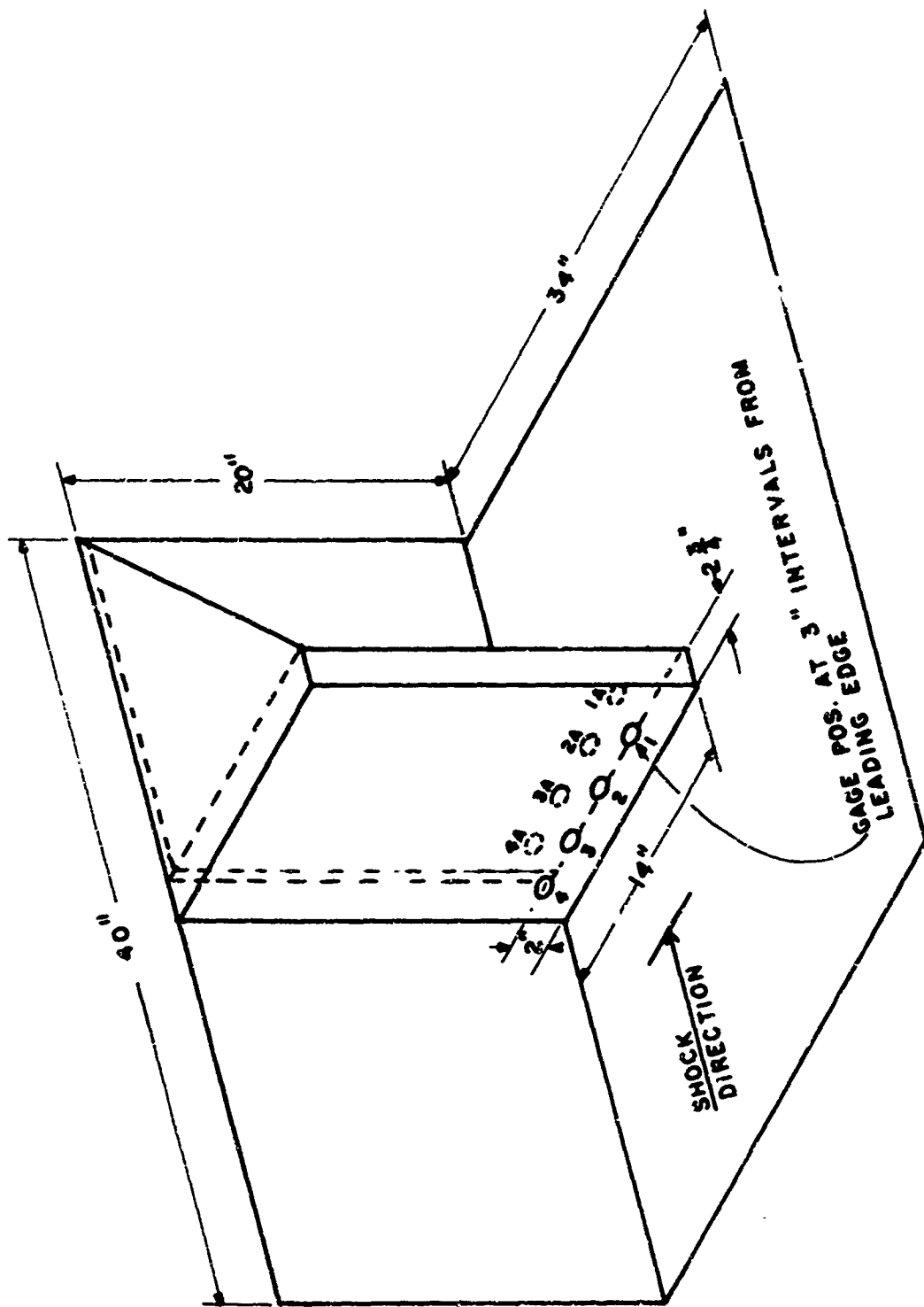


Figure 2. Model 38 - Two-Dimensional Loading Experiment

In both experiments, the differential records were obtained by differential operational amplifiers which electronically combined the output of each set of exterior-interior (or upstream-downstream) transducers.

B. Two-Dimensional Smoke Grid Experiment

The smoke-grid model (Model 39) was designed to simulate a basement type shelter when the above ground floors are assumed destroyed by the blast wave. Figure 3 shows a sketch of the model mounted in the 4 x 15 in. shock tube photographic test section. A high speed framing camera was used to record the motion of the smoke grids as the air was disturbed inside the model.

III. RESULTS

The results are presented in two sections; (A), the results of the differential loading experiments, and (B), those from the basement model.

A. Differential Loading

The complete set of pressure-time records from the loading experiments are placed in Appendix A. The records for Model 37 are shown first in the order of front wall, side wall, and back wall. After these are shown records obtained with Model 38; and last are the records for the input shock waves. These records display oscillations caused by reflections from the model.

Three representative sets of pressure-time histories of the wall loading of Model 37 are shown in Figures 4 - 6. Figure 7 shows the first set of traces recorded at the gage location nearest to the edge of Model 38. Table II summarizes the data obtained with both models. All arrival times referred to in this report indicate the time of arrival at the front of the models and are not shown on these traces, but are listed in Table II.

Figure 4(A) shows the pressure-time history for Position 3 on the outside of the front wall of Model 37. There are three main regions of interest that can be observed. Initially, the incoming shock wave was

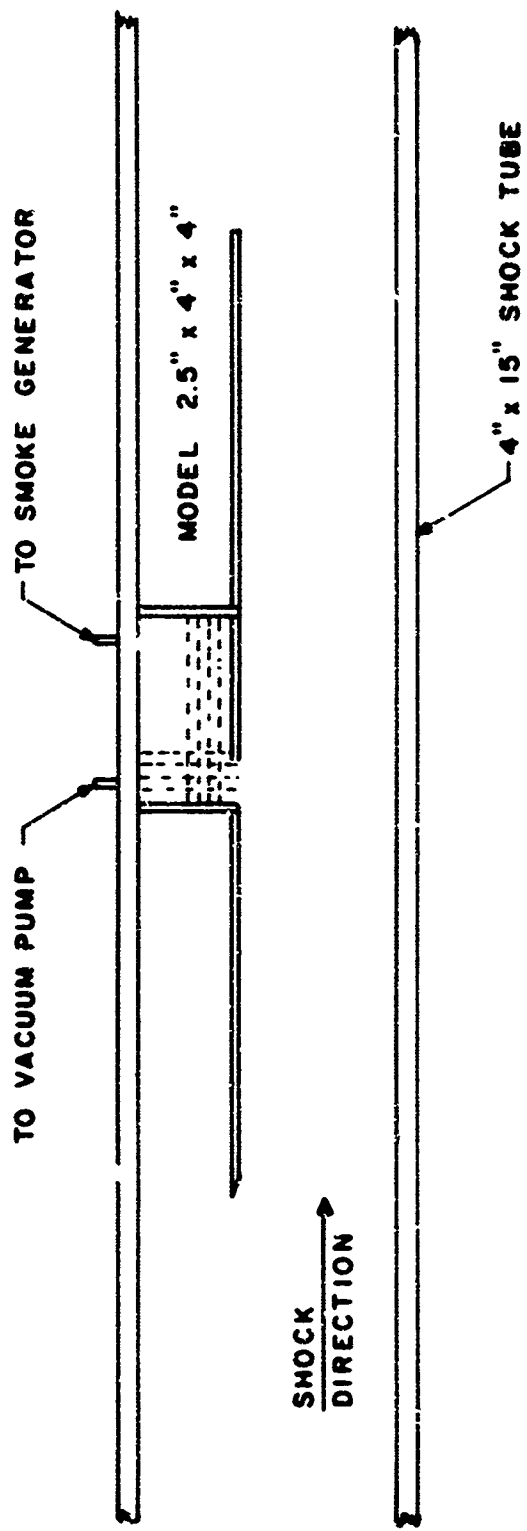


Figure 3. Model 39 - Air Flow Experiments

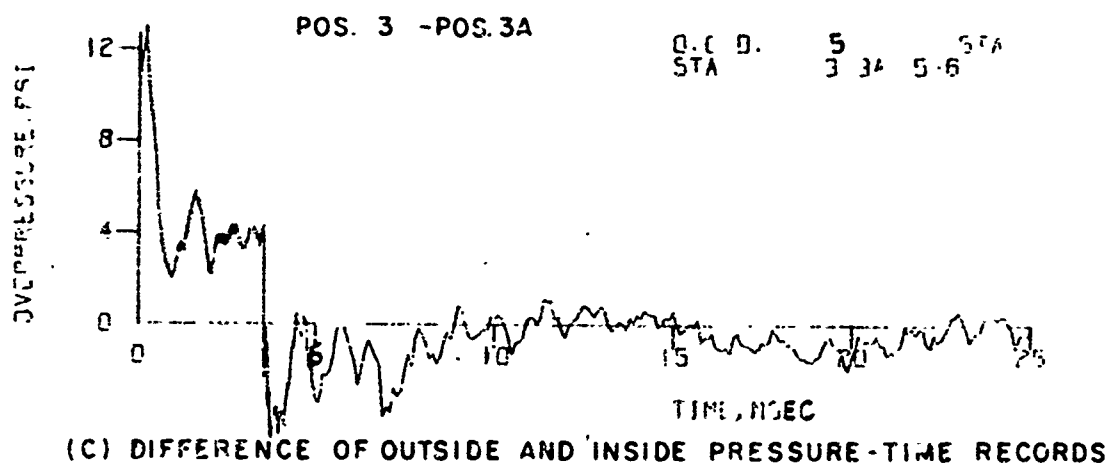
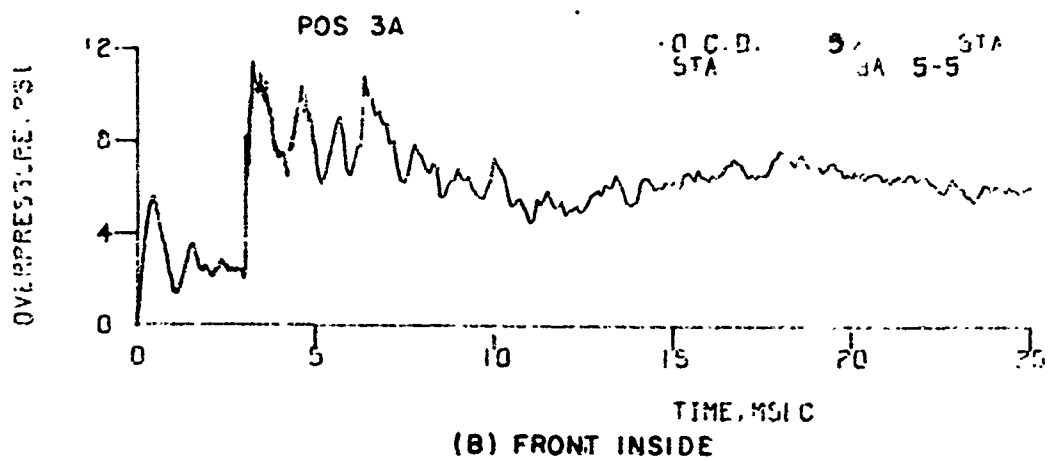
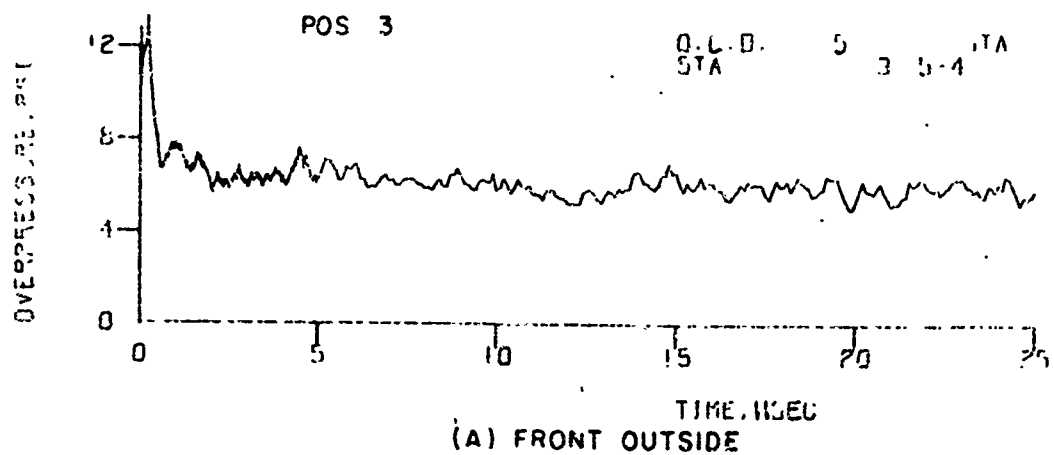


Figure 4. Pressure-Time Records - Front Wall of Model 37

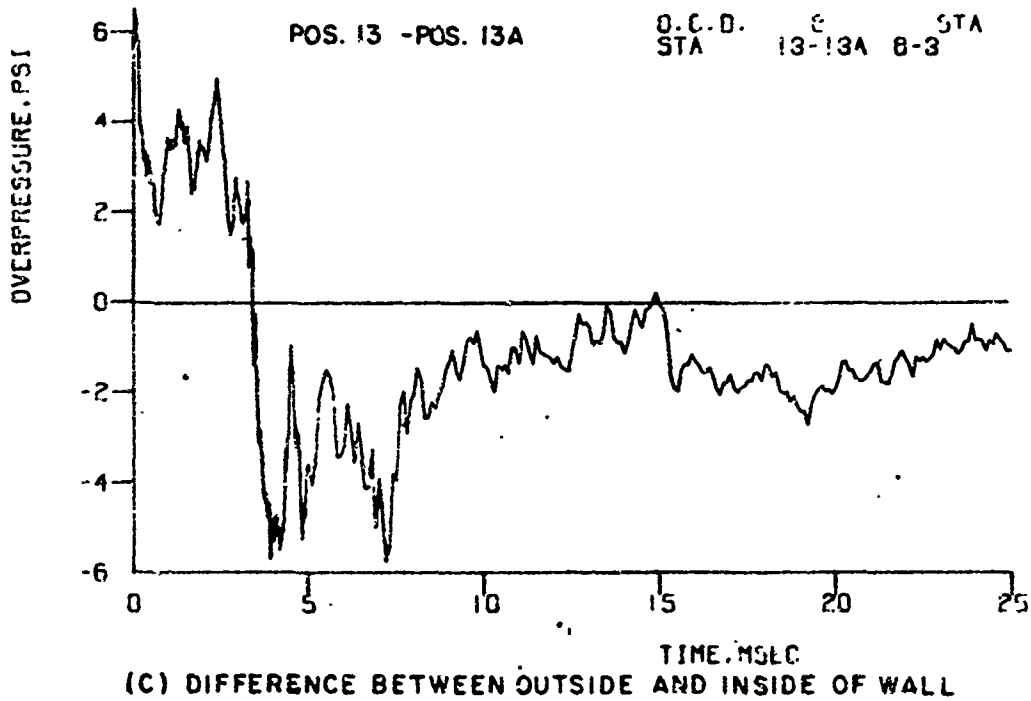
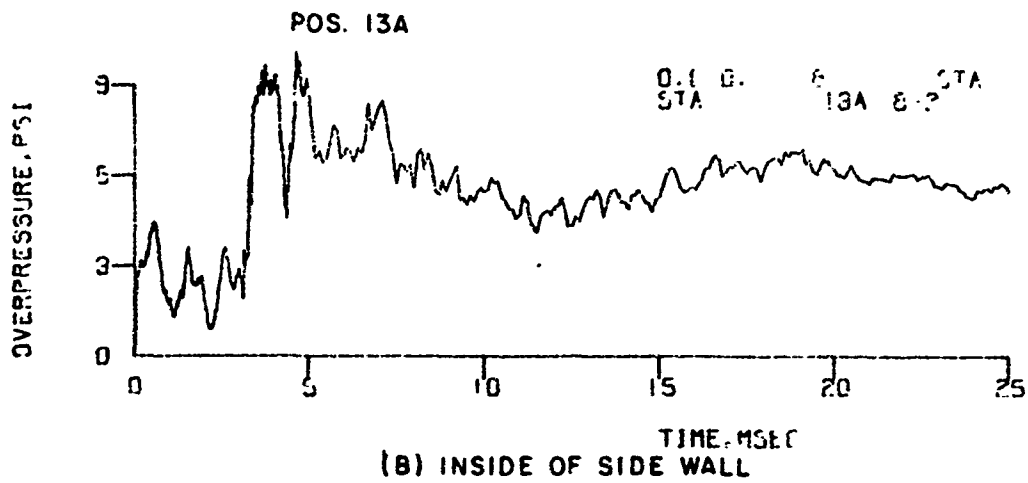
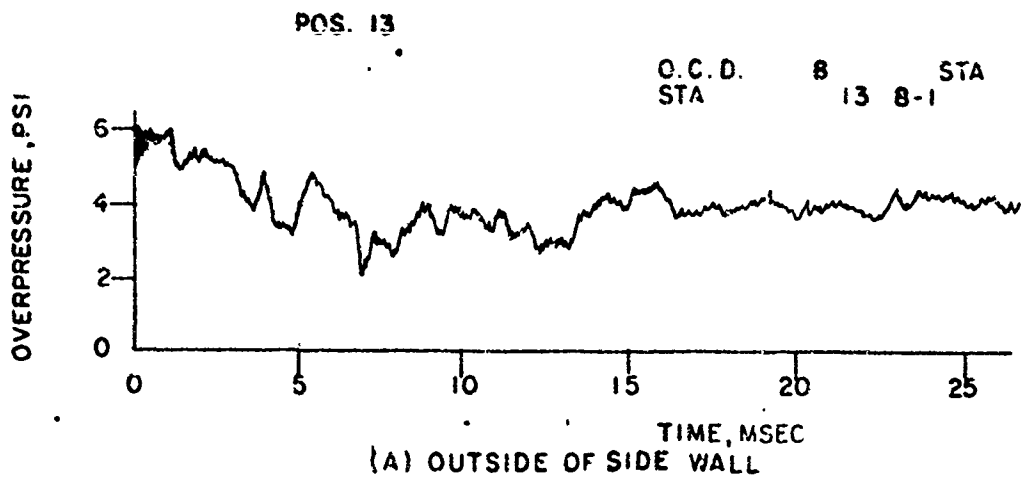
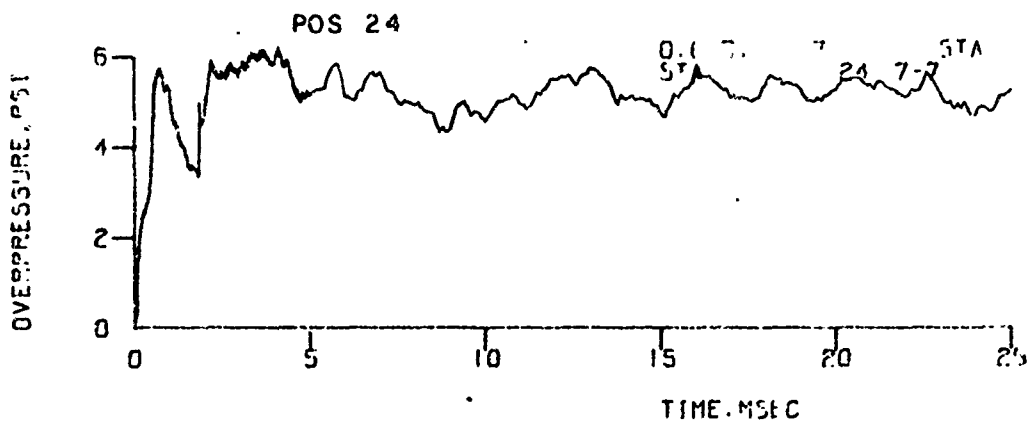
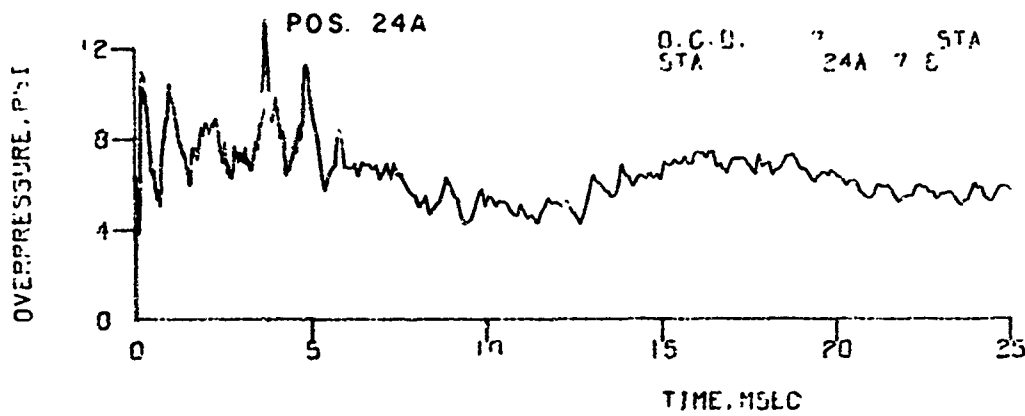


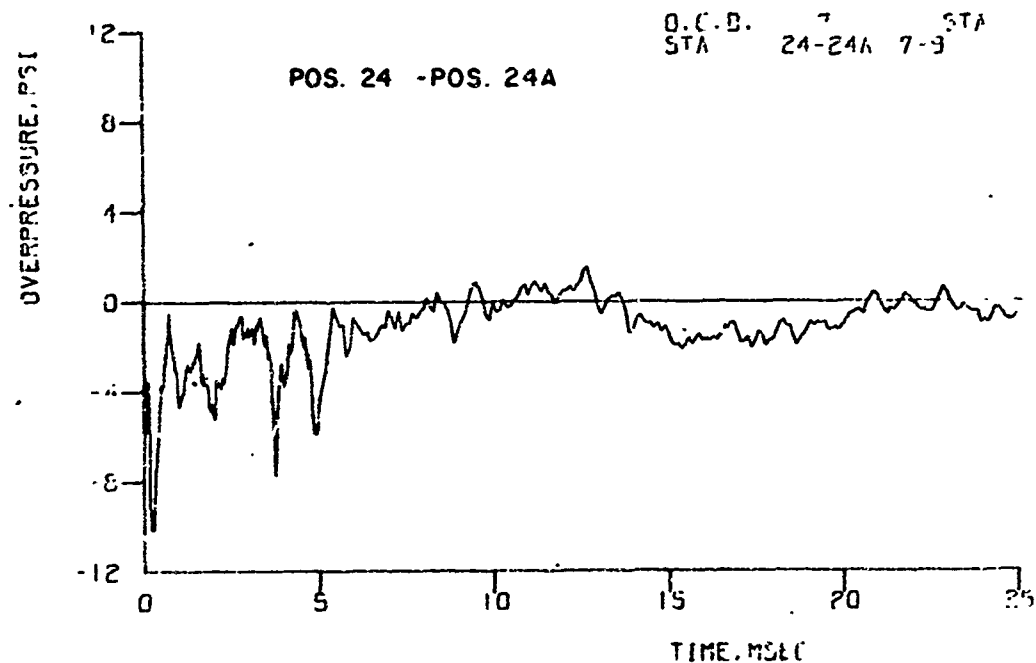
Figure 5. Pressure-Time Records - Side Wall of Model 37



(A) OUTSIDE OF BACK WALL

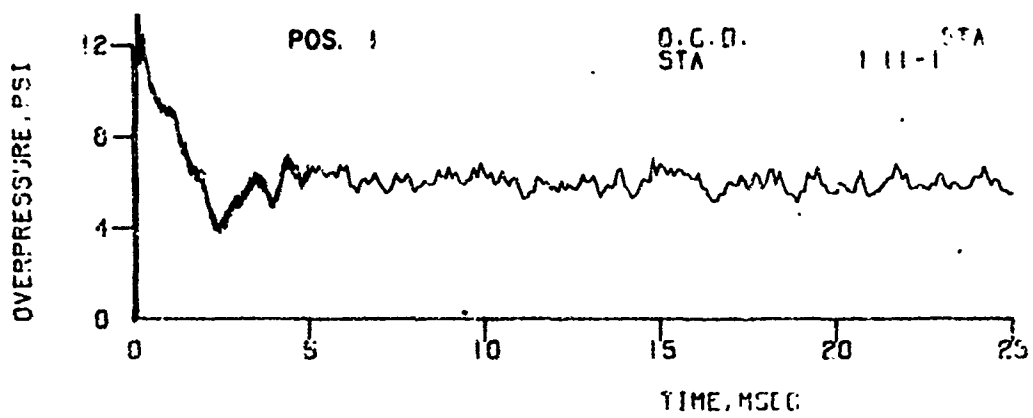


(B) INSIDE OF BACK WALL

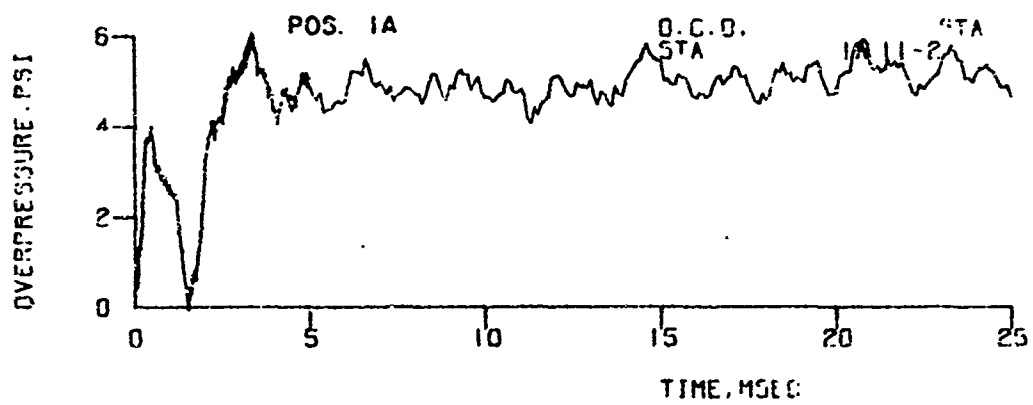


(C) DIFFERENCE BETWEEN OUTSIDE AND INSIDE OF WALL

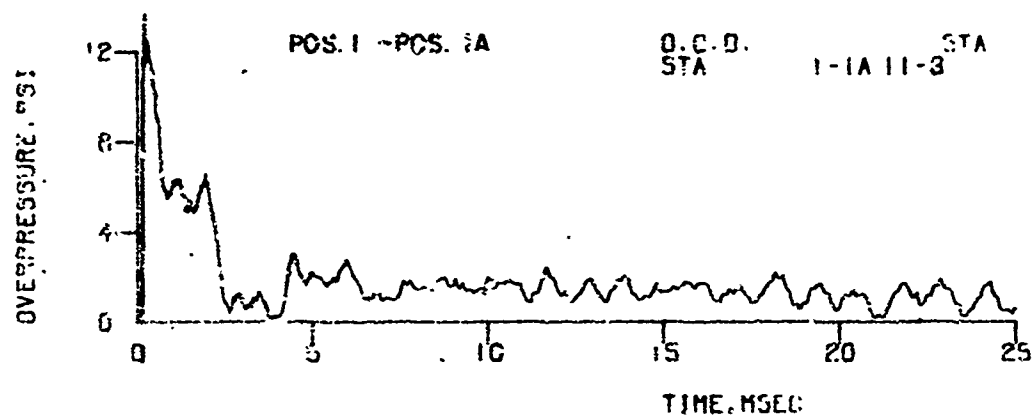
Figure 6. Pressure-Time Records - Back Wall of Model 37



(A) FRONT SIDE OF WALL



(B) BACK SIDE OF WALL



(C) DIFFERENCE BETWEEN FRONT AND BACK SIDES OF WALL

Figure 7. Pressure-Time Records - Model 38

Table II. Summary of Results

A. Differential Loading Experiment

Shot	P_s , psi	Wall	Position	First Peak, psi	P_{max} , psi	Arriv- al Time, μ sec	Model	Remarks
5-70-5	5.5	Front	1	12.1	12.1	0	37	3-D Model
			1A	-	10.1	326		
			1-1A	12.0	12.0	-		
5-70-5	5.5	Front	3	11.9	11.9	0		Shot 5-70-5 $P_1 = 14.7$ psi $T_1 = 39.4^\circ\text{C}$ $A_1 = 1163$ ft/sec
			3A	-	10.8	436		
			3-3A	11.8	11.8	-		
5-70-5	5.5	Front	4	12.0	12.0	0		Position 2 Lost
			4A	1.5	9.7	320		
			4-4A	12.2	12.2	-		
5-70-5	5.5	Front	5	11.7	11.7	0		
			5A	1.7	10.6	343		
			5-5A	11.6	11.6	0		
5-70-10	5.3	Side	12	5.4	5.7	239	37	Shot 5-70-10 $P_1 = 14.9$ psi $T_1 = 27.5^\circ\text{C}$ $A_1 = 1141$ ft/sec
			12A	5.7	9.8	401		
			12-12A	5.6	-6.2	229		
5-70-8	5.5	Side	13	5.6	-	255		Shot 5-70-8 $P_1 = 14.8$ psi $T_1 = 29.4^\circ\text{C}$ $A_1 = 1145$ ft/sec
			13A	2.3	8.9	440		
			13-13A	5.7	-6.1	255		
5-70-8	5.5	Side	14	5.2	6.3	245		
			14A	2.8	7.7	449		
			14-14A	5.1	6.1	243		
5-70-9	5.9	Side	15	3.8	6.2	977		Shot 5-70-9 $P_1 = 14.8$ psi $T_1 = 33.9^\circ\text{C}$ $A_1 = 1153$ ft/sec
			15A	3.4	10.1	1090		
			15-15A	3.8	-4.8	989		

Table II. Summary of Results (Continued)

A. Differential Loading Experiment

Shot	P_s , psi	Wall	Position	First Peak, psi	P_{max} , psi	Arriv- al Time, μ sec	Model	Remarks
5-70-8	5.5	Side	16	4.7	6.5	1000		
			16A	3.4	9.6	1052		
			16-16A	4.5	-5.3	977		
5-70-9	5.9	Side	17	4.8	6.3	968		
			17A	4.7	9.2	1043		
			17-17A	4.8	-5.1	968		
5-70-9	5.9	Side	18	4.5	7.5	1710		
			18A	4.6	12.5	1833		
			18-18A	4.1	-6.4	1703		
5-70-8	5.5	Side	19	4.8	6.3	1713		
			19A	3.1	10.7	1829		
			19-19A	4.3	-5.7	1713		
5-70-9	5.3	Side	20	5.1	6.2	1703	37	Shot 5-70-9
			20A	2.4	10.3	1776		$P_1 = 14.8$ psi
			20-20A	5.1	-5.3	1695		$T_1 = 33.9^\circ\text{C}$ $A_1 = 1153$ ft/sec
5-70-7	5.5	Rear	21	3.4	5.7	2184	37	Shot 5-70-7
			21A	10.0	13.7	1915		$P_1 = 14.9$ psi
			20-20A	-9.8	-10.5	1912		$T_1 = 31.4^\circ\text{C}$ $A_1 = 1149$ ft/sec
5-70-10	5.3	Rear	22	1.1	6.6	2166		Shot 5-70-10
			22A	6.5	10.8	1861		$P_1 = 14.9$ psi
			22-22A	-6.6	-8.1	1861		$T_1 = 27.5^\circ\text{C}$ $A_1 = 1141$ ft/sec
5-70-7	5.5	Rear	23	1.4	5.9	2184		
			23A	7.0	10.6	1847		
			23-23A	-7.0	-8.8	1843		

Table II. Summary of Results (Continued)

A. Differential Loading Experiment

Shot	\bar{P}_s , psi	Wall	Position	First Peak, psi	P_{max} , psi	Arriv- al Time, μsec	Model	Remarks
5-70-7	5.5	Rear	24	1.5	6.2	2159		
			24A	5.3	13.8	1868		
			24-24A	-5.0	-10.0	1876		
5-70-10	5.3	Rear	25	1.1	7.4	2452		
			25A	3.3	10.7	1813		
			25-25A	-3.4	-9.0	1823		
5-70-7	5.5	Rear	26	3.1	6.9	2618		
			26A	3.8	15.6	1801		
			26-26A	-3.6	-8.4	1788		
5-70-11	5.6	Front	1	12.3	12.3	0	38	2-D Model $P_1 = 14.75$ psi $T_1 = 36.2^\circ\text{C}$ $A_1 = 1160$ ft/sec
			1A	1.4	6.0	401		
			1-1A	-	-	-		
			2	12.6	12.6	0		
			2A	1.2	6.9	656		
			2-2A	-	-	-		
			3	12.7	12.7	0		
			3A	1.1	6.8	822		
			3-3A	-	-	-		
			4	12.8	12.8	0		
			4A	0.6	7.5	1036		
4-4A	-	-	-					

Table II. Summary of Results (Continued)

B. Flow Experiment

Shot	P_s , psi	Grid Position	Time, usec	Velocity ft/sec	Q lb/ft ²	Model	A/A _{IN}	Remarks
359	4.9	Front	165	11-456	0-261	39	.25	→ Shock  Model 39 1 in. entrance All Shots $P_1 = 14.8$ psi $T_1 = 20.7^\circ\text{C}$
			206-288	5-311	0-194			
			330-371	7-239	0-106			
			412-453	11-372	0-159			
			494-535	8-278	0-106			
363	4.9	Middle	124	2-144	0-23	39	.25	$T_1 = 21.2^\circ\text{C}$
			166-208	2-251	0-72			
			249-332	42-730	1-752			
			374-457	19-230	1-64			
			498-623	9-267	0-47			
365	4.9	No Smoke Grid				39	.25	$T_1 = 21.7^\circ\text{C}$
366	10.1	No Smoke Grid				39	.25	$T_1 = 21.7^\circ\text{C}$
368	10.0	No Smoke Grid				39	.25	$T_1 = 21.0$

reflected by the model front surface to a value determined by the input shock wave strengths. A series of rarification waves from the edges of the entrance and front wall reduce the pressure to some average stagnation pressure value. Other positions on the outside wall experienced similar loads with some pressure-time variations depending on the nearness of the relieving edges.

Figure 4(B) shows the position on the inside of the front wall corresponding to Figure 4(A). A more complicated pressure-time history exists on the inside than on the outside. The shadowgraphs shown in Figure 8 (taken from Reference 4) illustrate the complicated multiple reflections of the incoming shock wave. The first group of reflections (0 - 3 msec) come from the near side walls, and later from the rear wall (3 - 10 msec). A third, larger period of oscillations compared to first two groups correspond to a fill-time frequency.

Figure 4(C) is obtained by the electronic subtraction of the second from the first trace. The result is the differential loading for a position. The front loading is first inward (positive) until the reflected shock wave returns from the back wall and the loading becomes outward (negative). This outward force remains until an equal pressure is established on both sides of the front wall.

Figure 5 shows a similar set of traces representative of the side wall data taken at Positions 13, 13A, and the difference of the traces. The outside wall pressure is about equal to the pressure of the input shock wave (5.5 psi) at early times. Subsequently there is some decay to a lower pressure (3.0 psi) and an increase back to an average value of about 4 psi.

The pressure record of Position 13A on the inside of the side wall resembles the record from the inside of the front wall, second trace, Figure 4. As in Figure 4, there is an initial group of side-wall reflections, followed by a second group with larger amplitudes. There seems to be a lack of any sudden low pressures dip indicating the presence of a strong vortex created by the nearest edge, 3 1/2 in. away. The

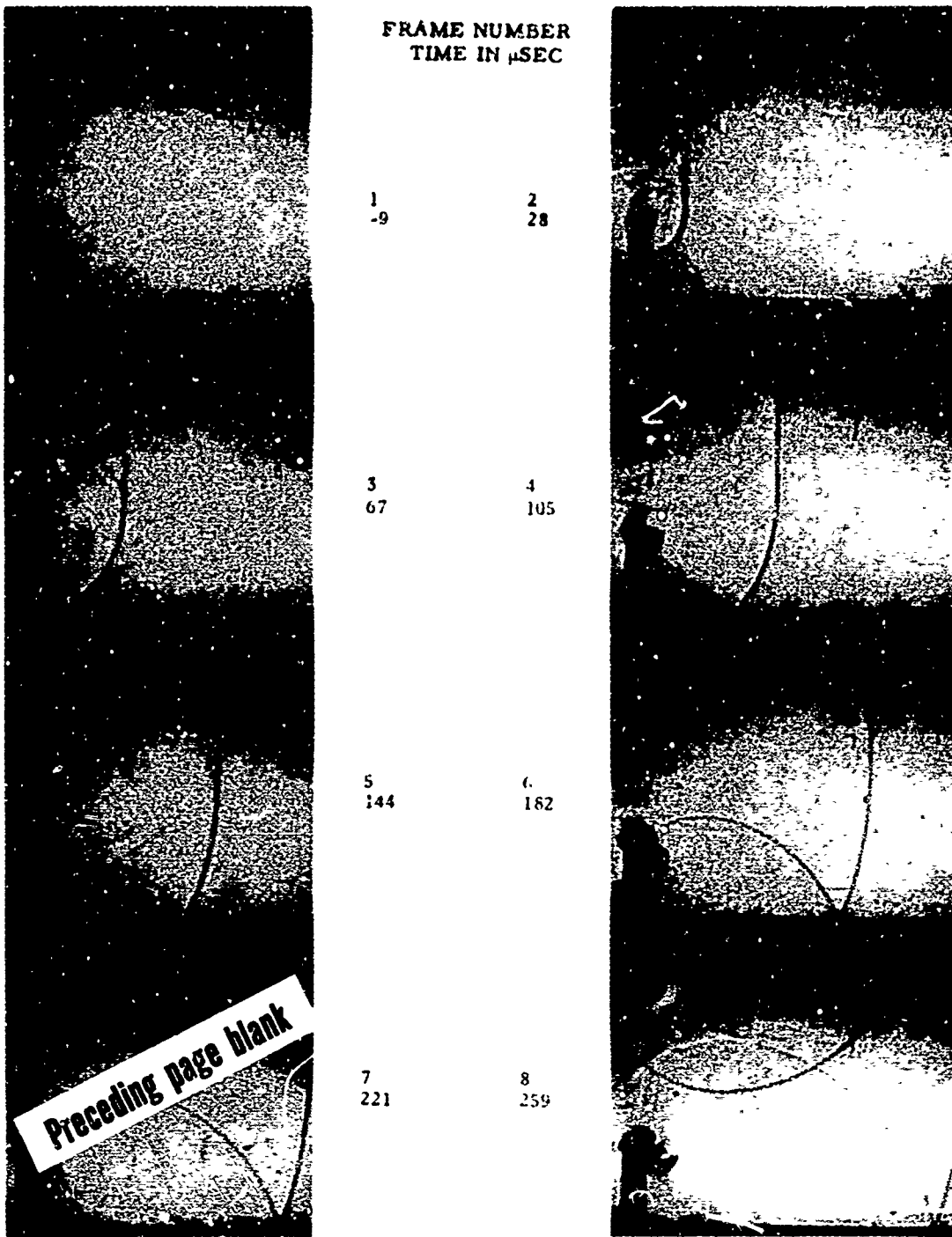


Figure 8. A Shock Wave Entering the Front of a Model

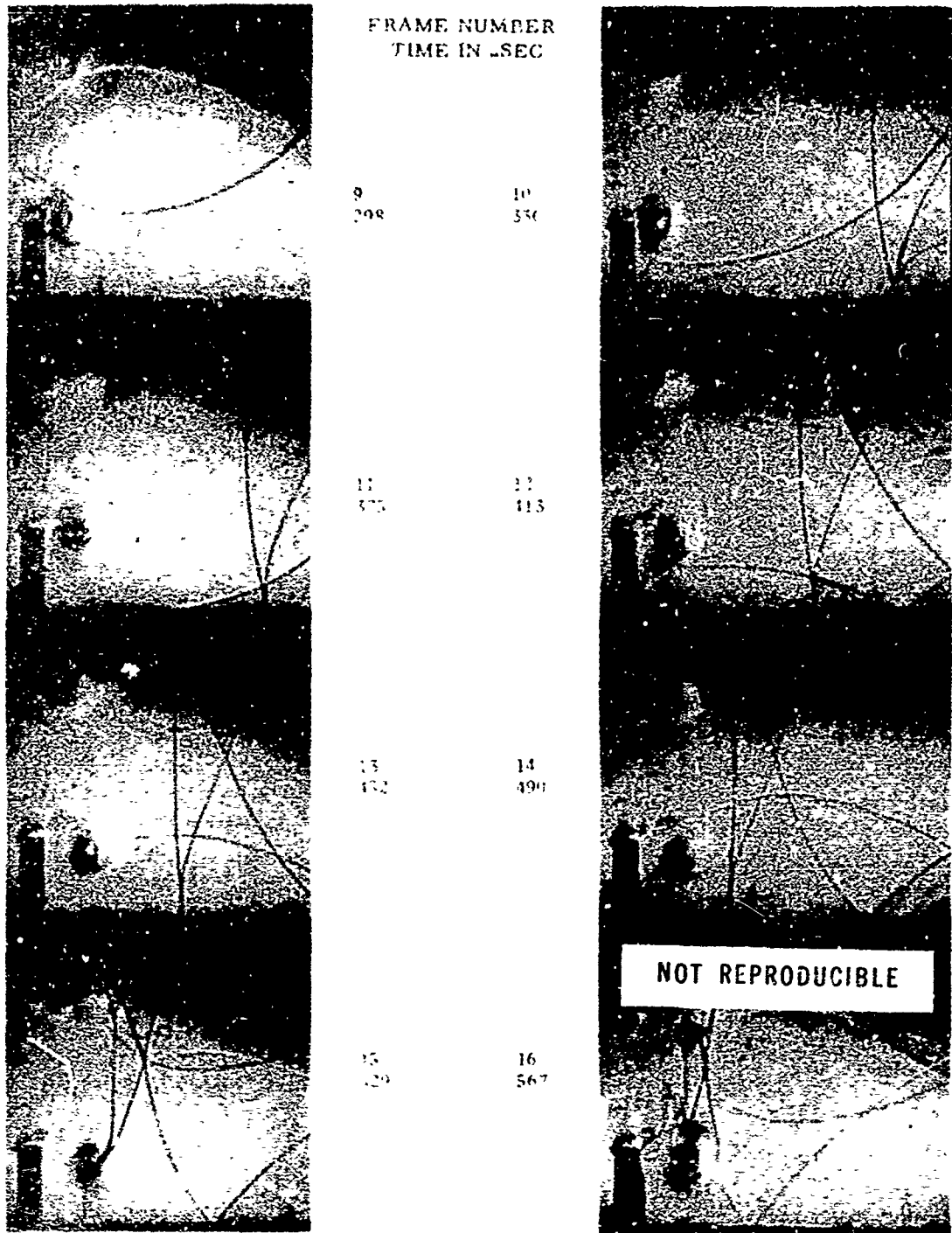


Figure 8. A Shock Wave Entering the Front of a Model (Continued)

first portion of the bottom trace, Figure 4(C), shows a positive, inward pressure which results in a positive differential pressure where the second group of reflections arrive from the inside back wall. The difference becomes negative, or outward. Appendix A shows the records from the remaining side wall positions.

Figure 6 shows a set of traces taken from the back wall of the model at Positions 24, 24A, and the difference between them. The upper trace, from the outside wall, shows an increasing rise to a pressure equal or above that of the input pressure* of $P_s = 5.5$ psi. A noticeable pressure dip follows which was possibly caused by a vortex propagated from the rear edge of the model top.

The corresponding inside Position 24A, shows pressure oscillations similar to those seen at Positions 3A and 13A. Because of these large oscillations in the pressure, the difference trace between 24A and 24 gives an almost all negative, or outward result. Again, the remaining records for the rear surface are to be found in Appendix A.

The results of the second differential loading experiment are given in Table II for Model 38, shown in Figure 2. The model positions are numbered from the outside free wall edge, toward the bottom plate. Upstream facing positions are numbered Positions 1 - 4, and positions behind the wall are labeled Positions 1A - 4A. Referring back to Figure 7, records from Positions 1, 1A, and the difference between them are shown.

The upper record, taken at the front of the wall shows a pressure decay from the initial reflection of the input wave to some value near stagnation pressure. Three portions of this decaying part of the record corresponded to arrival of rarefaction waves from the different relieving edges of the model wall. Only the first rarefaction is really two-dimensional. Mounting plate edges cause additional relief after this initial two-dimensional relief phase. An undershoot in pressure in

*This *stepwise* pressure growth is to be reported in more detail in a BRL Memorandum Report to be published.

the decay phase occurs which lowers the pressure below stagnation pressure; then pressure builds up again to about the value for stagnation pressure.

The second trace shows the pressure-time record from the rear of the wall, Position 1A. During the time of this trace, the shock wave has diffracted over the wall and down the back with a corresponding pressure decay. The sharp dip to zero pressure is caused by the vortex from the back edge of the wall. The pressure builds again to a value somewhat below the side-on value of input pressure.

The difference trace, shown at the bottom of Figure 7 shows a positive loading against the front of the wall during the recording time.

Records for the remaining positions on Model 38 may be found in Appendix A, Figure A-4. Examination of these traces does not show the vortex dip, as was observed at Position 1A. The last three positions in this group, Figure A-4, show a small negative difference for a short time. This net inward pressure on the outside of the rear wall is caused by reflections of the shock wave at the base of the rear wall.

B. Flows in the Basement Model

Preliminary results from a two-dimensional basement model are presented in this section. The shock wave was allowed to approach over the top of the model; it then moved into the model through the overhead entrance.

Photographs of the entrance-shock wave interaction display a relatively complicated process. Previous work (Reference 4) showed the shock wave as it entered through the front entrance of a geometrically similar model. A comparison of the two types of entrance effects are shown in Figures 8 and 9. The reflection processes of the shock wave appear similar in the two models. However, the flow into the model from the top entrance as indicated by the general direction the vortices are moving appears to be directed primarily downward in Figure 9. The

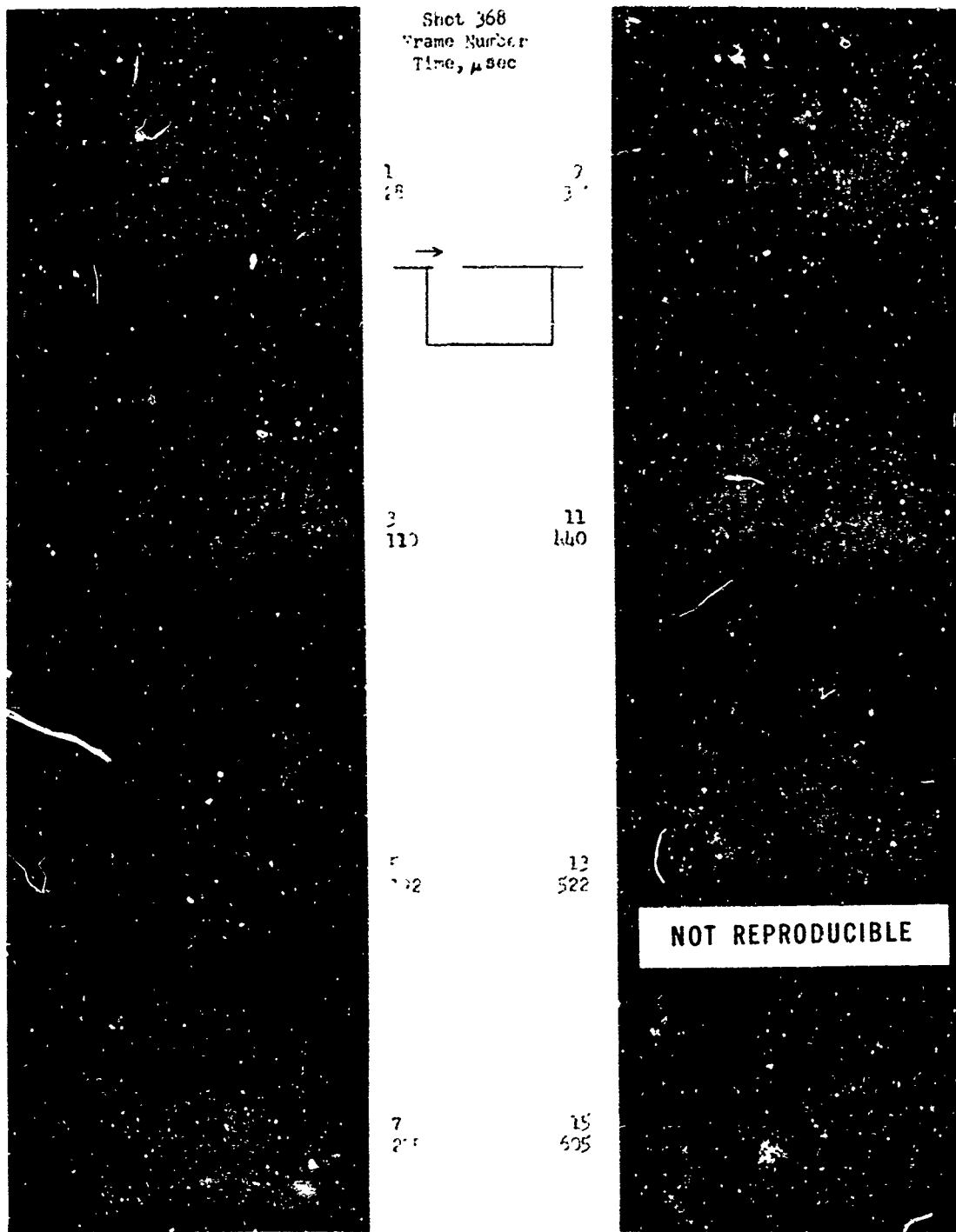


Figure 9. A Shock Wave Entering Model of Basement Shelter

direction of the vortices is not towards the far end of the model as expected. The vortices stay near the front of the model instead of crossing the model.

Table II presented before, summarizes the average air flow speeds at discrete times, measured from the time when the shock wave reaches the inside of the entrance. The range of speeds is quite wide and speeds of several hundred feet per second were calculated. This agrees with earlier work which was discussed in Reference 5. Similar flow speeds were found for a variety of entrance configurations at the same input pressure.

Appendixes C and D contain the photographs, air flow tables, and vector plots of data from Model 39.

IV. COMPARISONS OF RESULTS WITH THEORY

The purpose of this section is two-fold; first, to present an empirically derived computer program prediction for the pressure loading by a step shock wave on the front wall of a structure with or without an opening.* Second, the results of the present differential loading experiments will be compared with the structure loading prediction methods of Reference 6.

A. Front Wall

The pressure-time records from the outside of the front wall show three main divisions of pressure which will affect the wall loading. Initially, the input shock wave loads all position on the wall with reflected pressure at a given position. The reflected loading remains until a rarefaction wave arrives from the nearest edge. This second phase, or unloading process, continues as other rarefactions reach the position from the other edges and openings until the stagnation pressure

* A more general case allowing multiple openings and a general waveform for the input shock wave will be reported later as a BRL Memorandum Report.

for the input wave is reached. The unloading process occurs in some clearing time for the entire front face. The front wall load lasts at a higher level for a longer time than is predicted from Reference 6. A semi-log plot of the pressure-time curves led to the assumption that the decay portion of the loading might be represented by two exponential decay equations. These equations together with their time bounds are shown in Figure 10 with a schematic of a front wall with an opening.

For the computer program, the front wall is divided into general zones with incremental area subdivisions, then calculations for pressure-time loading at each of one-hundred increments of area are performed. The total loading is calculated by summing the incremental pressures over the area for each of fifty time increments. An example of the output format is shown in Table III. The Fortran IV program is listed in Appendix D.

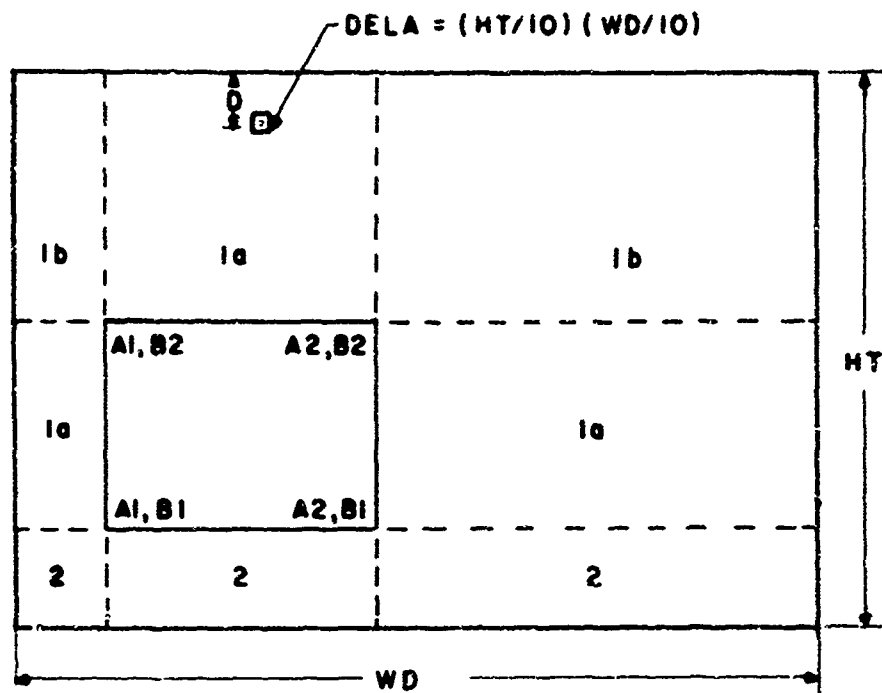
Figure 11 shows a sketch of a rectangular model (Model 38-A) with no openings, used in the experiments of Reference 7. Predictions from the machine program are compared in Figure 12(A) with experimental records obtained from Positions A and C. Figure 12(B) compares the experimental pressure loading obtained from Positions A, B, and C with the computer prediction and the loading prediction from Reference 6 using the method below.

The clearing time is given by

$$t_c = 3h' / C_{refl} \quad , \quad (8)$$

where h' is height of Model 38-A since $h < \text{width}/2$ and C_{refl} is the sound speed for reflected shock. For $P_s = 5$ psi, and $t_c = 852$ μsec . The average loading curve is drawn as now identified. The average loading predicted in this way is higher than the experimental results.

Figure 13(B) shows a similar average loading comparison for Model 37, which has an entrance. The notation is that used in Reference 6.



$$TR = D/CREF \quad (1)$$

$$DR = \text{least of } WD/2 \text{ or } HT \quad (2)$$

$$TC = 2.5 DR/CREF \quad (3)$$

$$P = PREF, 0 < T \leq TR \quad (4)$$

$$P/PREF = \text{EXP} \left[-0.232(T-TR)/TR \right] \quad (5)$$

$$TR < T < 2.5 TR$$

$$P/PREF = (0.70) \text{EXP} \left[-0.36(T-2.5TR)/(TC-2.5TR) \right] \quad (6)$$

$$2.5 TR \leq T \leq TC$$

$$P = PSTAG, T > TC \quad (7)$$

Figure 10. Notation and Equations for Computer Program - Loading of Outside of Front Wall

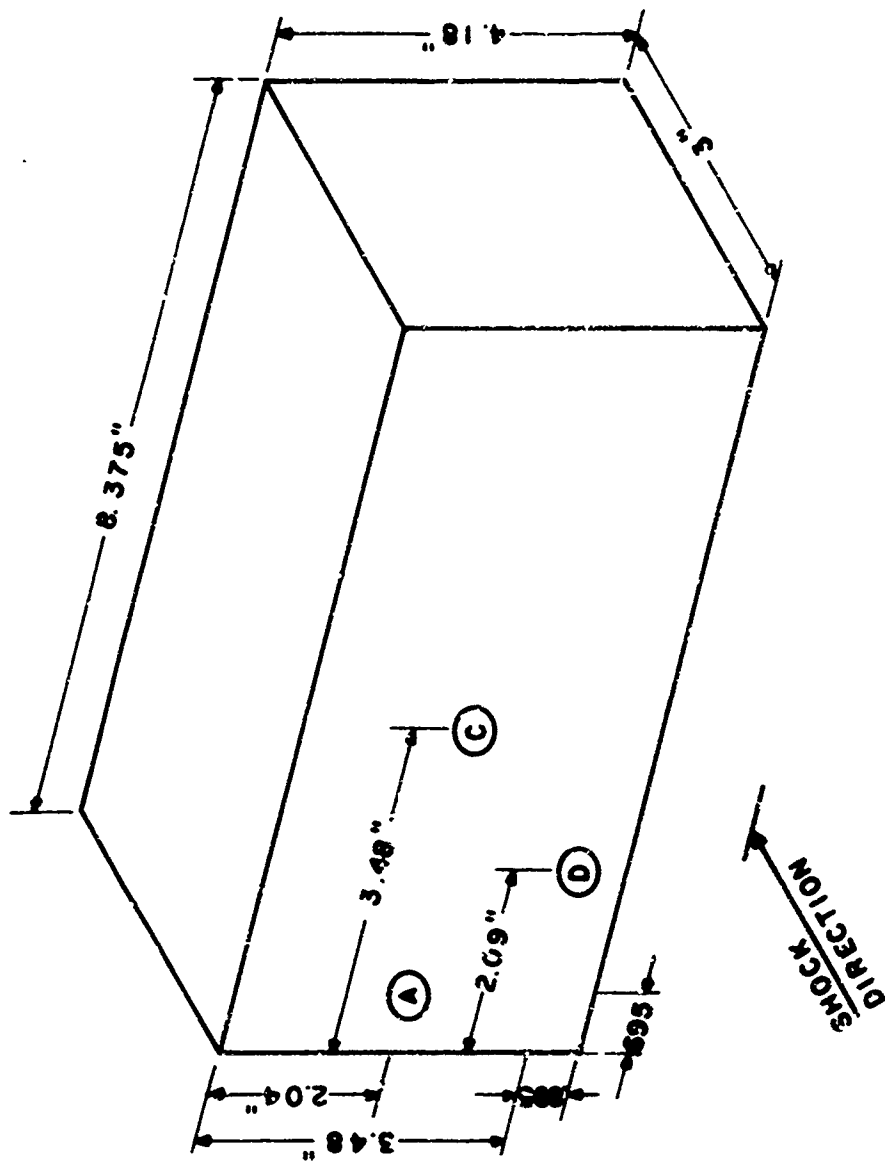
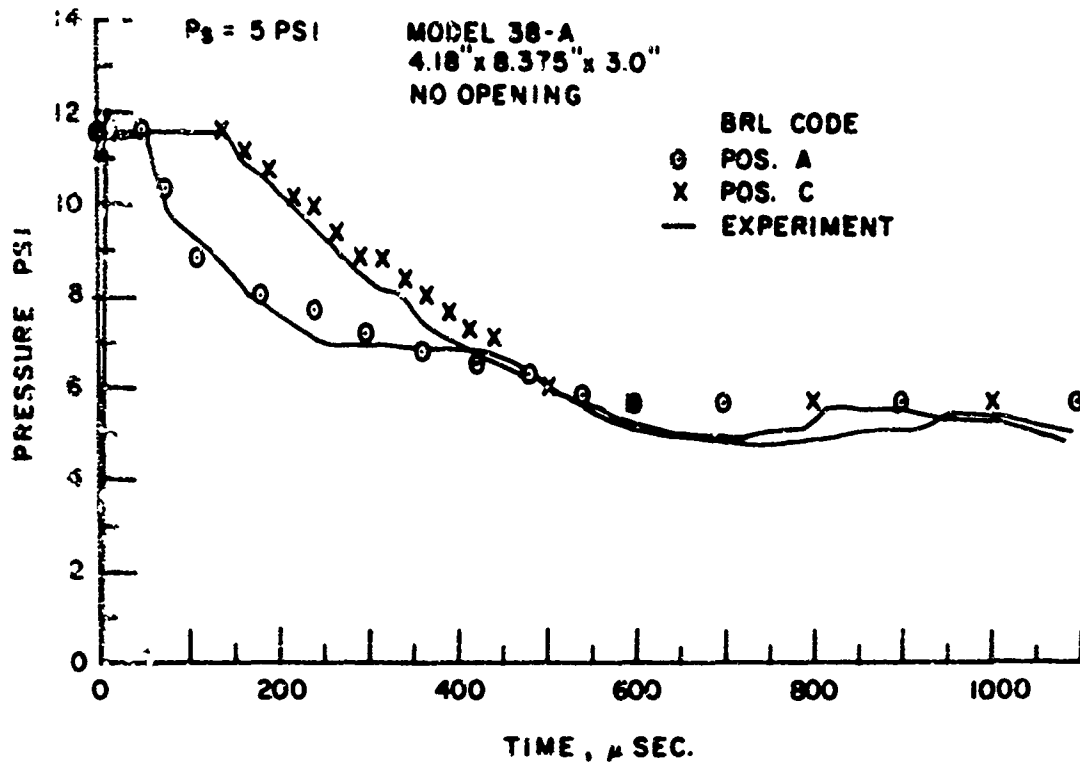
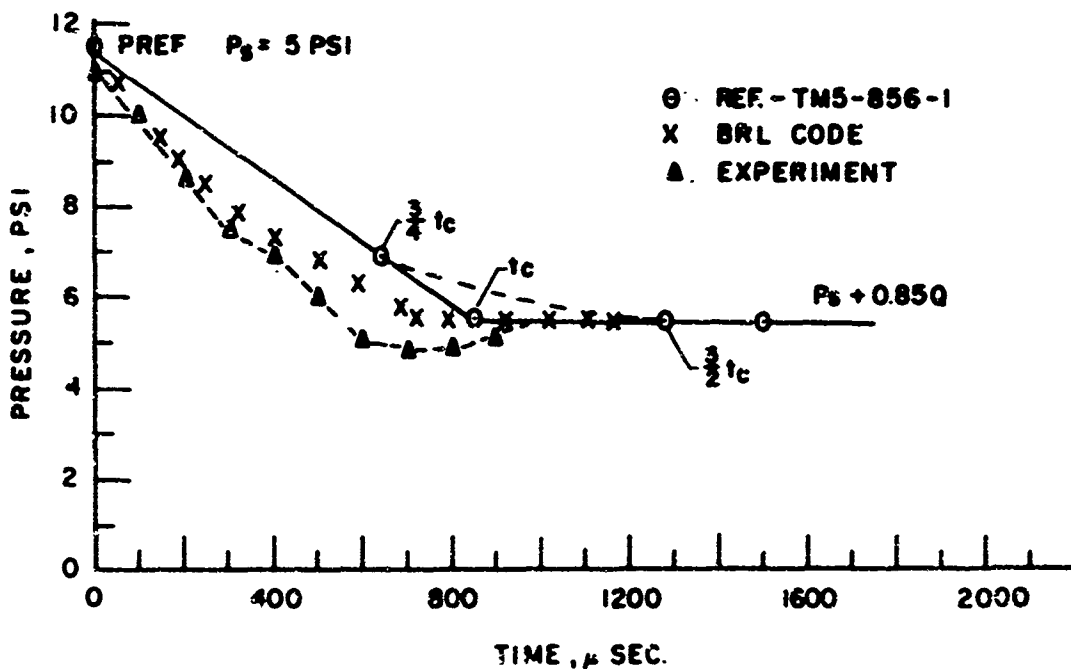


Figure 11. Sketch of Model 38(A), No Openings

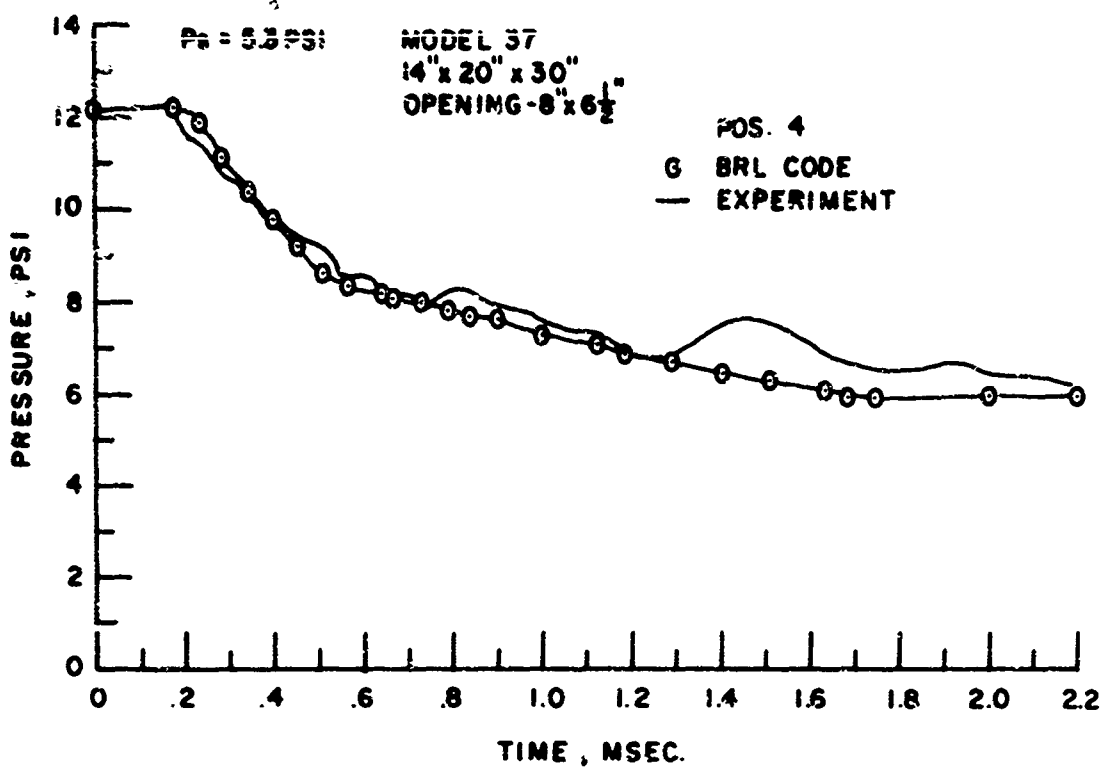


(A) PRESSURE - TIME LOADING ON THE FRONT WALL

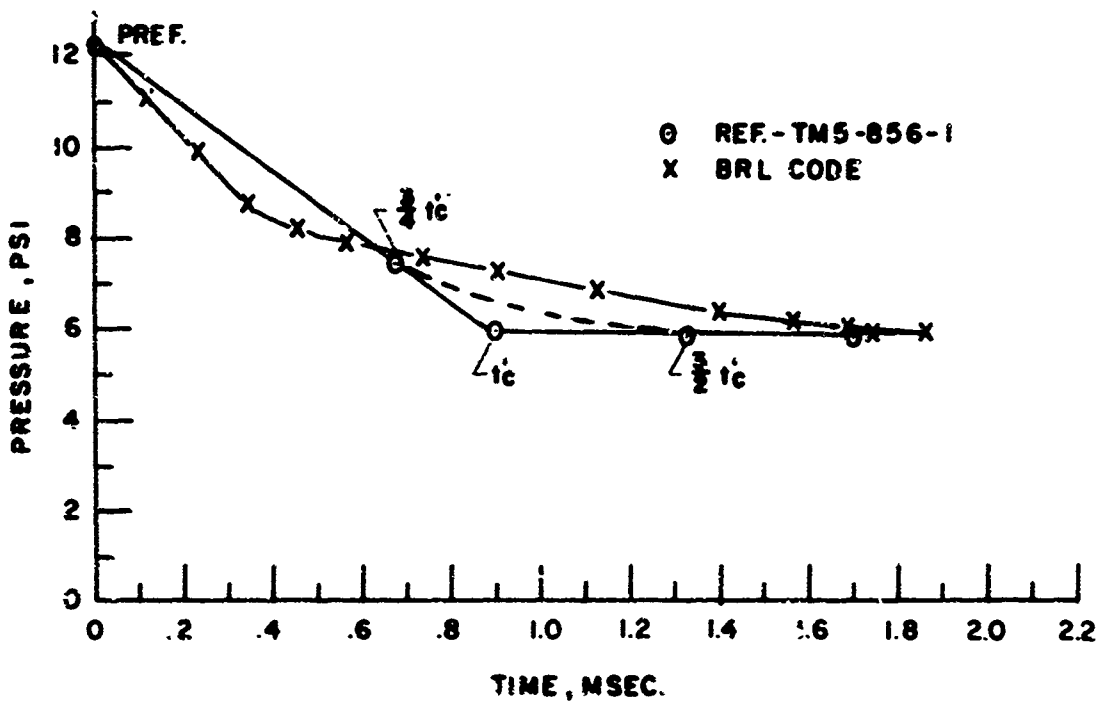


(B) PREDICTED AVERAGE PRESSURE LOADING ON THE FRONT WALL

Figure 12. Loading for Front Wall of Model 38(A)



(A) PRESSURE-TIME LOADING ON OUTSIDE OF FRONT WALL



(B) PREDICTED AVERAGE PRESSURE LOADING ON OUTSIDE OF FRONT WALL

Figure 13. Loading for Outside of Front Wall - Model 37

Table III. Example of Machine Program Output

W-FT	H-FT	TIME-SEC	PRESSURE-PSI	FORCE-LBS	P-T PSI-SEC
.083	.058	.000001	12.200	34.177	.000016
.083	.058	.000057	12.200	34.177	.000700
.083	.058	.000113	10.426	29.206	.001285
.083	.058	.000170	8.539	23.921	.001764
.083	.058	.000226	8.427	23.606	.002237
.083	.058	.000282	8.315	23.295	.002703
.083	.058	.000338	8.206	22.988	.003164
.083	.058	.000394	8.098	22.685	.003618
.083	.058	.000450	7.991	22.386	.004066
.083	.058	.000506	7.886	22.091	.004508
.083	.058	.000562	7.782	21.800	.004945
.083	.058	.000618	7.679	21.512	.005376
.083	.058	.000674	7.578	21.229	.005801
.083	.058	.000731	7.478	20.949	.006220
.083	.058	.000787	7.380	20.673	.006634
.083	.058	.000843	7.282	20.400	.007043
.083	.058	.000899	7.186	20.132	.007446
.083	.058	.000955	7.092	19.866	.007844
.083	.058	.001011	6.998	19.604	.008236
.083	.058	.001067	6.906	19.346	.008624
.083	.058	.001123	6.815	19.091	.009006
.083	.058	.001179	6.725	18.839	.009383
.083	.058	.001235	6.636	18.591	.009756
.083	.058	.001292	6.549	18.346	.010123
.083	.058	.001348	6.463	18.104	.010486
.083	.058	.001404	6.378	17.866	.010843
.083	.058	.001460	6.293	17.630	.011196
.083	.058	.001516	6.211	17.398	.011545
.083	.058	.001572	6.129	17.169	.011889
.083	.058	.001628	6.048	16.942	.012228
.083	.058	.001684	5.968	16.719	.012563
.083	.058	.001740	5.960	16.696	.012897
.083	.058	.001796	5.960	16.696	.013231
.083	.058	.001853	5.960	16.696	.013566
.083	.058	.001909	5.960	16.696	.013900
.083	.058	.001965	5.960	16.696	.014234
.083	.058	.002021	5.960	16.696	.014568
.083	.058	.002077	5.960	16.696	.014901
.083	.058	.002133	5.960	16.696	.015235
.083	.058	.002189	5.960	16.696	.015568
.083	.058	.002245	5.960	16.696	.015902
.083	.058	.002301	5.960	16.696	.016235
.083	.058	.002357	5.960	16.696	.016569
.083	.058	.002413	5.960	16.696	.016902
.083	.058	.002469	5.960	16.696	.017236
.083	.058	.002525	5.960	16.696	.017569
.083	.058	.002581	5.960	16.696	.017903
.083	.058	.002637	5.960	16.696	.018236
.083	.058	.002693	5.960	16.696	.018570
.083	.058	.002749	5.960	16.696	.018903
.083	.058	.002805	5.960	16.696	.019237
.083	.058	.002861	5.960	16.696	.019570
.083	.058	.002917	5.960	16.696	.019904
.083	.058	.002973	5.960	16.696	.020237
.083	.058	.003029	5.960	16.696	.020571
.083	.058	.003085	5.960	16.696	.020904
.083	.058	.003141	5.960	16.696	.021238
.083	.058	.003197	5.960	16.696	.021571
.083	.058	.003253	5.960	16.696	.021905
.083	.058	.003309	5.960	16.696	.022238
.083	.058	.003365	5.960	16.696	.022572
.083	.058	.003421	5.960	16.696	.022905
.083	.058	.003477	5.960	16.696	.023239
.083	.058	.003533	5.960	16.696	.023572
.083	.058	.003589	5.960	16.696	.023906
.083	.058	.003645	5.960	16.696	.024239
.083	.058	.003701	5.960	16.696	.024573
.083	.058	.003757	5.960	16.696	.024906
.083	.058	.003813	5.960	16.696	.025240
.083	.058	.003869	5.960	16.696	.025573
.083	.058	.003925	5.960	16.696	.025907
.083	.058	.003981	5.960	16.696	.026240
.083	.058	.004037	5.960	16.696	.026574
.083	.058	.004093	5.960	16.696	.026907
.083	.058	.004149	5.960	16.696	.027241
.083	.058	.004205	5.960	16.696	.027574
.083	.058	.004261	5.960	16.696	.027908
.083	.058	.004317	5.960	16.696	.028241
.083	.058	.004373	5.960	16.696	.028575
.083	.058	.004429	5.960	16.696	.028908
.083	.058	.004485	5.960	16.696	.029242
.083	.058	.004541	5.960	16.696	.029575
.083	.058	.004597	5.960	16.696	.029909
.083	.058	.004653	5.960	16.696	.030242
.083	.058	.004709	5.960	16.696	.030576
.083	.058	.004765	5.960	16.696	.030909
.083	.058	.004821	5.960	16.696	.031243
.083	.058	.004877	5.960	16.696	.031576
.083	.058	.004933	5.960	16.696	.031910
.083	.058	.004989	5.960	16.696	.032243
.083	.058	.005045	5.960	16.696	.032577
.083	.058	.005101	5.960	16.696	.032910
.083	.058	.005157	5.960	16.696	.033244
.083	.058	.005213	5.960	16.696	.033577
.083	.058	.005269	5.960	16.696	.033911
.083	.058	.005325	5.960	16.696	.034244
.083	.058	.005381	5.960	16.696	.034578
.083	.058	.005437	5.960	16.696	.034911
.083	.058	.005493	5.960	16.696	.035245
.083	.058	.005549	5.960	16.696	.035578
.083	.058	.005605	5.960	16.696	.035912
.083	.058	.005661	5.960	16.696	.036245
.083	.058	.005717	5.960	16.696	.036579
.083	.058	.005773	5.960	16.696	.036912
.083	.058	.005829	5.960	16.696	.037246
.083	.058	.005885	5.960	16.696	.037579
.083	.058	.005941	5.960	16.696	.037913
.083	.058	.005997	5.960	16.696	.038246
.083	.058	.006053	5.960	16.696	.038580
.083	.058	.006109	5.960	16.696	.038913
.083	.058	.006165	5.960	16.696	.039247
.083	.058	.006221	5.960	16.696	.039580
.083	.058	.006277	5.960	16.696	.039914
.083	.058	.006333	5.960	16.696	.040247
.083	.058	.006389	5.960	16.696	.040581
.083	.058	.006445	5.960	16.696	.040914
.083	.058	.006501	5.960	16.696	.041248
.083	.058	.006557	5.960	16.696	.041581
.083	.058	.006613	5.960	16.696	.041915
.083	.058	.006669	5.960	16.696	.042248
.083	.058	.006725	5.960	16.696	.042582
.083	.058	.006781	5.960	16.696	.042915
.083	.058	.006837	5.960	16.696	.043249
.083	.058	.006893	5.960	16.696	.043582
.083	.058	.006949	5.960	16.696	.043916
.083	.058	.007005	5.960	16.696	.044249
.083	.058	.007061	5.960	16.696	.044583
.083	.058	.007117	5.960	16.696	.044916
.083	.058	.007173	5.960	16.696	.045250
.083	.058	.007229	5.960	16.696	.045583
.083	.058	.007285	5.960	16.696	.045917
.083	.058	.007341	5.960	16.696	.046250
.083	.058	.007397	5.960	16.696	.046584
.083	.058	.007453	5.960	16.696	.046917
.083	.058	.007509	5.960	16.696	.047251
.083	.058	.007565	5.960	16.696	.047584
.083	.058	.007621	5.960	16.696	.047918
.083	.058	.007677	5.960	16.696	.048251
.083	.058	.007733	5.960	16.696	.048585
.083	.058	.007789	5.960	16.696	.048918
.083	.058	.007845	5.960	16.696	.049252
.083	.058	.007901	5.960	16.696	.049585
.083	.058	.007957	5.960	16.696	.049919
.083	.058	.008013	5.960	16.696	.050252
.083	.058	.008069	5.960	16.696	.050586
.083	.058	.008125	5.960	16.696	.050919
.083	.058	.008181	5.960	16.696	.051253
.083	.058	.008237	5.960	16.696	.051586
.083	.058	.008293	5.960	16.696	.051920
.083	.058	.008349	5.960	16.696	.052253
.083	.058	.008405	5.960	16.696	.052587
.083	.058	.008461	5.960	16.696	.052920
.083	.058	.008517	5.960	16.696	.053254
.083	.058	.008573	5.960	16.696	.053587
.083	.058	.008629	5.960	16.696	.053921
.083	.058	.008685	5.960	16.696	.054254
.083	.058	.008741	5.960	16.696	.054588
.083	.058	.008797	5.960	16.696	.054921
.083	.058	.008853	5.960	16.696	.055255
.083	.058	.008909	5.960	16.696	.055588
.083	.058	.008965	5.960	16.696	.055922
.083	.058	.009021	5.960	16.696	.056255
.083	.058	.009077	5.960	16.696	.056589
.083	.058	.009133	5.960	16.696	.056922
.083	.058	.009189	5.960	16.696	.057256
.083	.058	.009245	5.960	16.696	.057589
.083	.058	.009301	5.960	16.696	.057923
.083	.058	.009357	5.960	16.696	.058256
.083	.058	.009413	5.960	16.696	.058590
.083	.058	.009469	5.960	16.696	.058923
.083	.058	.009525	5.960	16.696	.059257
.083	.058	.009581	5.960	16.696	.059590
.083	.058	.009637	5.960	16.696	.059924
.083	.058	.009693	5.960	16.696	.060257
.083	.058	.009749	5.960	16.696	.060591
.083	.058	.009805	5.960	16.696	.060924
.083	.058	.009861	5.960	16.696	.061258
.083	.058	.009917	5.960	16.696	.061591
.083	.058	.009973	5.960	16.696	.061925
.083	.058	.010029	5.960	16.696	.062258
.083	.058	.010085	5.960	16.696	.062592
.083	.058	.010141	5.960	16.696	.062925
.083	.058	.010197	5.960	16.696	.063259
.083	.058	.010253	5.960	16.696	.063592
.083	.058	.010309	5.960	16.696	.063926
.083	.058	.010365	5.960	16.696	.064259
.083	.058	.010421	5.960	16.696	.064593
.083	.058	.010477	5.960	16.696	.064926
.083	.058	.010533	5.960	16.696	.065260
.083	.058	.010589	5.960	16.696	.065593
.083	.058	.010645	5.960	16.696	.065927

Table III. Example of Machine Program Output (Continued)

FORCE ON FRONT

TIME-SEC	TOTAL FORCE-LB,	AVERAGE PRESSURE-PSI
0.000001	2734.1	12.20
0.000057	2717.7	12.13
0.000113	2486.9	11.10
0.000170	2290.1	10.22
0.000226	2211.7	9.87
0.000282	2117.5	9.45
0.000338	2030.9	9.06
0.000394	1957.7	8.74
0.000450	1894.4	8.45
0.000506	1840.5	8.21
0.000562	1804.1	8.05
0.000618	1773.4	7.91
0.000674	1747.2	7.80
0.000731	1721.4	7.68
0.000787	1696.0	7.57
0.000843	1671.0	7.46
0.000899	1646.4	7.35
0.000955	1622.1	7.24
0.001011	1598.2	7.13
0.001067	1574.7	7.03
0.001123	1551.5	6.92
0.001179	1528.6	6.82
0.001235	1506.1	6.72
0.001292	1484.0	6.62
0.001348	1462.1	6.52
0.001404	1440.6	6.43
0.001460	1419.4	6.33
0.001516	1398.6	6.24
0.001572	1378.0	6.15
0.001628	1357.7	6.06
0.001684	1337.8	5.97
0.001740	1335.7	5.96
0.001796	1335.7	5.96
0.001853	1335.7	5.96
0.001909	1335.7	5.96
0.001965	1335.7	5.96
0.002163	1335.7	5.96
0.002362	1335.7	5.96
0.002560	1335.7	5.96
0.002759	1335.7	5.96
0.002957	1335.7	5.96
0.003156	1335.7	5.96
0.003354	1335.7	5.96
0.003553	1335.7	5.96
0.003751	1335.7	5.96
0.003950	1335.7	5.96
0.004148	1335.7	5.96
0.004347	1335.7	5.96
0.004545	1335.7	5.96
0.004744	1335.7	5.96

The clearing time,

$$t_c' = 3h_f' / C_{refl} \quad , \quad (9)$$

where

$$h_f' = \sum \frac{\delta_n h_n A_n}{A_f} \leq h_f' \quad ; \quad (10)$$

where A_f is net area of front, A_n is area of zones on front. (See Figure 10), h_n equals the distance between edges which relieve the pressure in zones 1a, h_n equals the smaller of height or width for zones 1b, and h_n equals the distance between the edge relieving and the opposite side of zone 2. δ_n equals one-half for the zones designated 1a and equals one for all other zones. h_f' equals the smaller value of the height or half-width of the front. The values of t_c' equals 892 μ sec for Model 37, where h_f' equals 4.38 in. and C_{refl} equals 1236 ft/sec.

A similar prediction can be made for the inside front wall of Model 37, where

$$h_{if}' = \sum \frac{\delta_n h_n A_n}{A_{if}'} = 3.5 \text{ in.} \quad (11)$$

From Figure 14, P_{soi} equals 1.82 psi, the average inside peak pressure for an opening 17 percent of the total front wall area. For the ambient sound speed, C_o , of 1163 ft/sec for the experiment, then,

$$U_{io} = C_o \left(1 + \frac{6 P_{soi}}{7 P_o} \right)^{1/2} = 1198 \text{ ft/sec,} \quad (12)$$

the speed of the shockwave inside with pressure P_{soi} . The reflected pressure for P_{soi} at an ambient pressure, P_o , of 14.7 psi is found from the Equation 13:

$$P_{i-refl} = 2 P_{soi} \left[\frac{7 P_o + 4 P_{soi}}{7 P_o + P_{soi}} \right] = 3.8 \text{ psi} \quad . \quad (13)$$

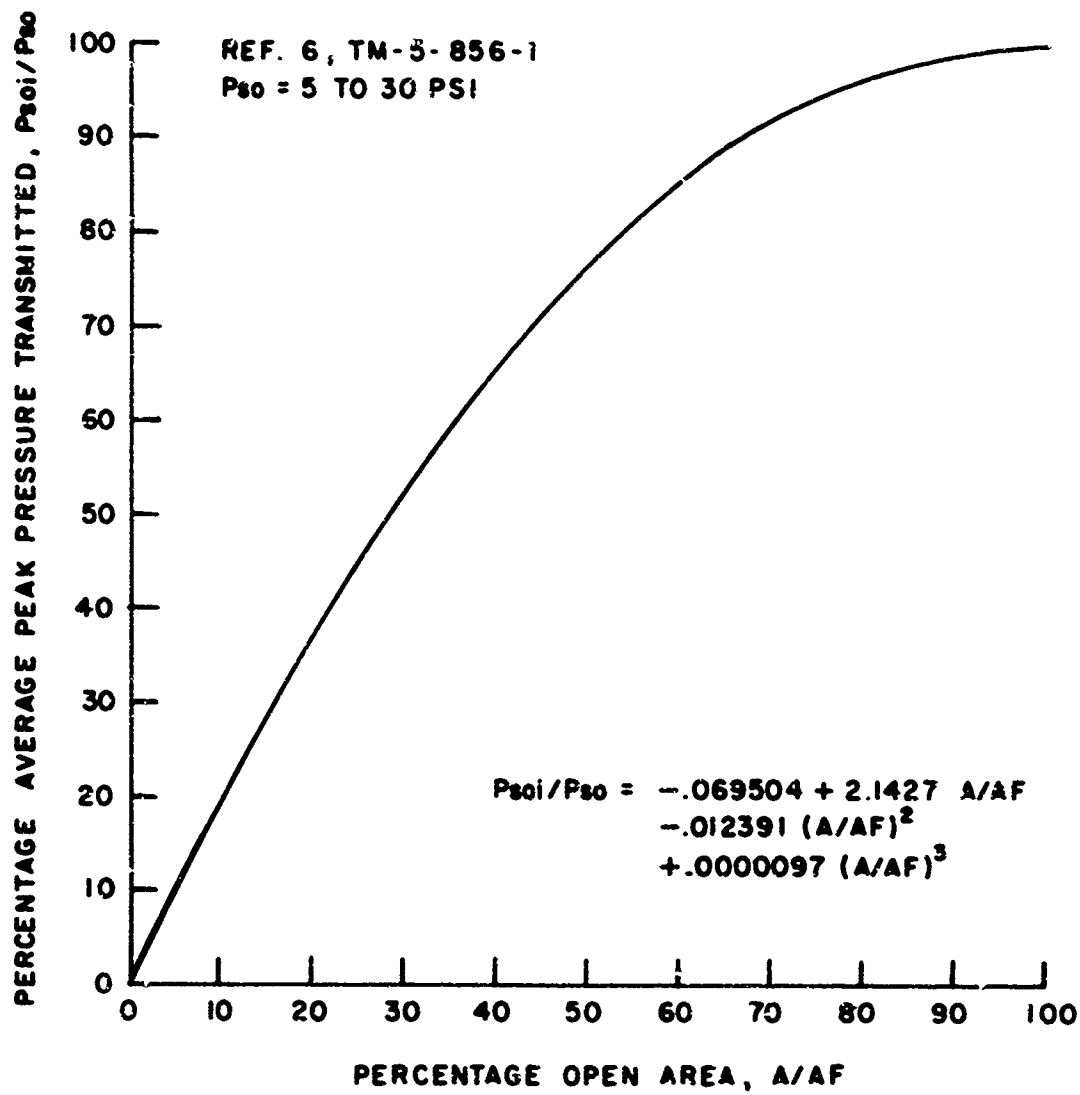


Figure 14. Average Transmitted Peak Pressure on Inside of Front Wall

The clearing time for the inside of the front wall is

$$t = 4 h'_{if}/C_o = 1 \text{ msec} \quad (14)$$

The time for the return of the first reflection from the back wall is:

$$L_i/U_{io} + L_i/C_o = 3.53 \text{ msec} \quad (15)$$

where, $L_i/C_o = 1.79 \text{ msec}$. The decay of the peak pressure to the outside value is calculated from Equation 16:

$$3 h'_{if}/C_o = 0.75 \text{ msec} \quad (16)$$

Figure 15 shows a comparison of particular loads on the front wall with the average predicted loads calculated from the equations of Reference 6. The particular load may be quite different from the average load calculated this way.

B. Side Wall

Particular records from Positions 17 and 17A are compared in Figure 16 with average loading predictions from Reference 6. The equations used in obtaining these predictions are listed below.

Calculations for the average outside, side wall loading are as follows:

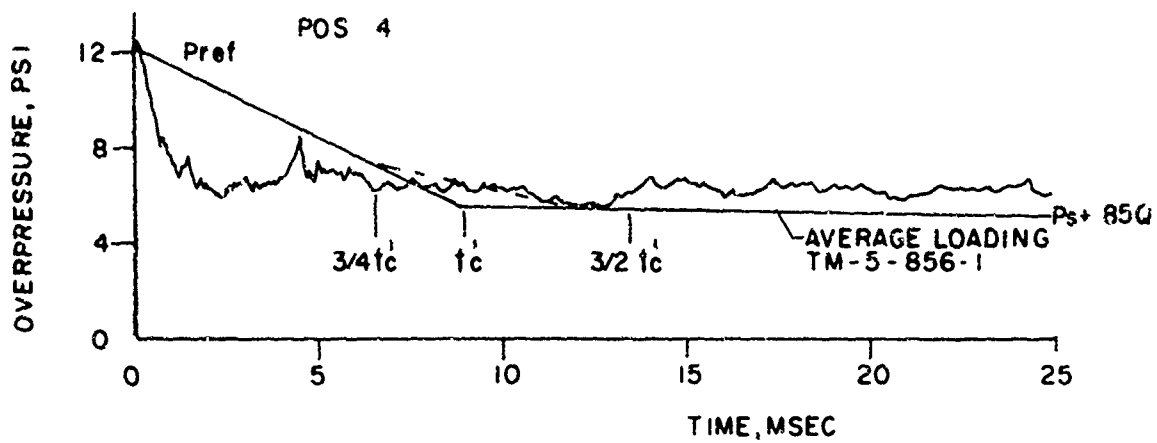
For $P_s = 5.5 \text{ psi}$, $U_s = 1336 \text{ ft/sec}$, $P_{so} = P_s$, $P_o = 14.7 \text{ psi}$, $L = 2.5 \text{ ft}$, and $h' = 1.167 \text{ f}$,

$$t_d = L/U_o = 1.87 \text{ msec} \quad (17)$$

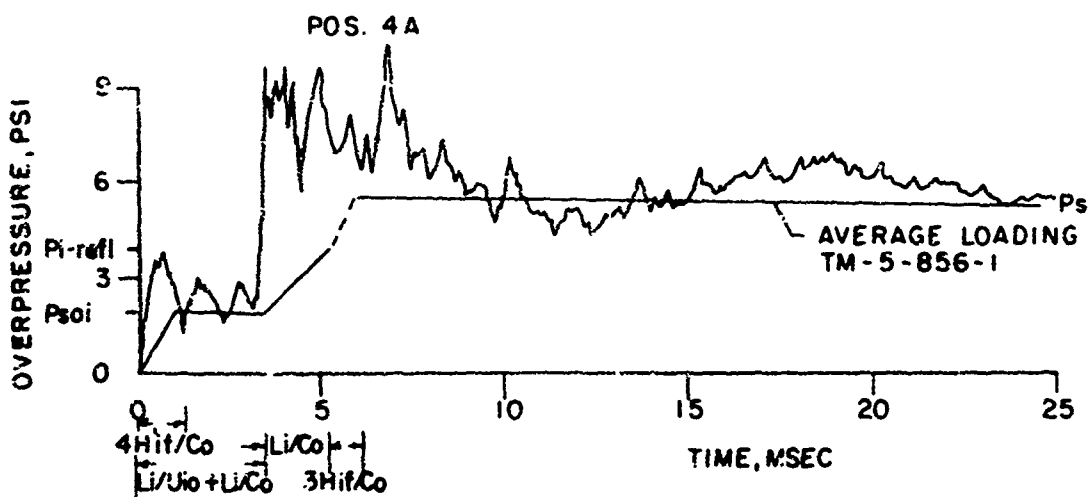
$$P'' = \bar{P}/P_s = 0.9 + 0.1 \left(1 - P_{so}/P_o \right)^2 = 0.94 \quad (18)$$

is the average pressure near the bottom of wall (zone 3 of Reference 6) when the shock wave has reached the rear corner; $\bar{P} = 5.2 \text{ psi}$.

$$P' = \bar{P}/P_s = 0.5 + 0.125 \left(2 - P_{so}/P_o \right)^2 = 0.83 \quad (19)$$

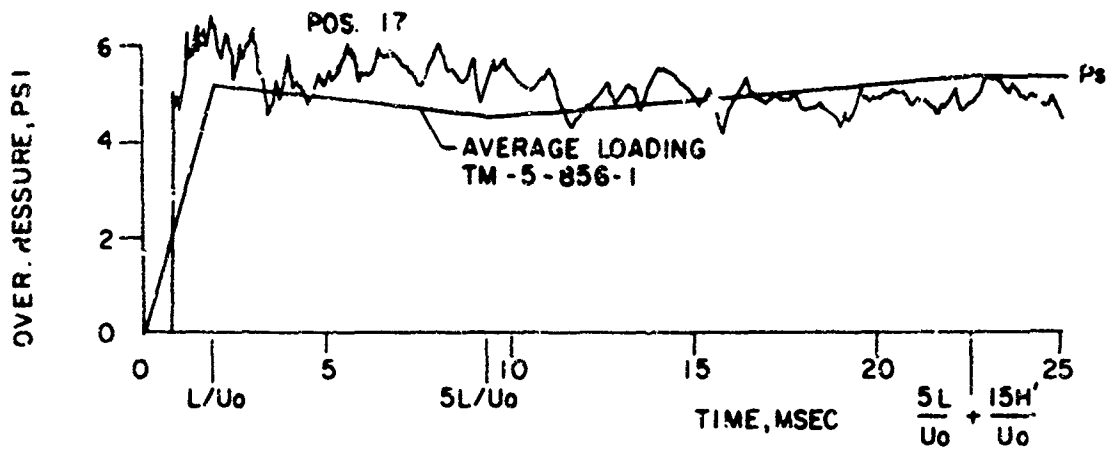


(A) RECORD FROM POS. 4 COMPARED WITH AVERAGE PREDICTED LOADING ON OUTSIDE OF FRONT WALL

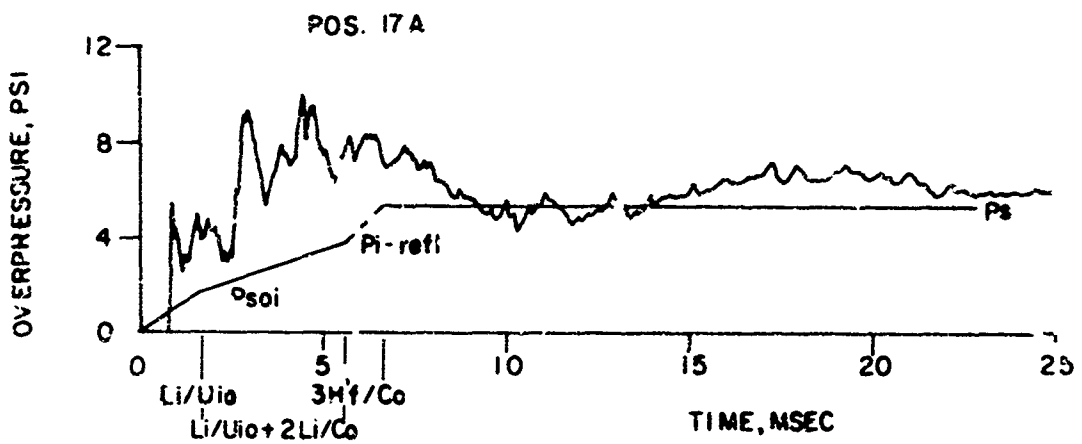


(B) RECORD FROM POS. 4A COMPARED WITH AVERAGE PREDICTED LOADING ON INSIDE OF FRONT WALL

Figure 15. Comparison of Pressure-Time Records with the Predicted Average Loading Curves on the Front Wall



(A) RECORD FROM POS. 17 COMPARED WITH AVERAGE PREDICTED LOADING ON OUTSIDE OF SIDE WALL



(B) RECORD FROM POS. 17A COMPARED WITH AVERAGE PREDICTED LOADING ON INSIDE OF SIDE WALL

Figure 15. Comparison of Records with the Average Predicted Loading on the Side Wall

and $\bar{P} = 4.6$ psi, the minimum average pressure.

$$5L/U_0 = 9.4 \text{ msec} \quad (20)$$

and

$$15 h' / U_0 = 13.1 \text{ msec} \quad (21)$$

where h' is least of $L/2$ and h .

Calculations for the average inside pressure are as follows:

Using the values of P_{soi} , P_{i-refl} , U_{i0} , hf' , and C_0 calculated from above and letting $L_i = 2.083$ ft, the following parameters may be calculated:

$$L_i / U_{i0} = 1.7 \text{ msec} \quad , \quad (22)$$

$$2 L_i / C_0 = 3.6 \text{ msec} \quad , \quad (23)$$

and

$$3 h' / C_0 = 0.94 \text{ msec} \quad . \quad (24)$$

Two observations may be made from the comparisons in Figure 16: First, it is obvious that there is, no loading at a given position until the shock wave arrives there. If an average loading value were used in this case a pressure would be predicted, even though in reality one does not exist. The second observation is that a low predicted value of the average transmittal peak pressure inside occurs. The back wall reflected wave therefore, is also too small.

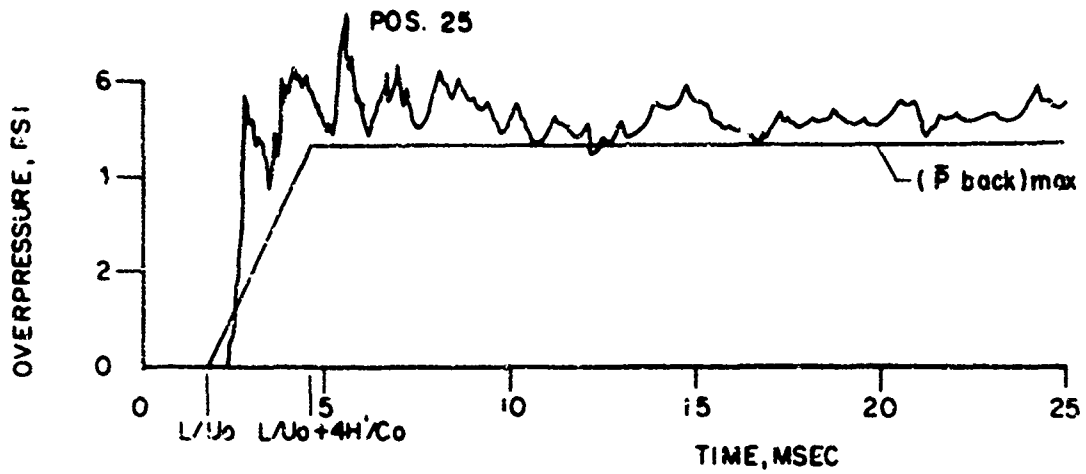
C. Back Wall

A comparison of records from Positions 25 and 25A (center of back wall) is made in Figure 17 with average loading predictions. The loading predictions were again made using the methods of Reference 6.

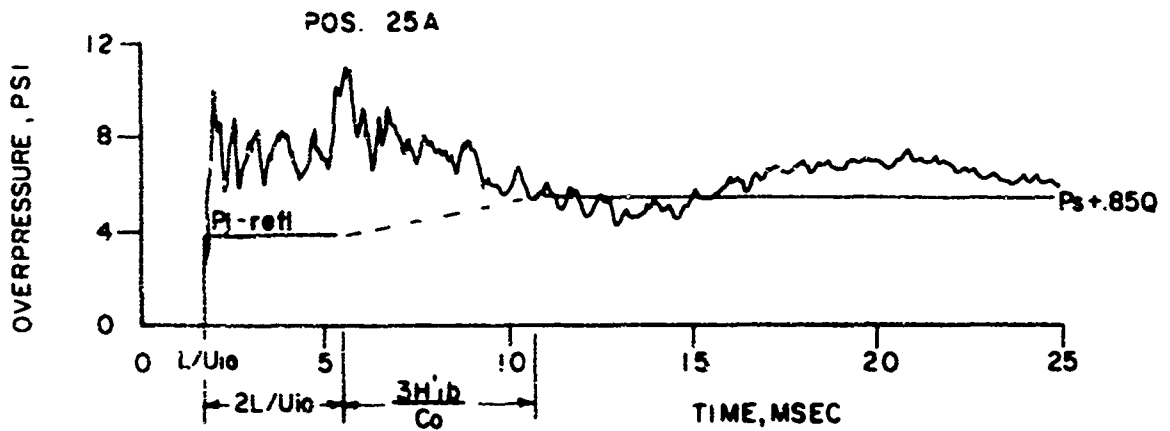
Calculations for the outside loading are as follows:

$$t_d = L/U_0 = 1.87 \text{ msec}, h' = \text{lesser of } h \text{ or } W/2 = W/2 = .833 \text{ ft} \quad .$$

$$\text{Back wall buildup time, } t_b = 4 h' / C_0 = 2.87 \text{ msec.} \quad (25)$$



(A) RECORD FROM POS 25 COMPARED WITH AVERAGE PREDICTED LOADING ON OUTSIDE OF BACK WALL



(B) RECORD FROM POS. 25A COMPARED WITH AVERAGE PREDICTED LOADING ON INSIDE OF BACK WALL

Figure 17. Comparison of Records with the Average Predicted Loading on the Back Wall

$$(\bar{P}_{\text{back}})_{\text{max}} = P_{\text{sb}} \left(\frac{1}{2}\right) [1 + (1 + \beta)l^{-\beta}] \quad , \quad (26)$$

which gives the average peak pressure at buildup time, t_b .

$$P_{\text{so}} = P_{\text{sb}} = P_s = 5.5 \text{ psi, for step shock wave.}$$

$$\beta = 0.5 P_{\text{so}}/P_o = 0.187 \quad , \quad (27)$$

and

$$(\bar{P}_{\text{back}})_{\text{max}} = 4.6 \text{ psi}$$

$$\frac{\bar{P}_{\text{back}}}{P_s} = \frac{(\bar{P}_{\text{back}})_{\text{max}}}{P_{\text{sb}}} + \left[1 - \frac{(\bar{P}_{\text{back}})_{\text{max}}}{P_{\text{sb}}} \right] \left[\frac{t - (t_d + t_b)}{t_o - t_b} \right]^2 \quad . \quad (28)$$

Calculations for average loading on the inside of the back wall are as follows:

$\tau_d = L_i/U_{i0} = 1.7 \text{ msec}$ and $h'_{ib} \cdot L_i$, since there are no openings in the back wall. $2 L_i/C_o = 3.6 \text{ msec}$.

$$3 h'_{ib}/C_o = 3 L_i/C_o = 5.4 \text{ msec} \quad . \quad (29)$$

$$P_{\text{soi}} = 1.82 \text{ psi, } P_{\text{i-refl}} = 3.8 \text{ psi, and } P_s + 0.85Q = 5.9 \text{ psi.}$$

For a step shock wave the positive duration, t_o , approaches infinity, and $\bar{P}_{\text{back}} = (\bar{P}_{\text{back}})_{\text{max}}$.

The major differences between the average loading predicted and the data records occur again for the inside loading. The reason for this was previously, an underprediction of P_{soi} and therefore, $P_{\text{i-refl}}$. If the predicted value for $P_{\text{i-refl}}$ should be much higher than the outside pressure, then $P_{\text{i-refl}}$ would fall to P_{stag} , instead of $P_s + 0.85Q$ as predicted.

The underprediction of P_{soi} seems to be a serious deficiency, of the method.

V. SUMMARY AND CONCLUSIONS

The Appendixes of this report contain the pressure-time loading records from the differential loading experiments, a computer program used to predict the outside wall loading from a step shock wave for the case of a single opening; high speed photographs of the two-dimensional basement model-shock wave interaction, and tables of the flow calculations.

From these data the following conclusions appear valid:

1. The time that is required for reflected pressure to clear from the outside front wall is proportional to the wall half-width or height dimension, whichever is smaller. The proportionality appears also to hold for the front wall with an opening. The clearing time is not proportional to a weighted sum of the opening-edge dimensions as indicated in Reference 6.
2. The internal reflections on the inside walls are more complex than is assumed in previous prediction methods. This causes larger inside loads than were predicted before. It is possible that an oscillatory loading function could be used to account for the reflections from the side walls.
3. The side and top wall areas influenced by the vortex motion from the model's edges are localized near the edges and the effects of vortices does not seem to extend too far from the edge (some few inches).
4. The basement shelter model results are quite preliminary, but they appear to show a strong air flow direction towards the floor from the entrance above. Additional experiments are being started with larger three-dimensional models instrumented with stagnation pressure transducers. It is planned to continue this phase of the work through the next work period.
5. Clearing time for the front wall and frequency of internal pressure reflections should scale for a full size room. An example is given in Appendix E.

ACKNOWLEDGMENTS

The author wishes to thank Messrs. R. Abrahams, R. Peterson, and K. Holbrook for the experimental work performed at the BRL 5.5 ft Shock Tube, and also to thank Mr. R. Rudolph for rewriting the smoke grid tracer program for the Fortran IV language.

REFERENCES

1. H. M. Childers, *et al.*, "Final Report - Open Shelter Feasibility Study," The Vertex Corporation, Kensington, Maryland, Vertex TR No. 68-1, October 1968.
2. E. L. Hill, *et al.*, "Determination of Shelter Configuration for Ventilation," Research Triangle Institute, Durham, North Carolina, Final Report R-OU-177, July 9, 1965.
3. S. J. Lis and H. F. Behls, "Ventilation Equipment Analysis for Basement Shelters," General American Research Division, Niles, Illinois, GARD Final Report 1278, February 1968.
4. George A. Coulter, "Air Shock Filling of Model Rooms," Ballistic Research Laboratories Memorandum Report No. 1916, March 1968.
5. George A. Coulter, "Flow in Rooms Caused by Air Shock Waves," Ballistic Research Laboratories Memorandum Report No. 2044, July 1970.
6. "Design of Structures to Resist the Effects of Atomic Weapons," Headquarters, Department of the Army, Washington, D.C., TM 5-856-1, November 1960.
7. William J. Taylor, To be published as a Ballistic Research Laboratories Memorandum Report.

APPENDIX A

PRESSURE-TIME RECORDS

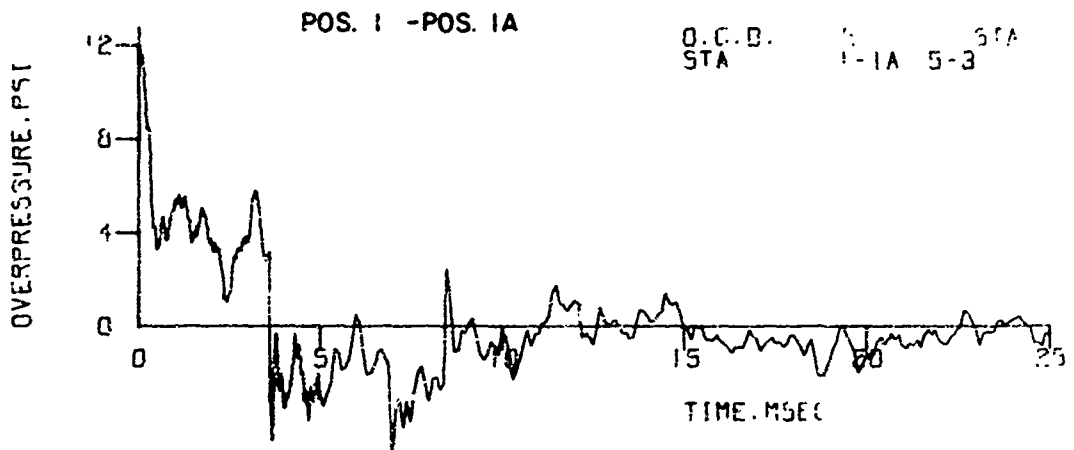
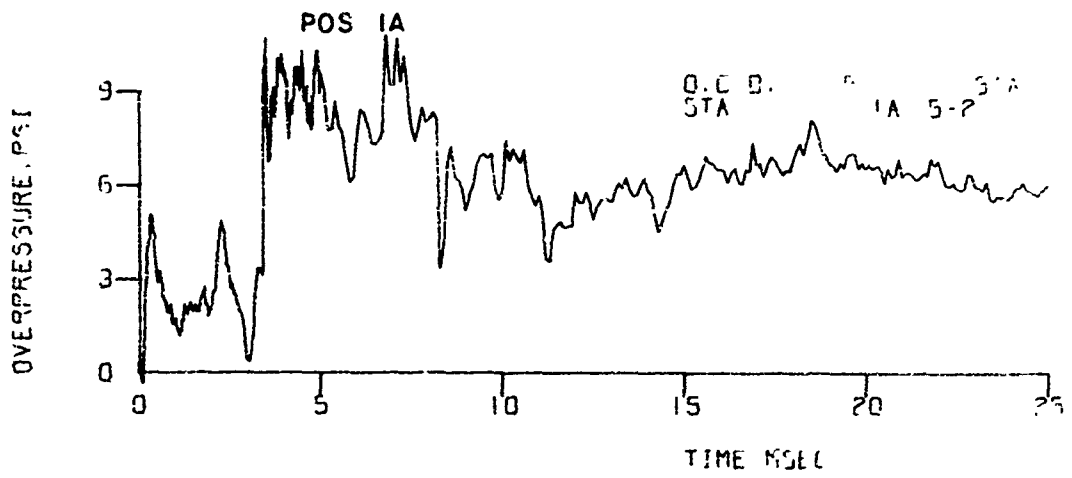
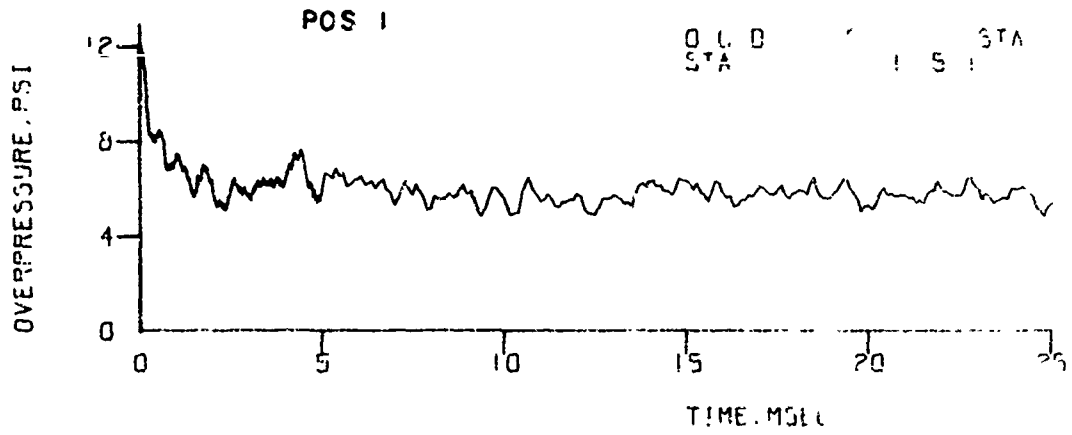


Figure A-1. Records from Front Wall - Model 37

Preceding page blank

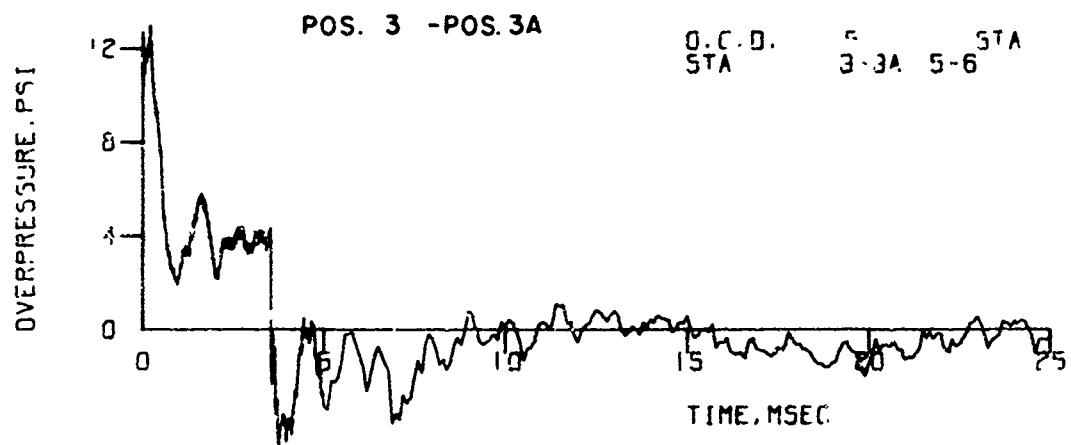
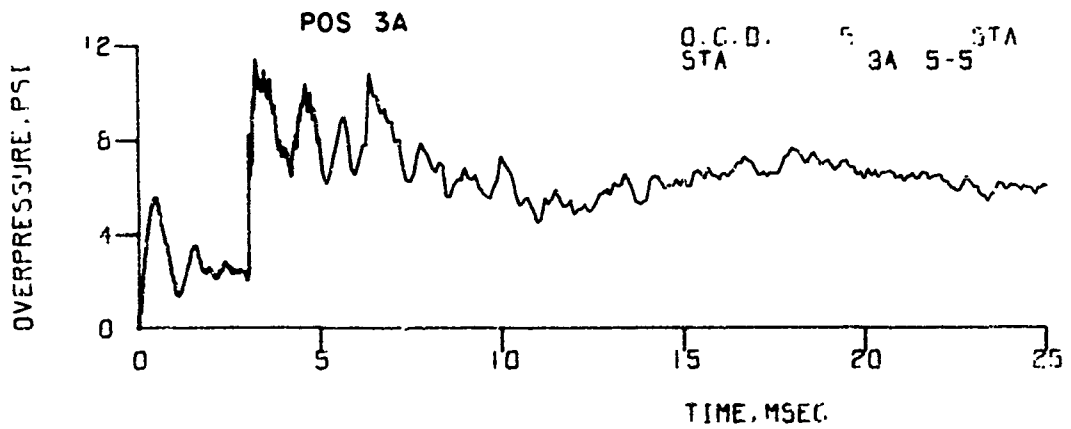
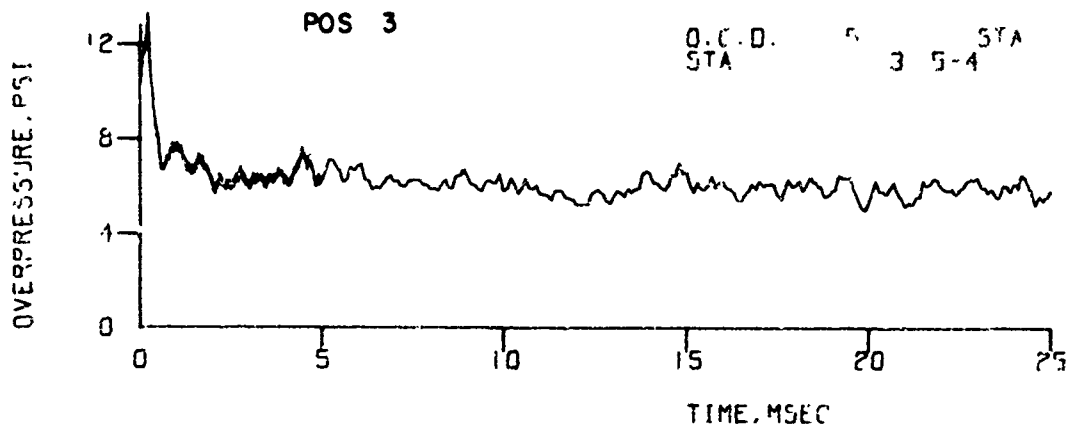


Figure A-1. Records from Front Wall - Model 37 (Continued)

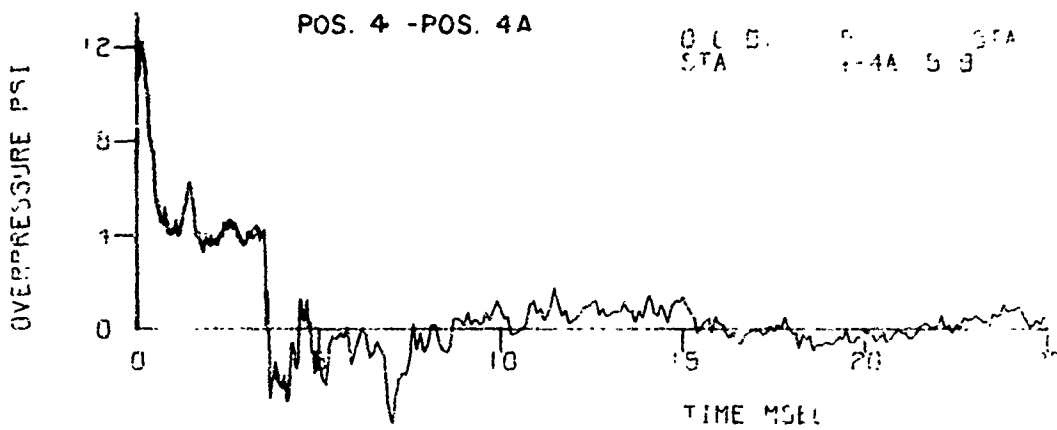
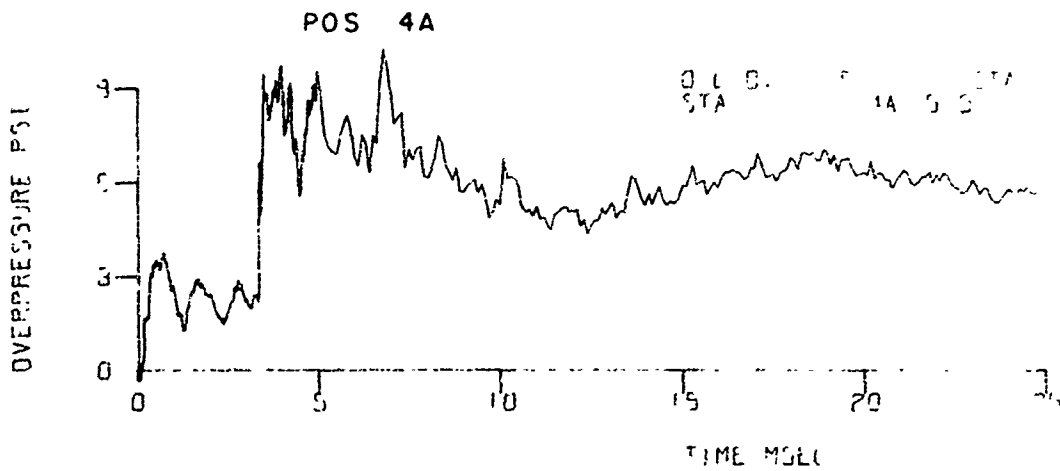
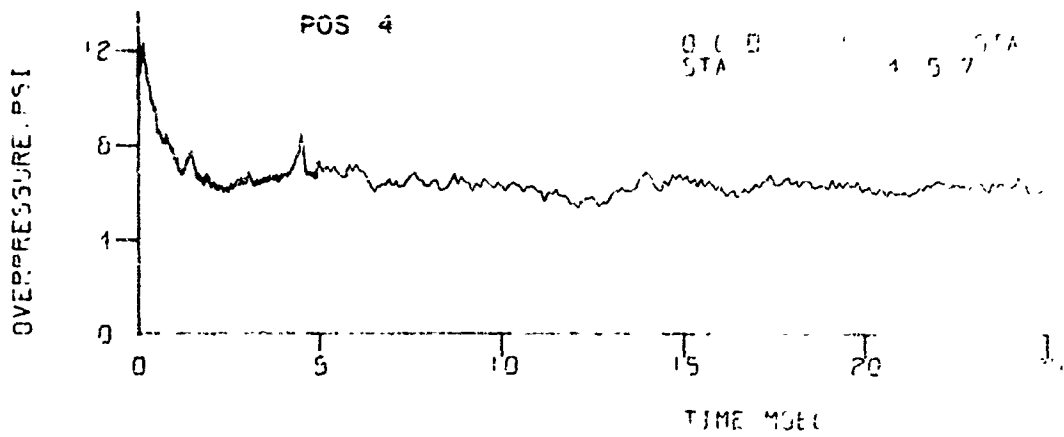


Figure A-1. Records from Front Wall - Model 37 (Continued)

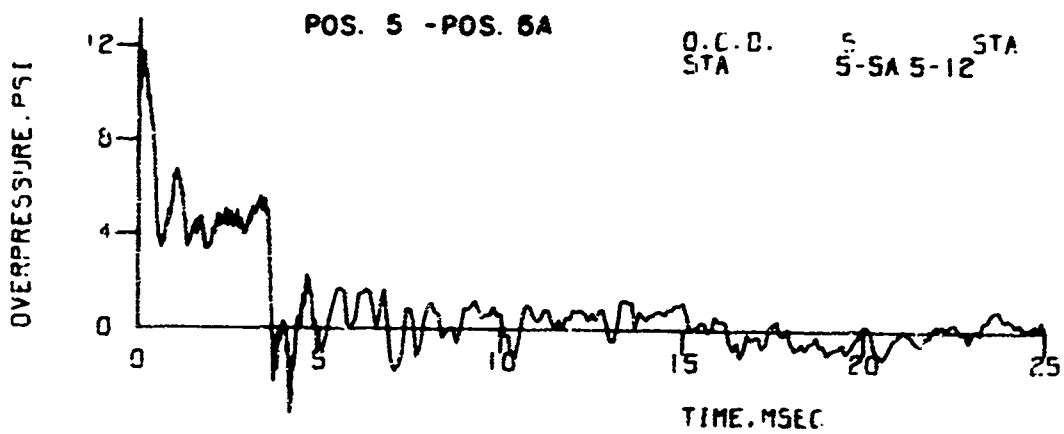
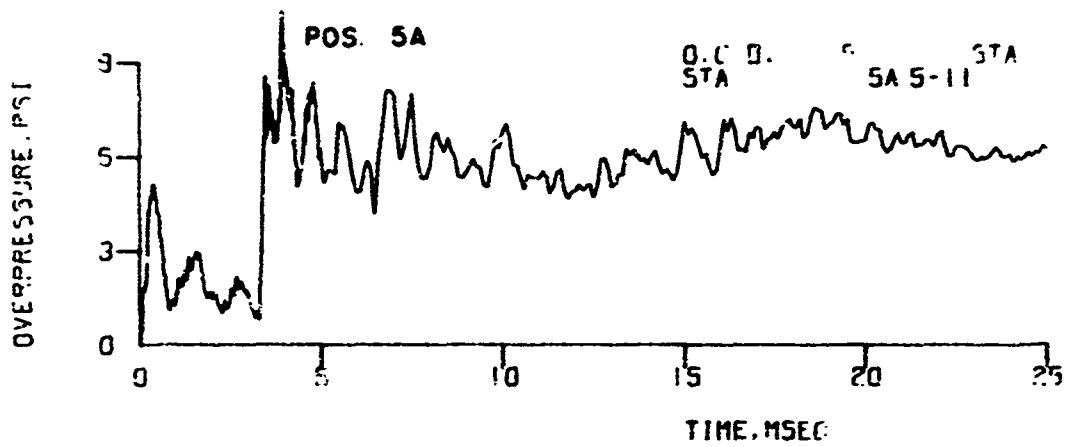
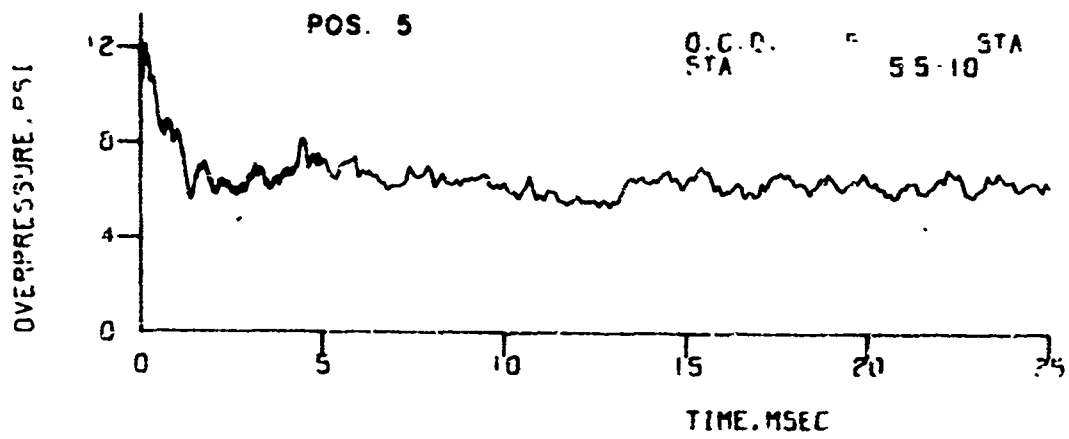


Figure A-1. Records from Front Wall - Model 37 (Continued)

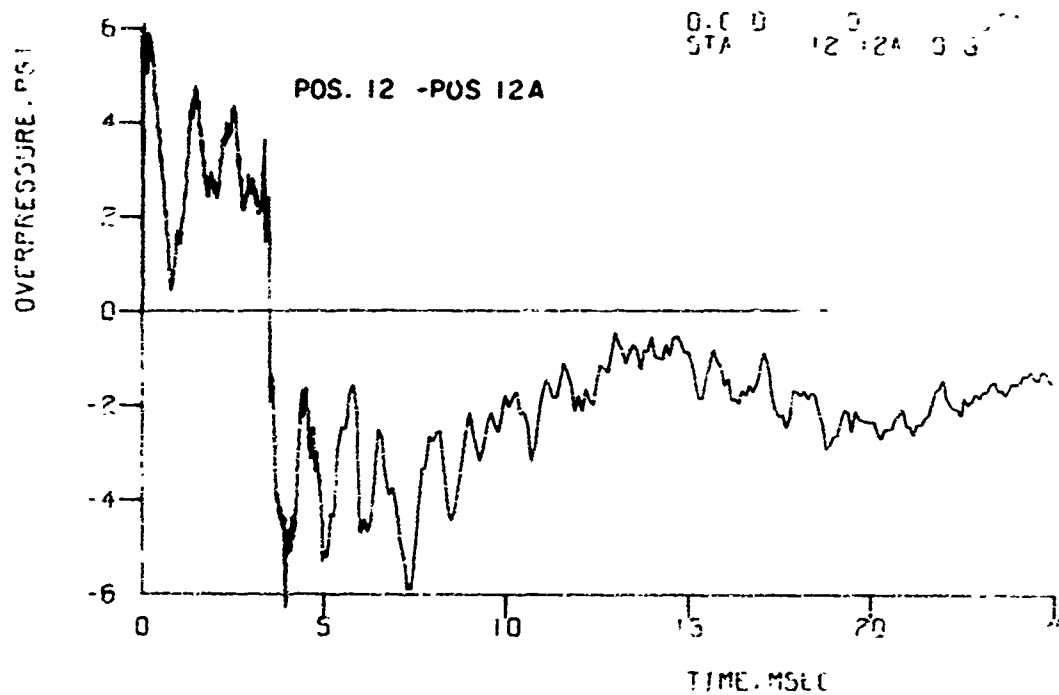
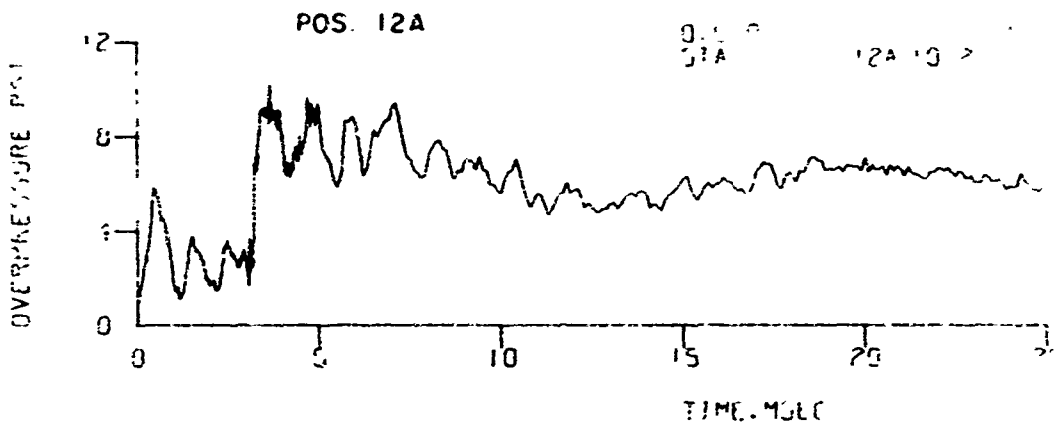
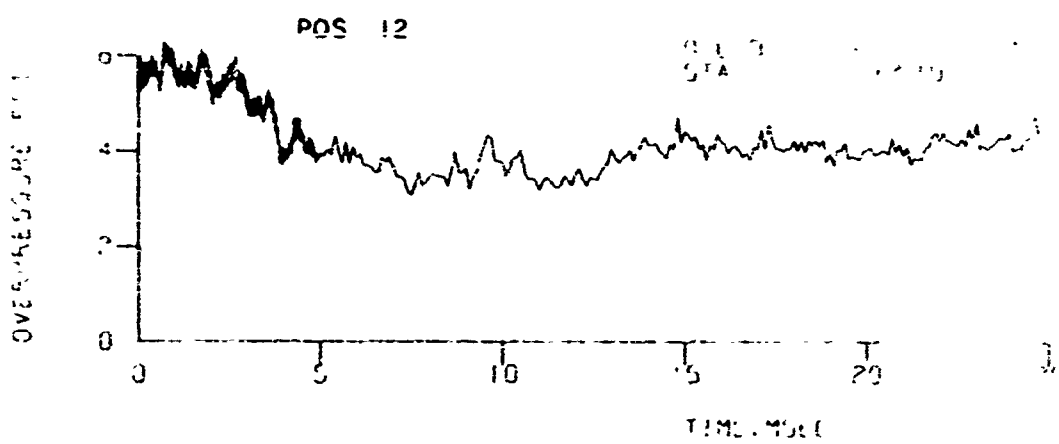


Figure A-2. Records from Side Wall - Model 37

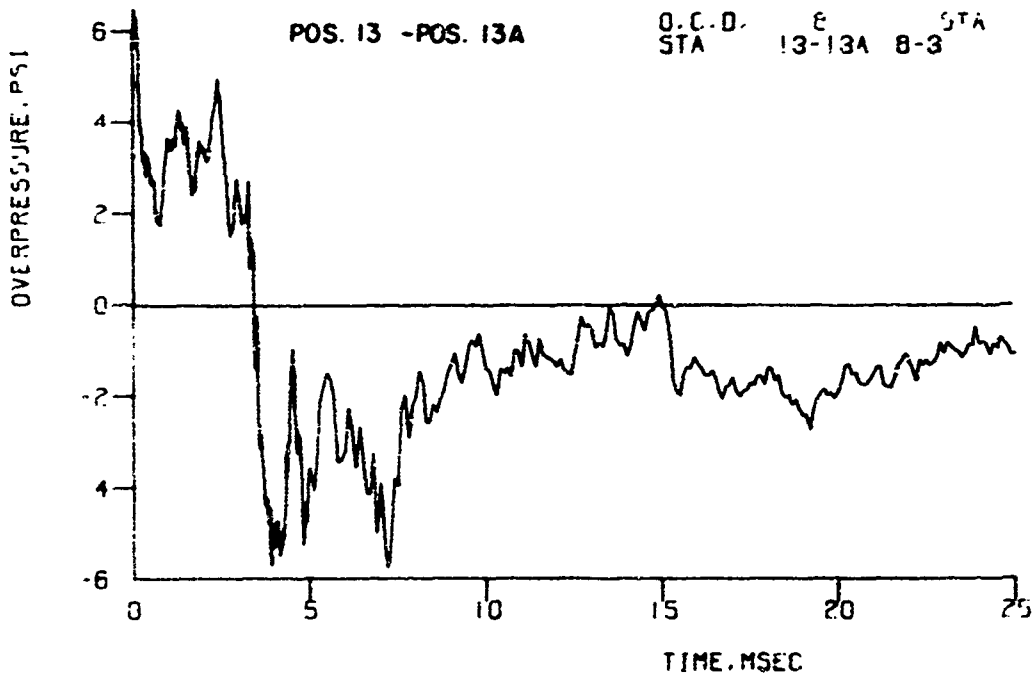
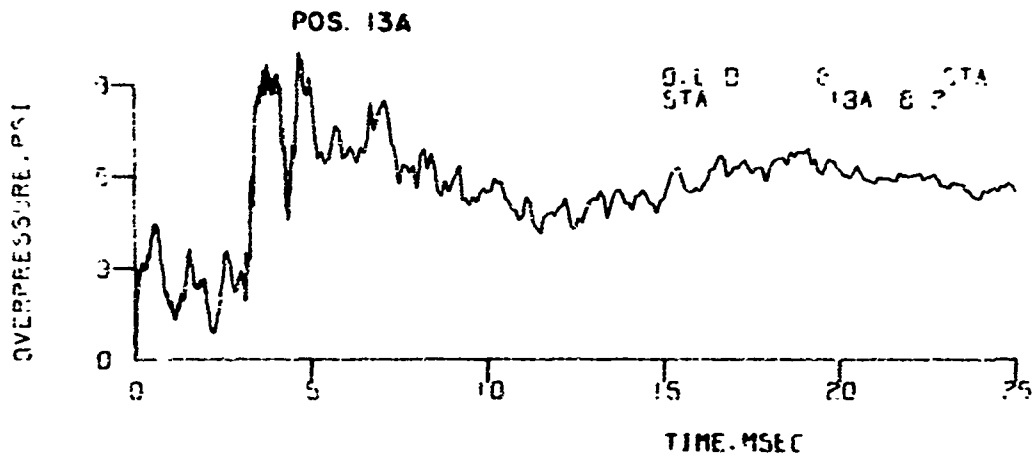
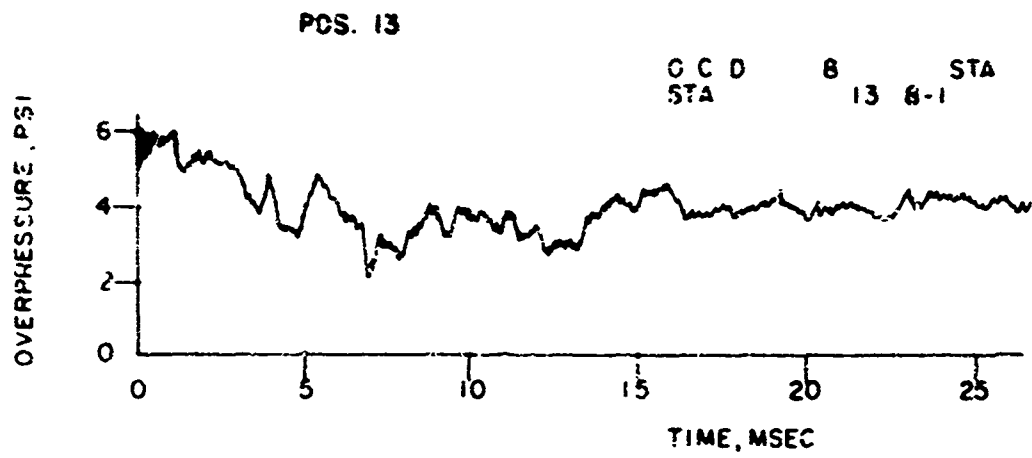


Figure A-2. Records from Side Wall - Model 37 (Continued)

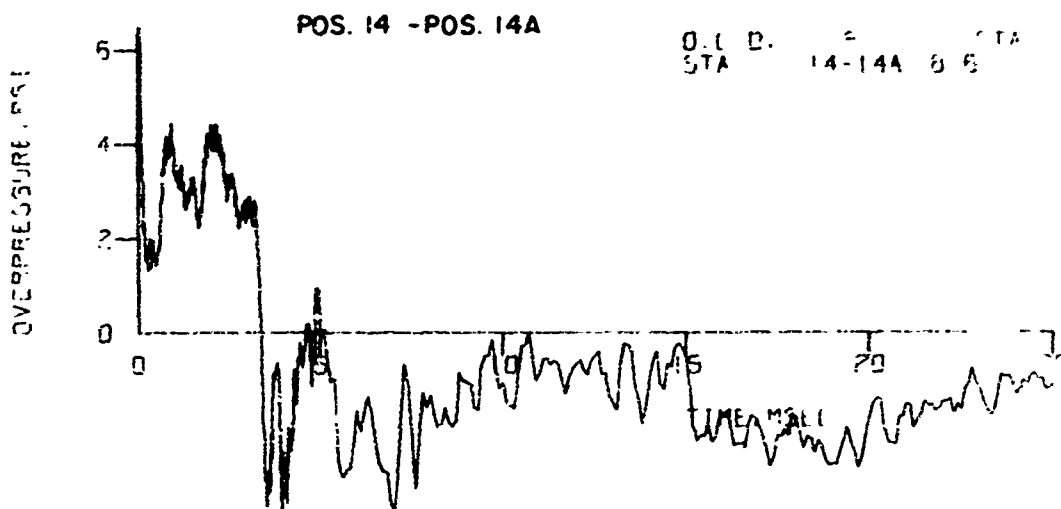
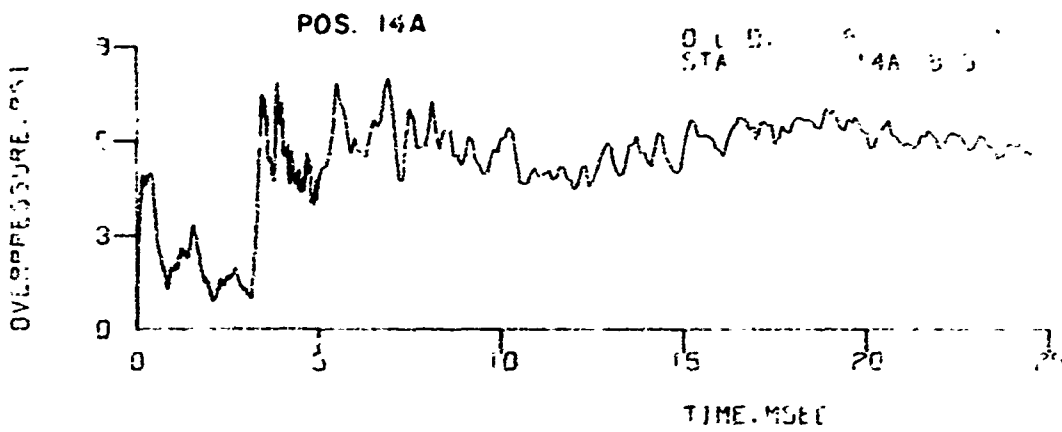
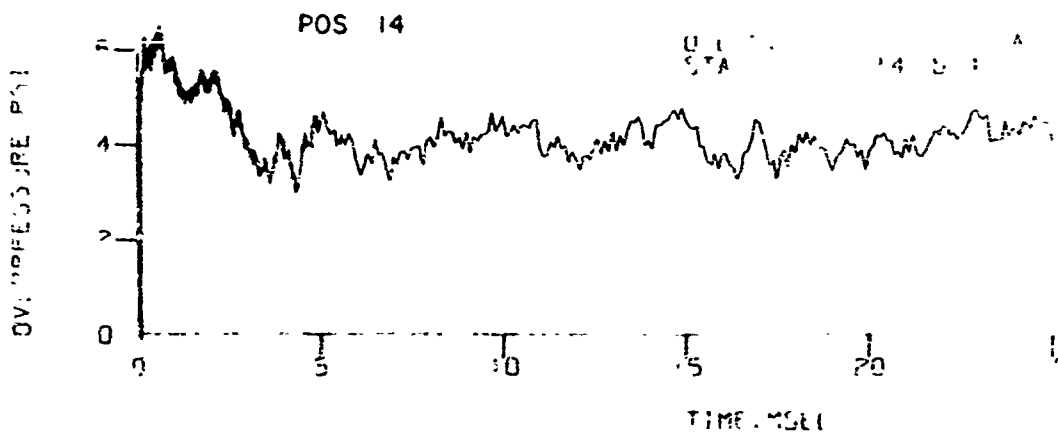


Figure A-2. Records from Side Wall - Model 37 (Continued)

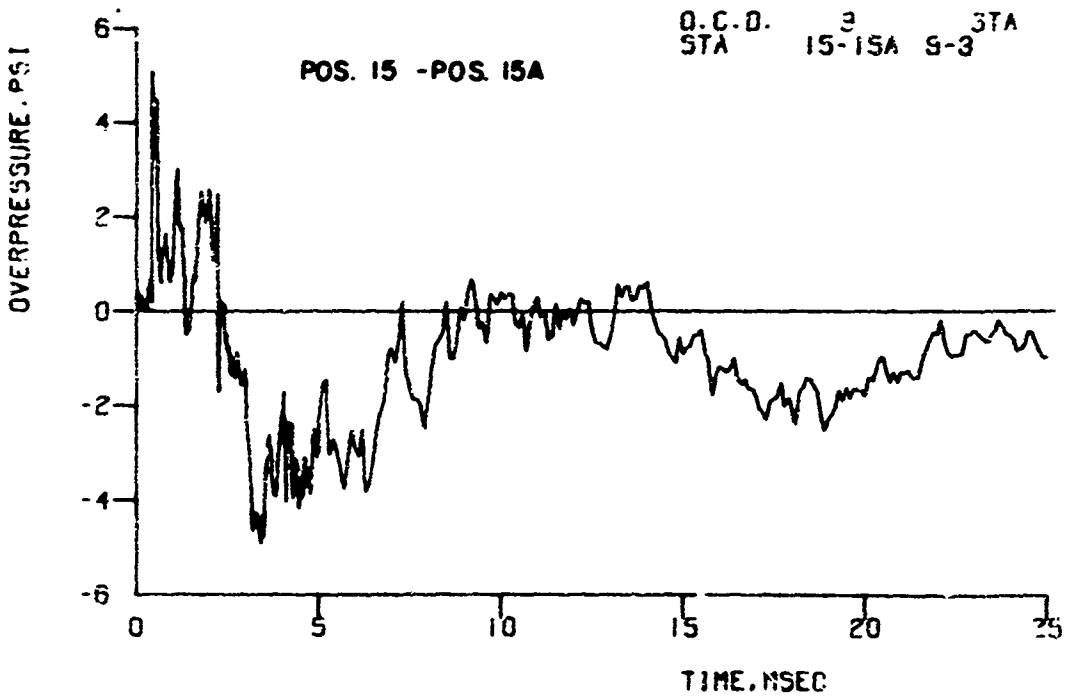
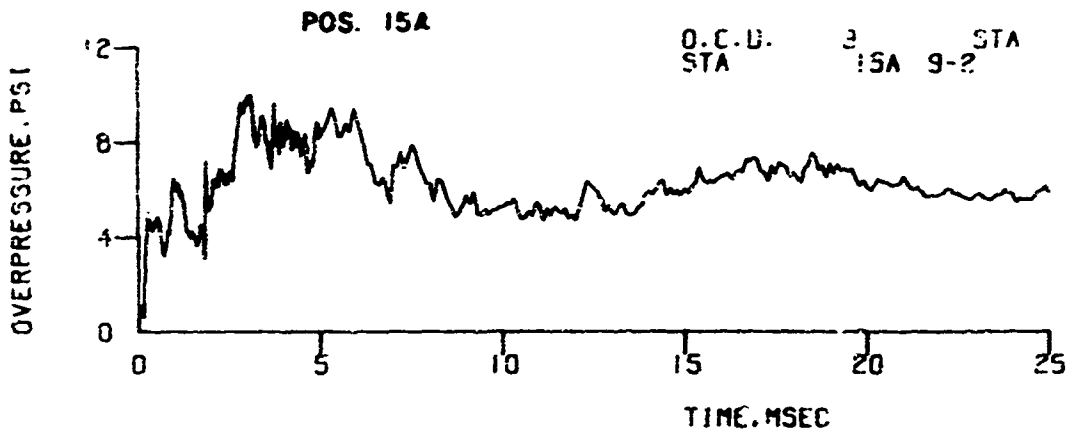
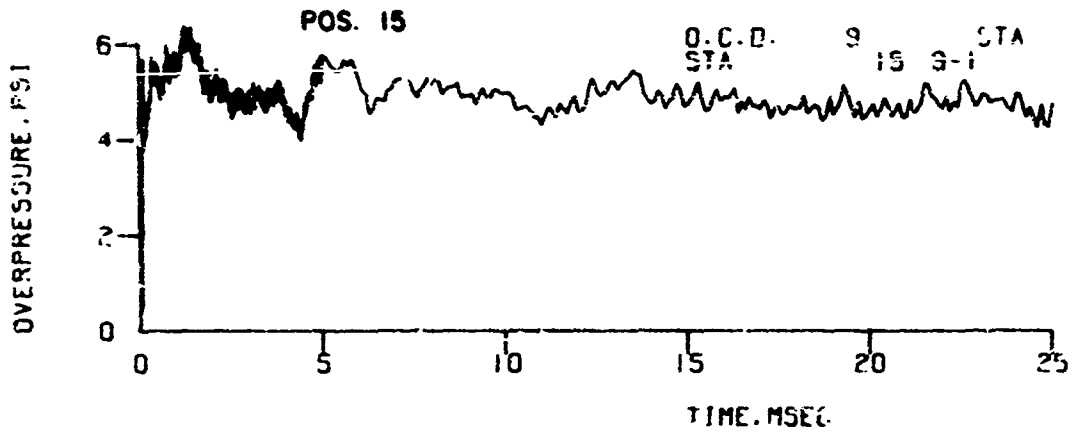


Figure A-2. Records from Side Wall - Model 37 (Continued)

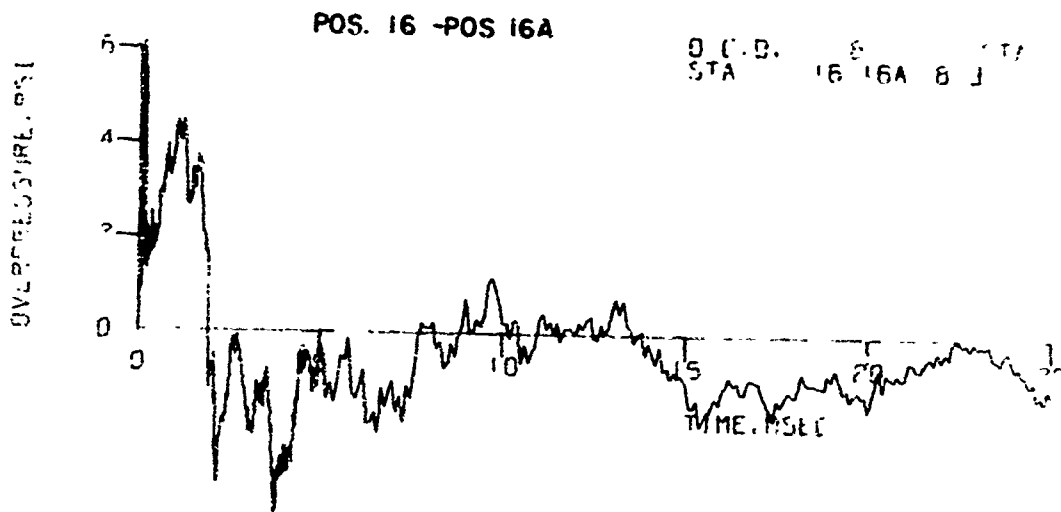
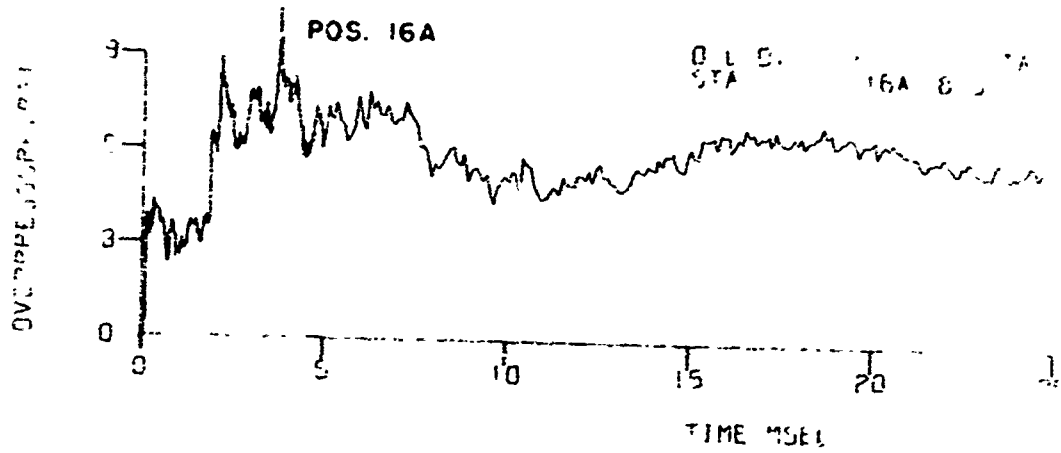
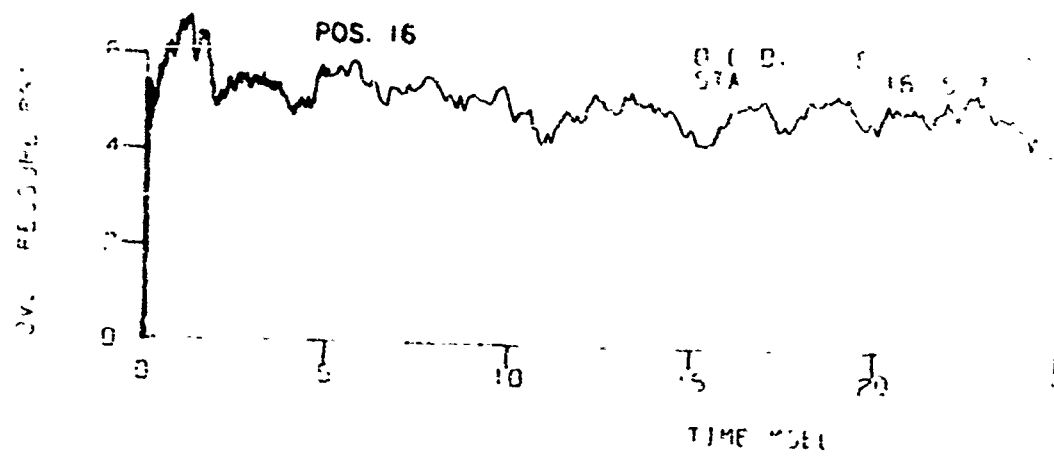


Figure A-2. Records from Side Wall - Model 37 (Continued)

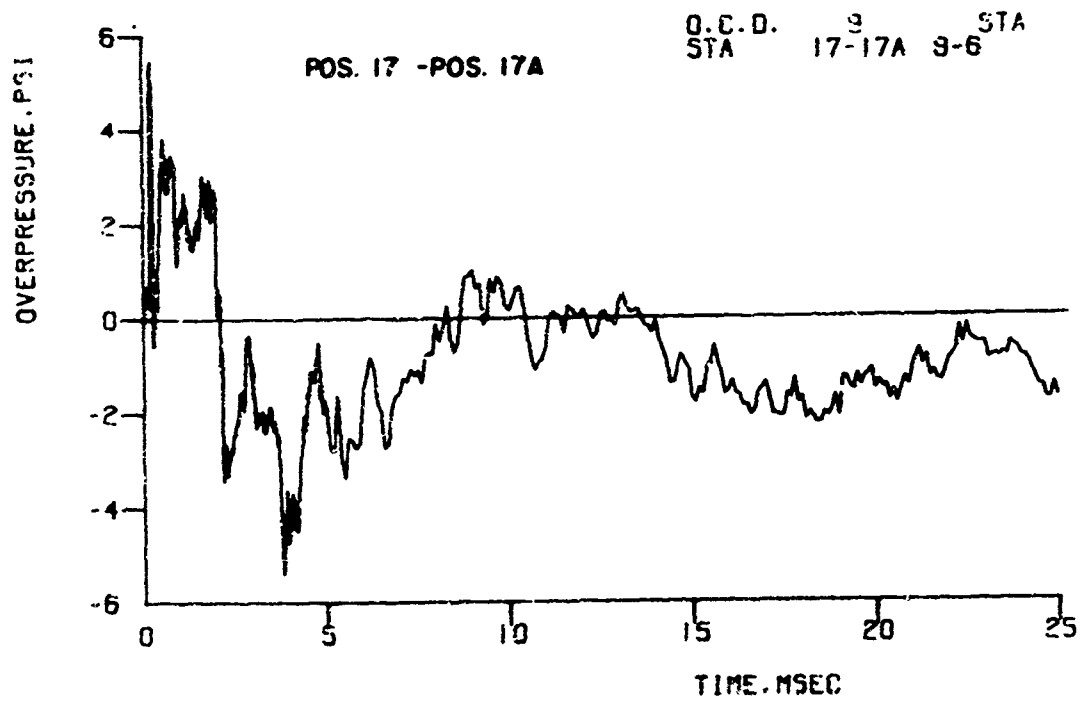
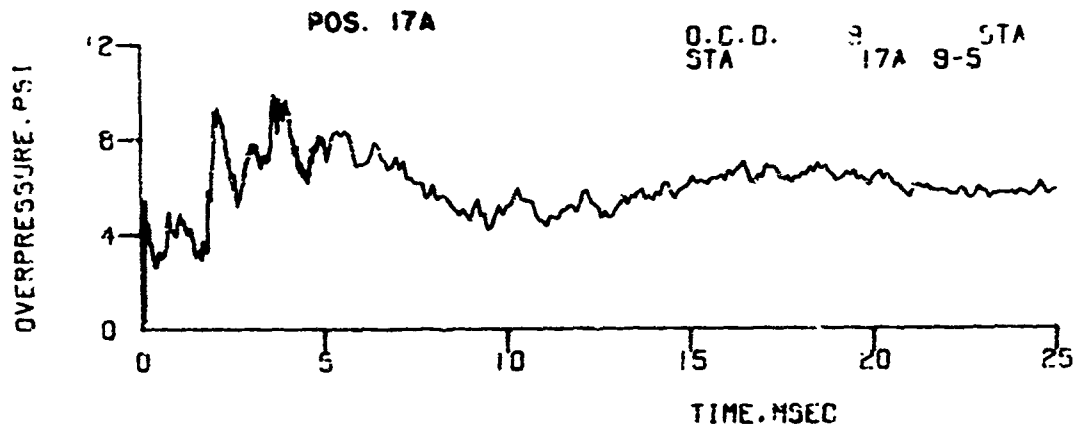
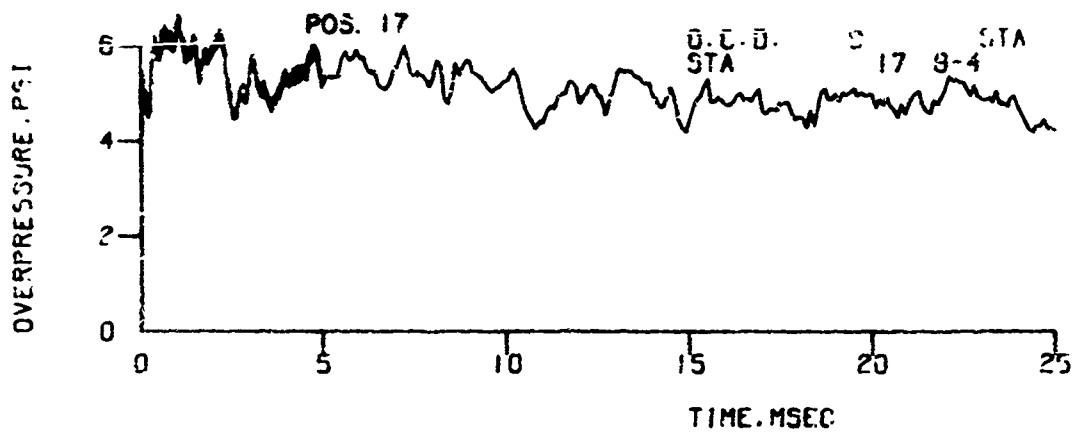


Figure A-2. Records from Side Wall - Model 37 (Continued)

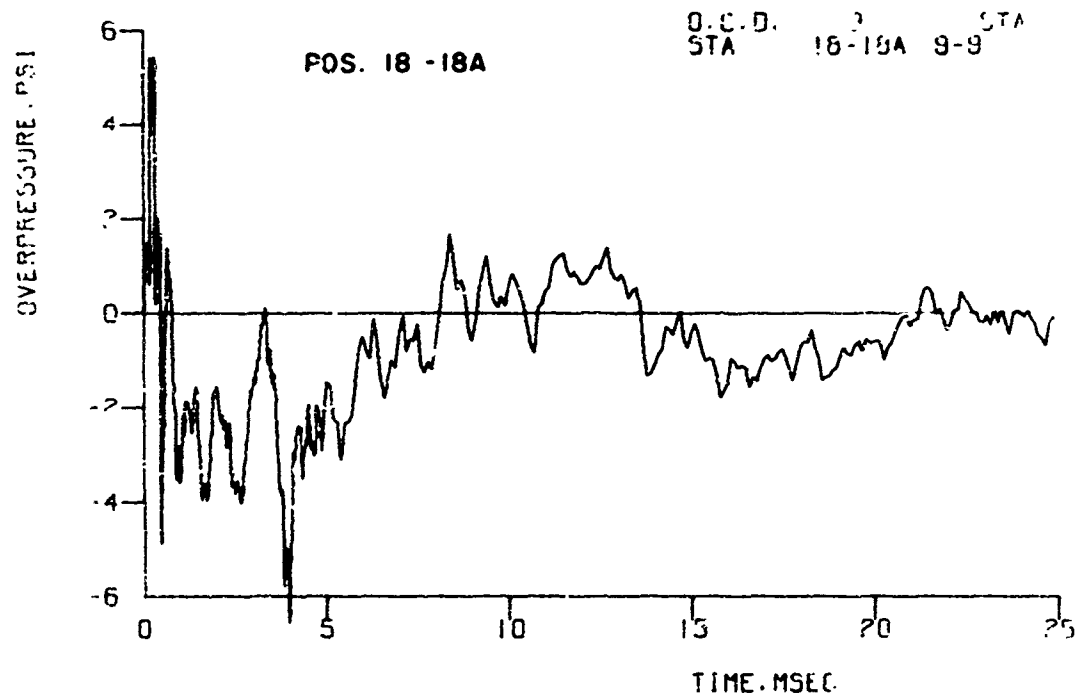
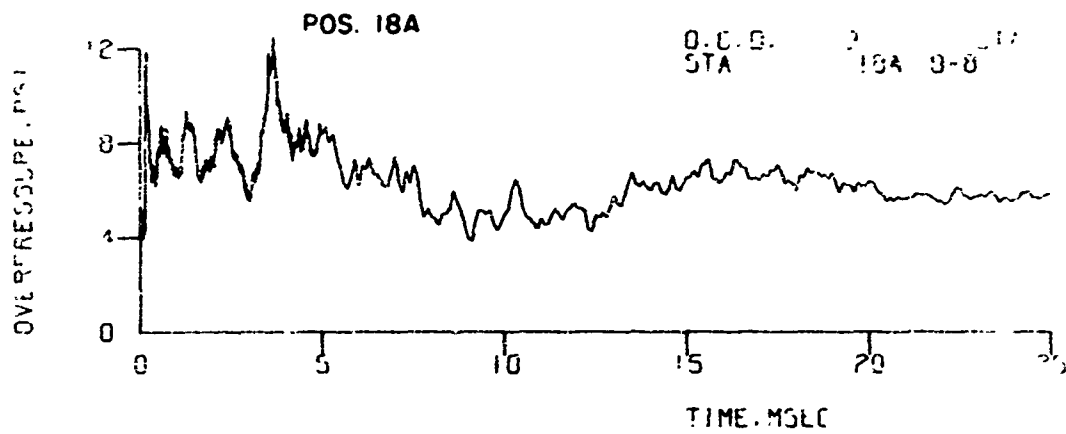
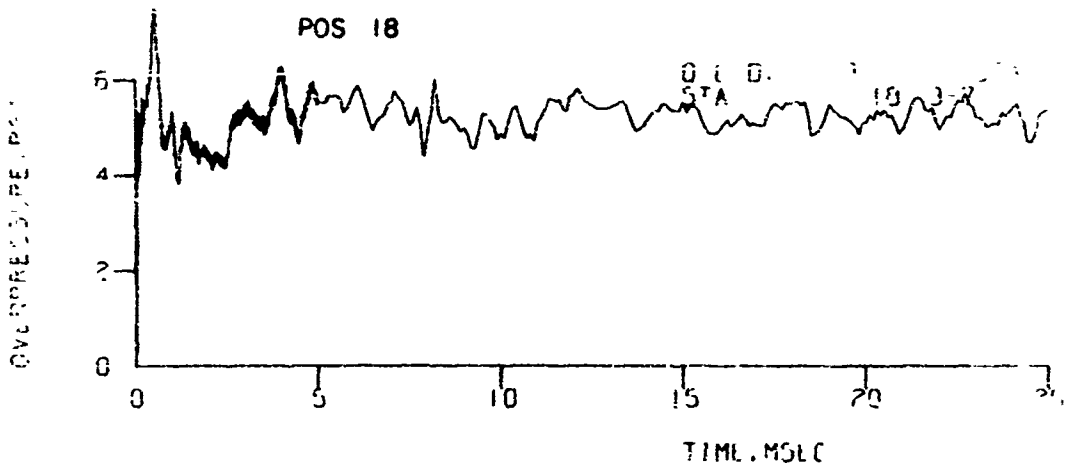


Figure A-2. Records from Side Wall - Model 37 (Continued)

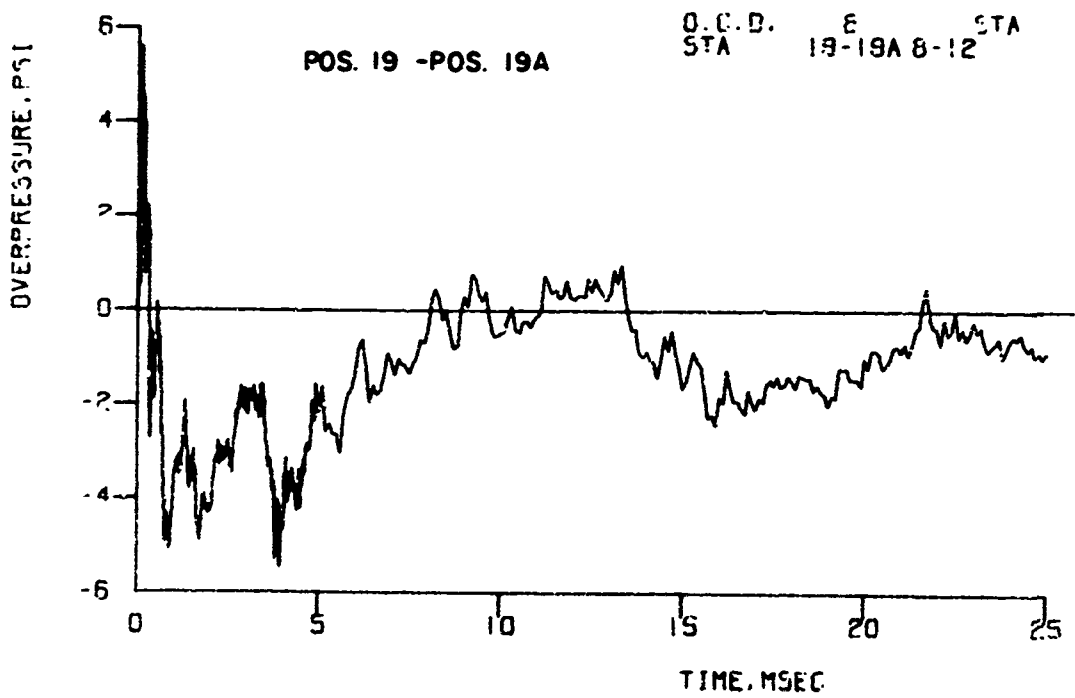
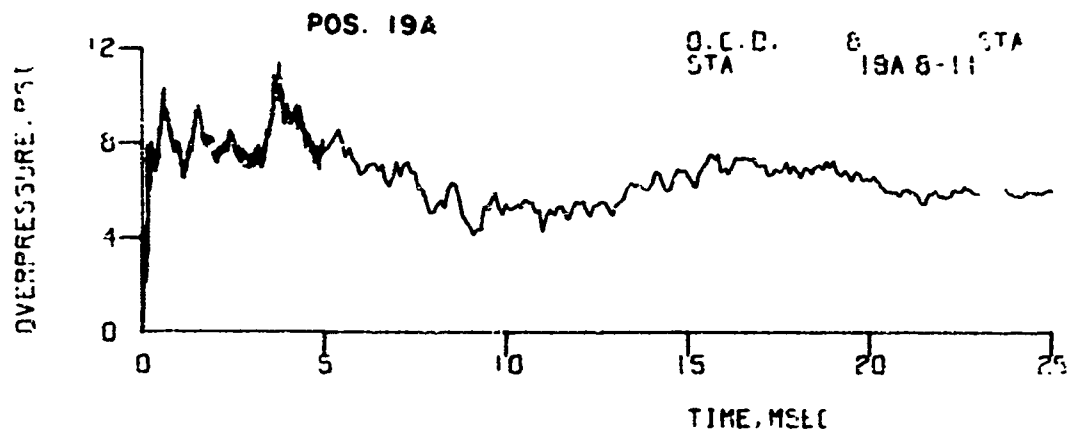
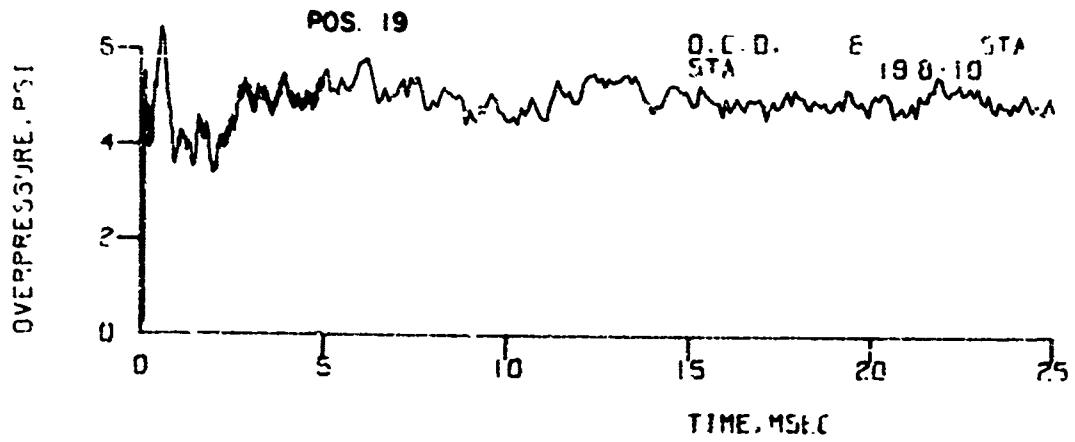


Figure A-2. Records from Side Wall - Model 3/ (Continued)

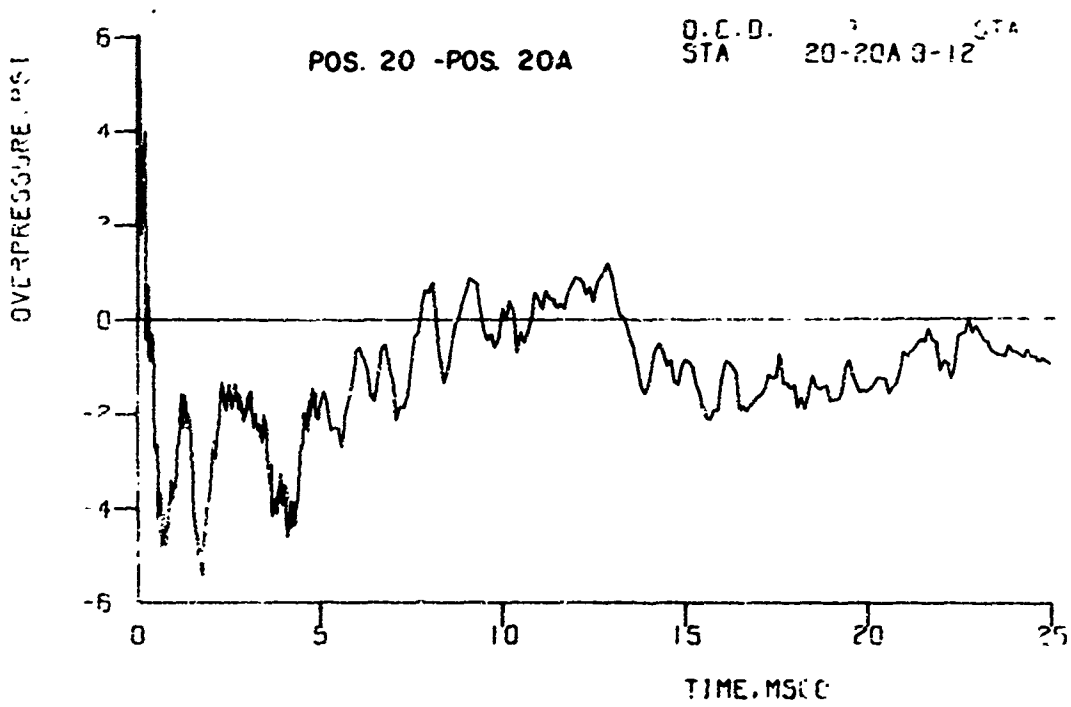
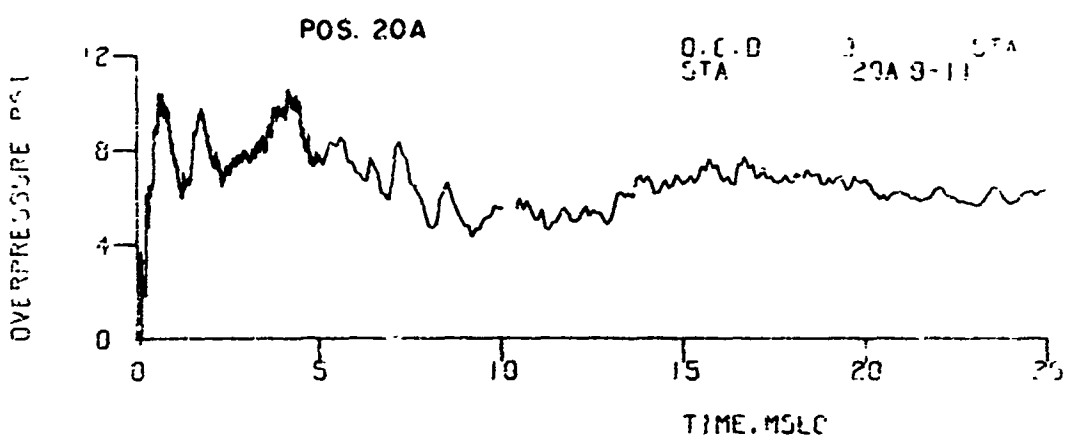
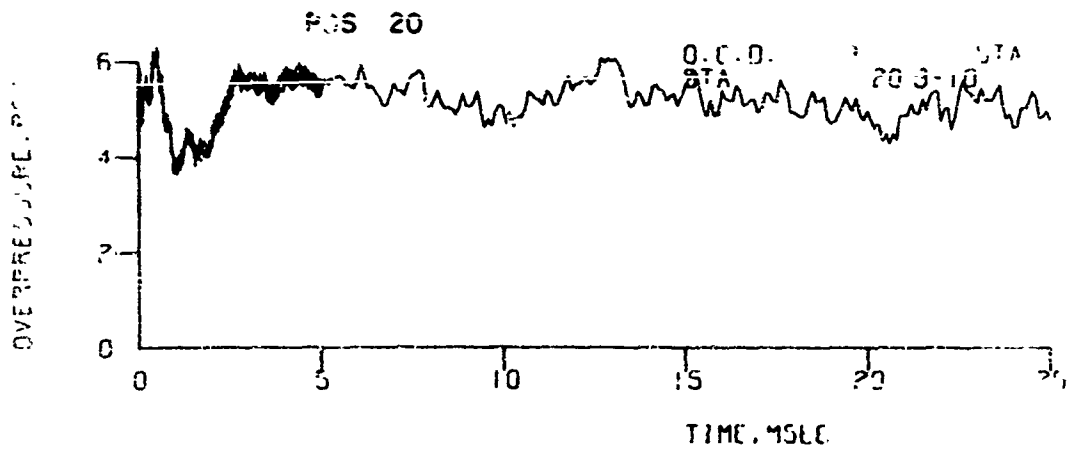


Figure A-2. Records from Side Wall - Model 37 (Continued)

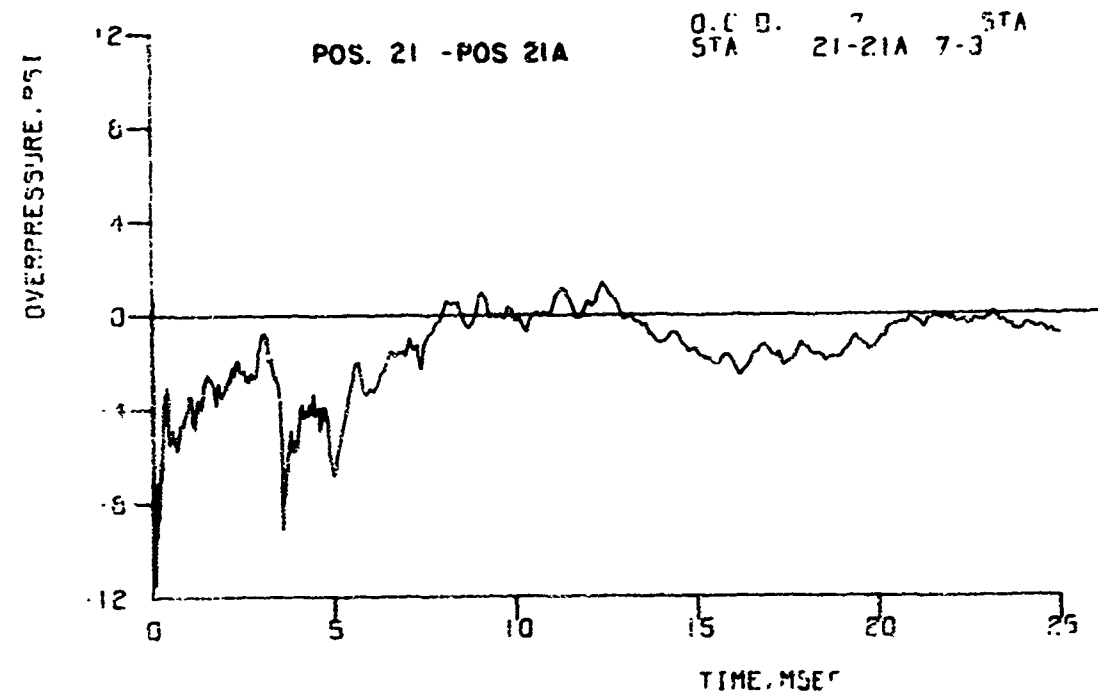
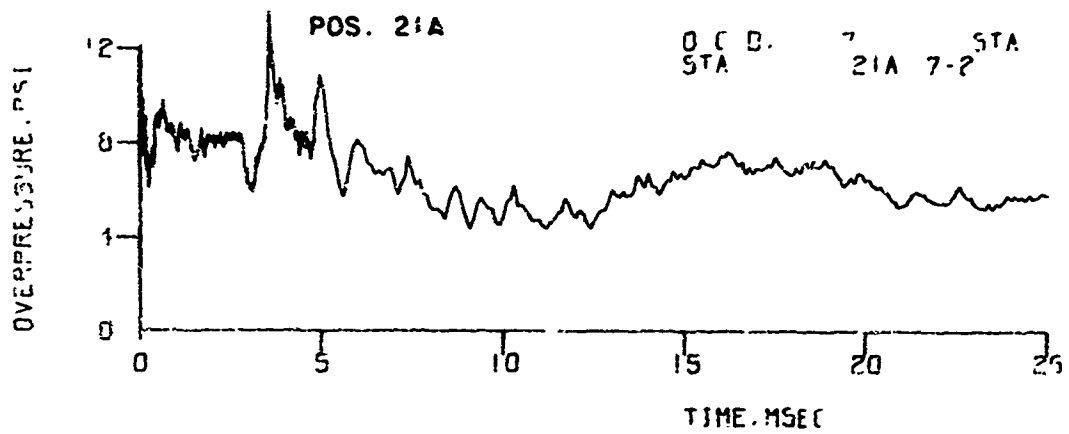
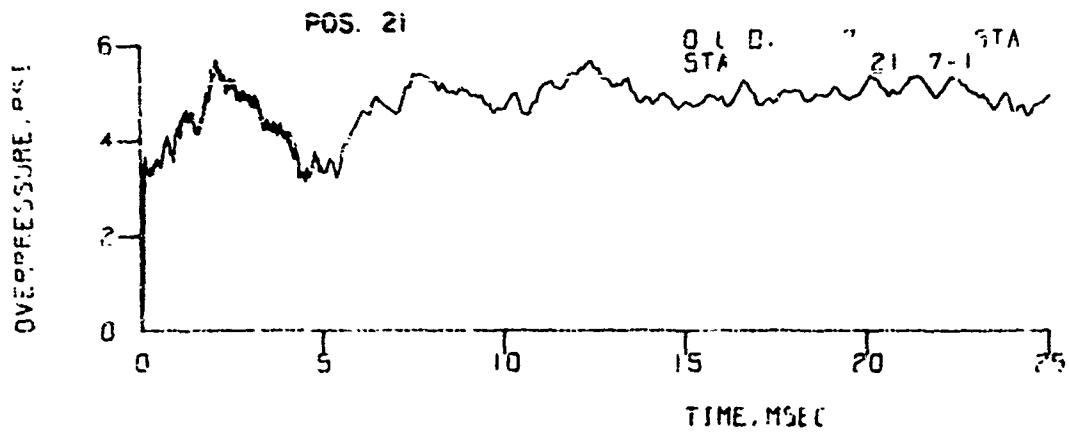


Figure A-3. Records from Rear Wall - Model 37

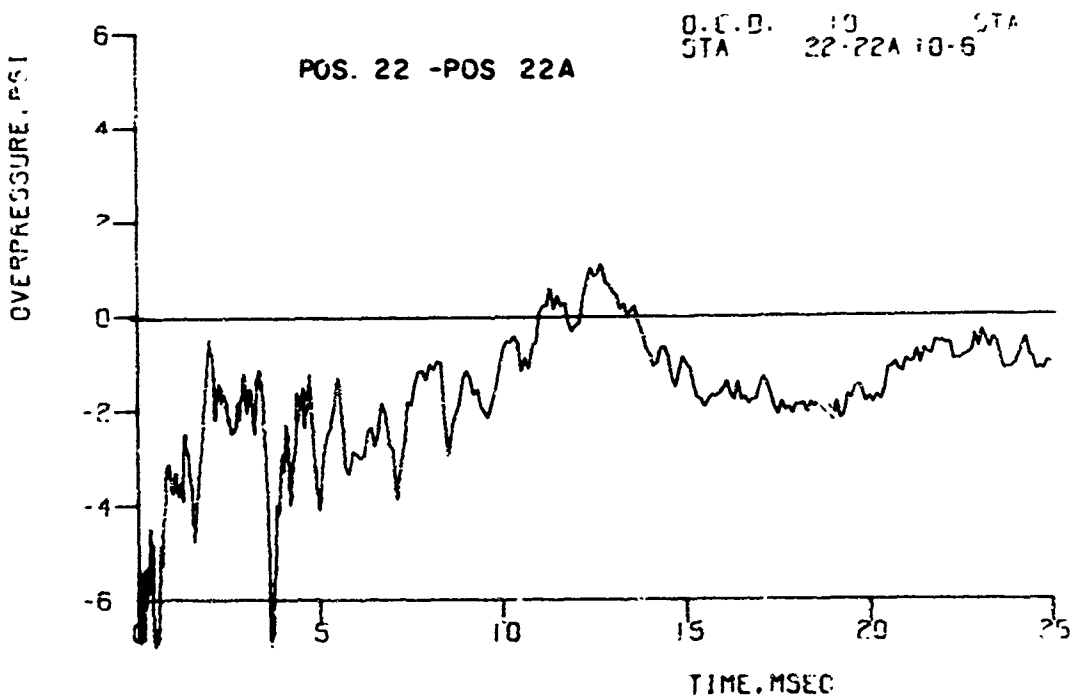
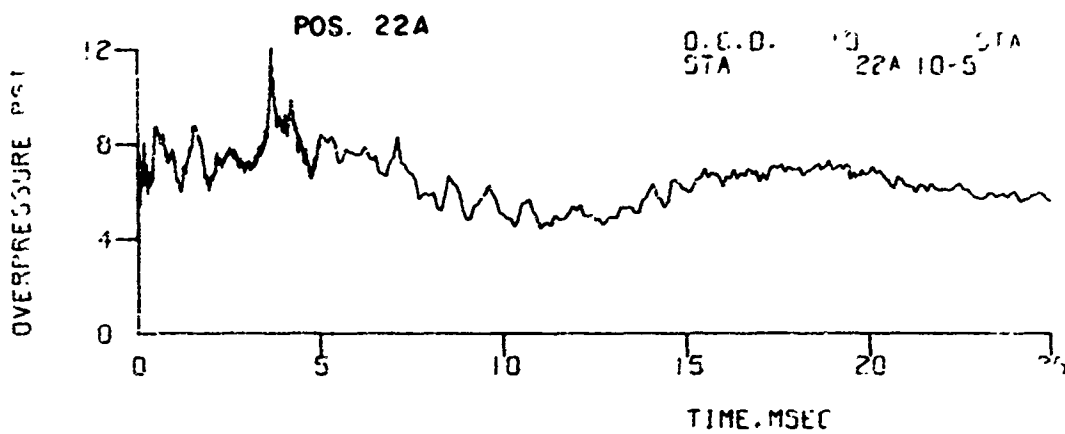
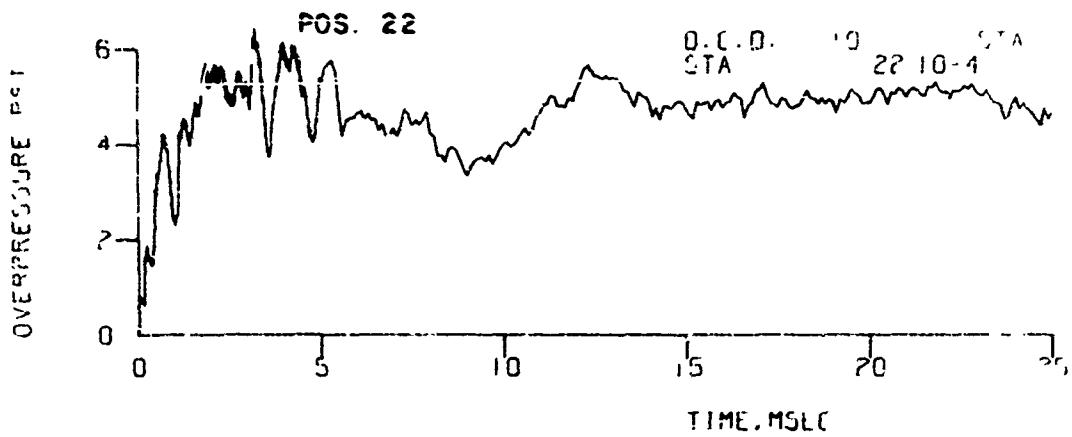


Figure A-3. Records from Rear Wall - Model 37 (Continued)

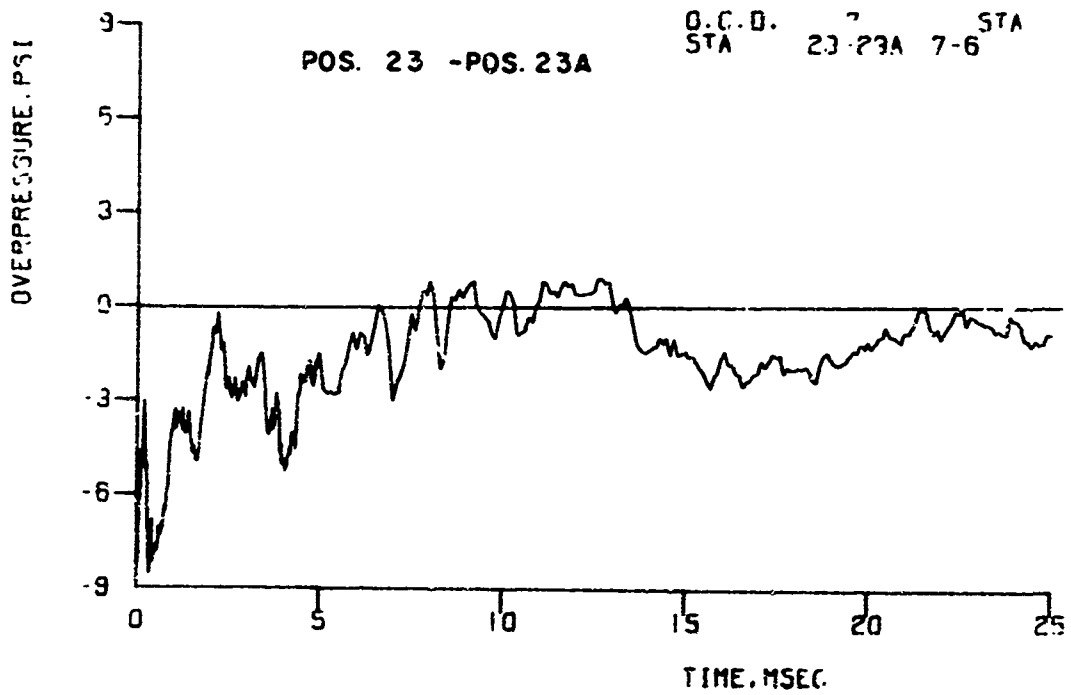
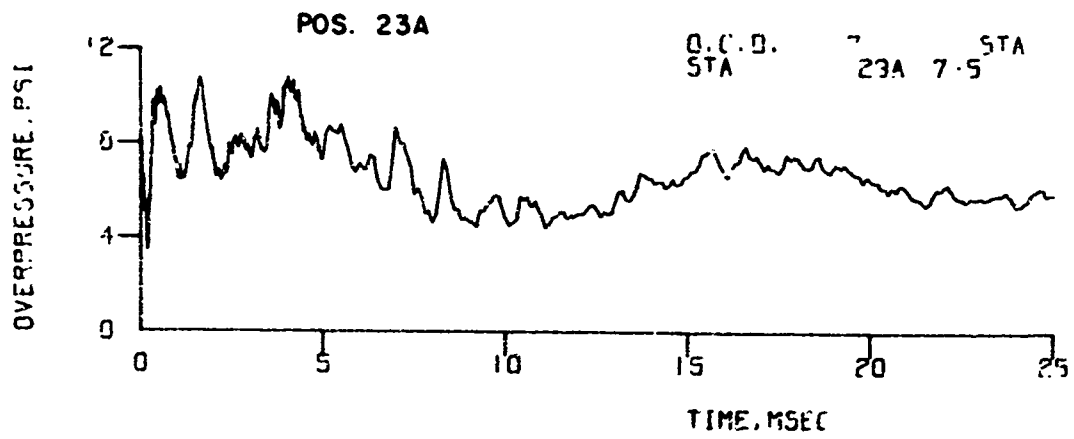
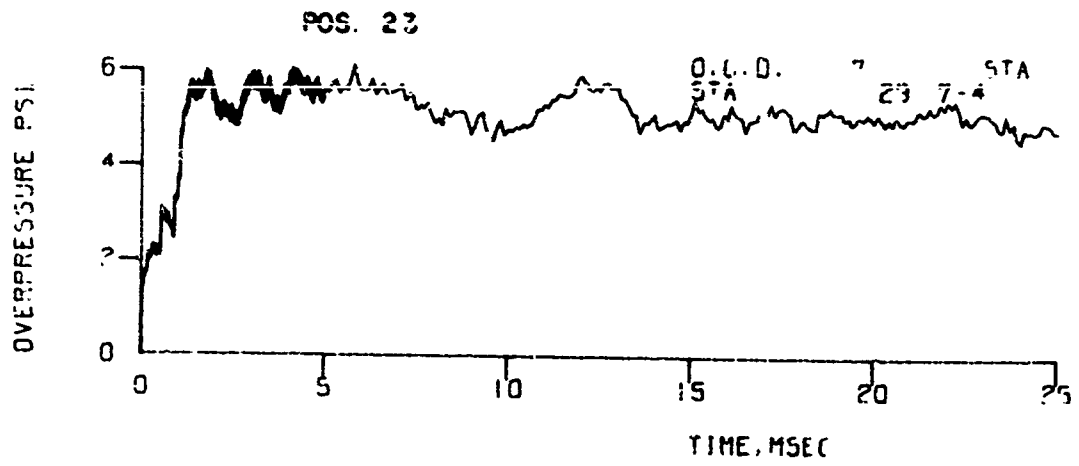


Figure A-3. Records from Rear Wall - Model 37 (Continued)

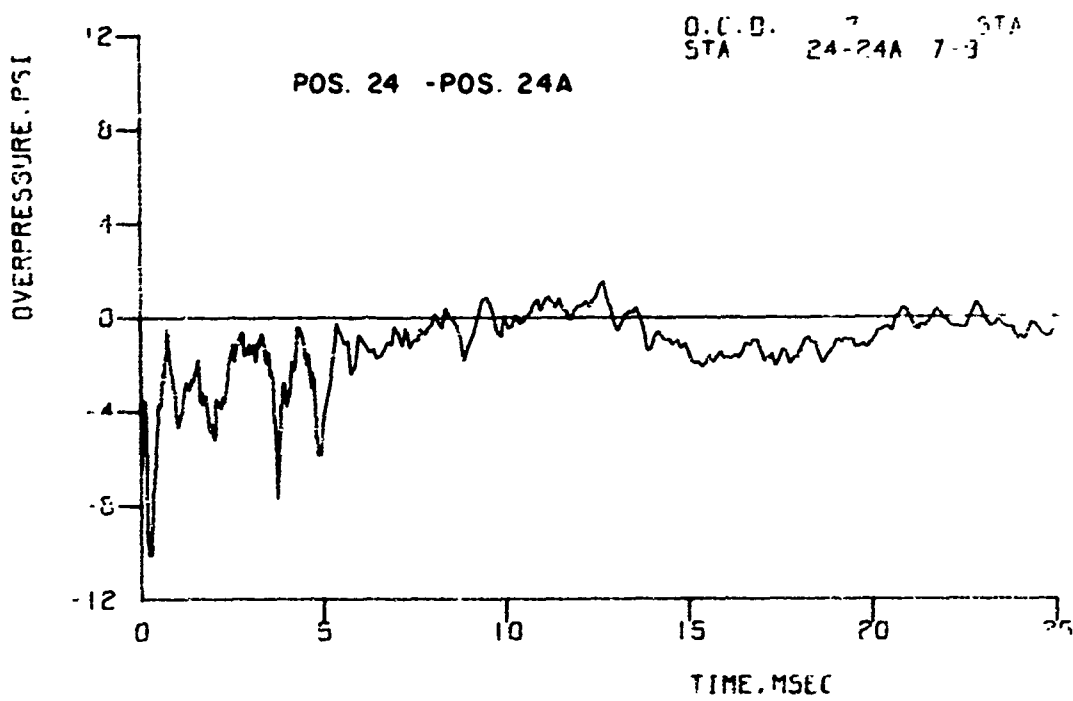
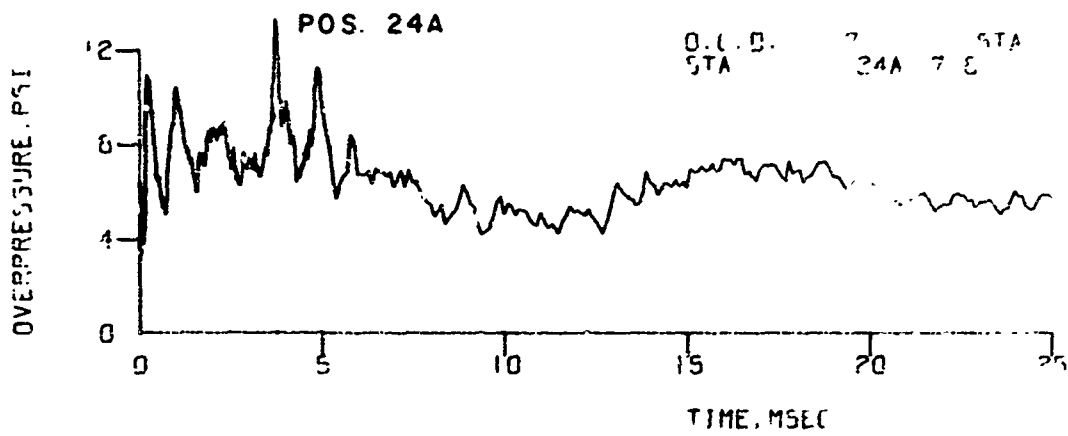
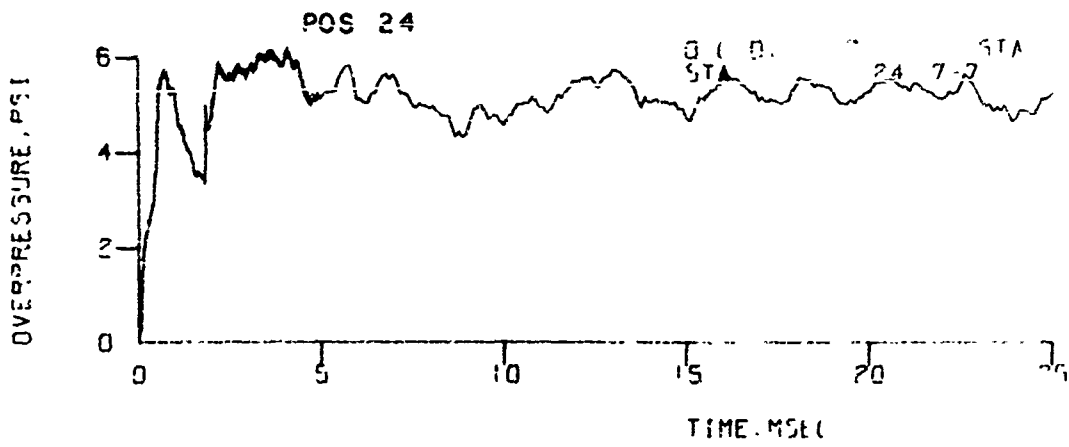


Figure A-3. Records from Rear Wall - Model 37 (Continued)

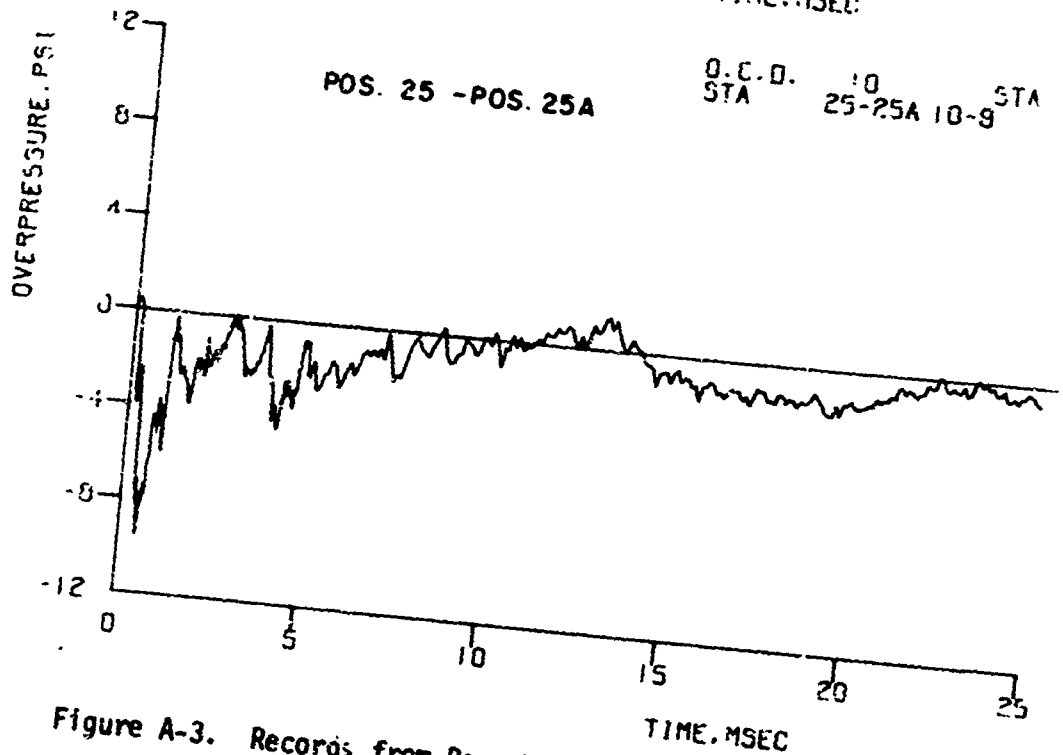
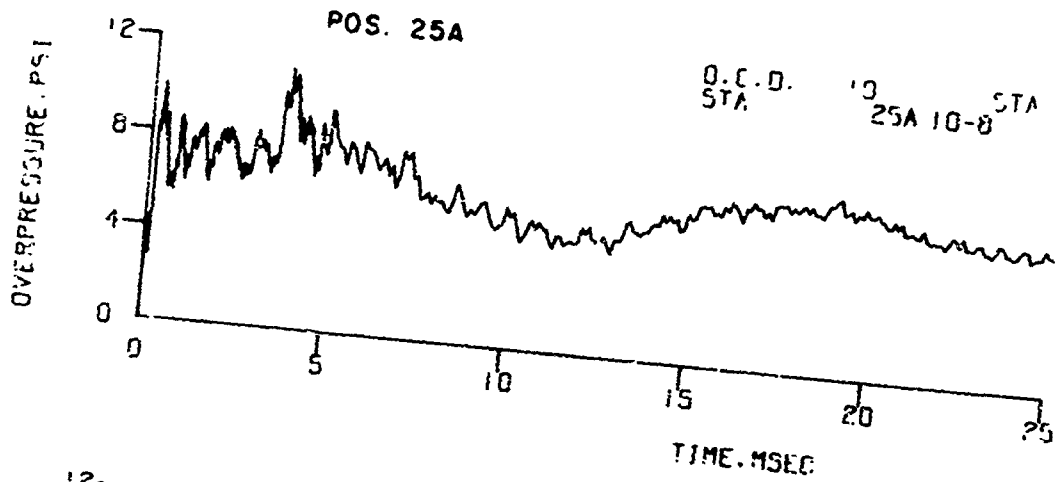
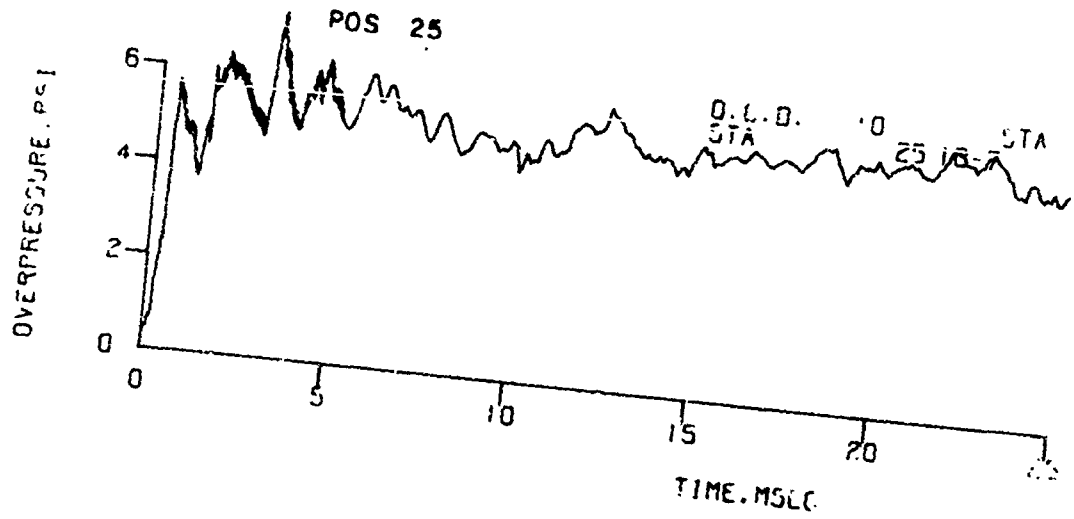


Figure A-3. Records from Rear Wall - Model 37 (Continued)

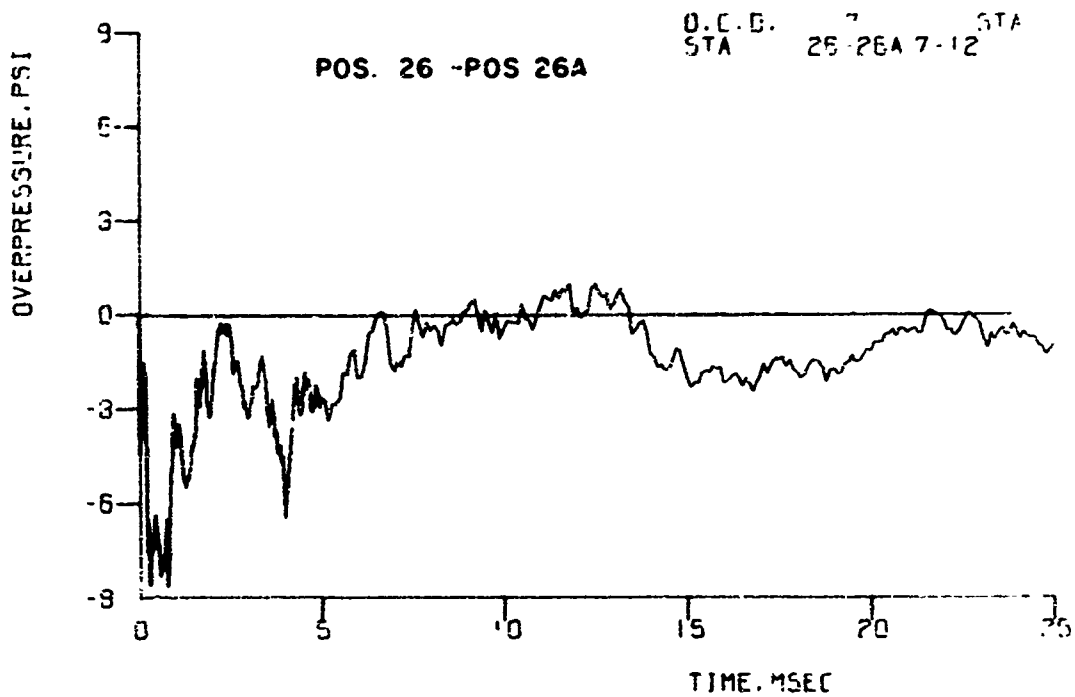
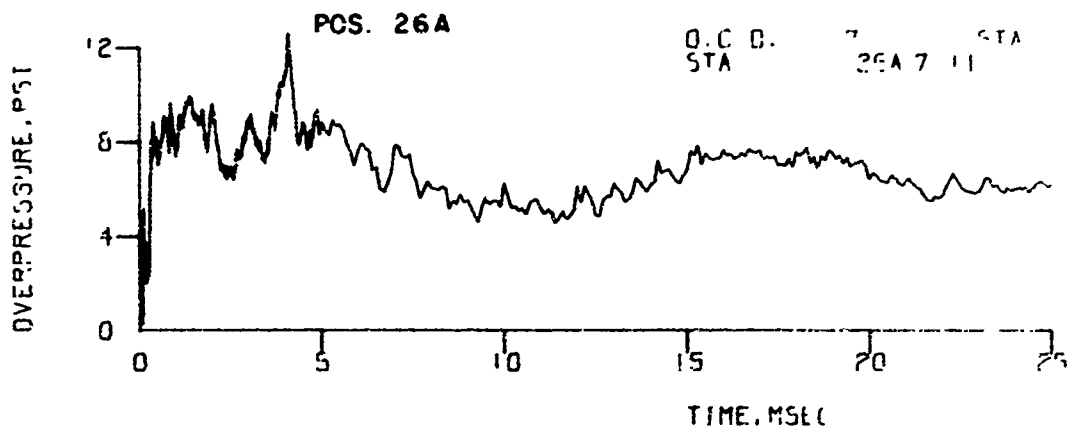
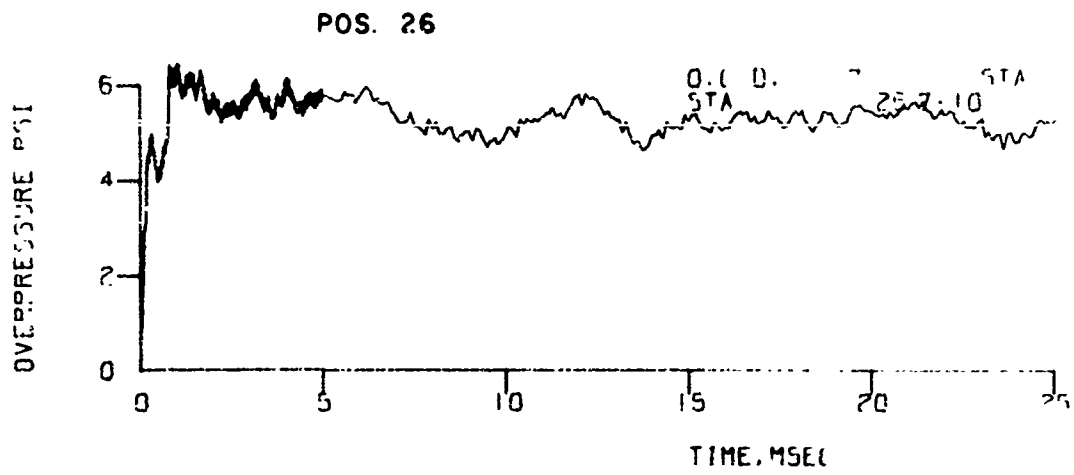


Figure A-3. Records from Rear Wall - Model 37 (Continued)

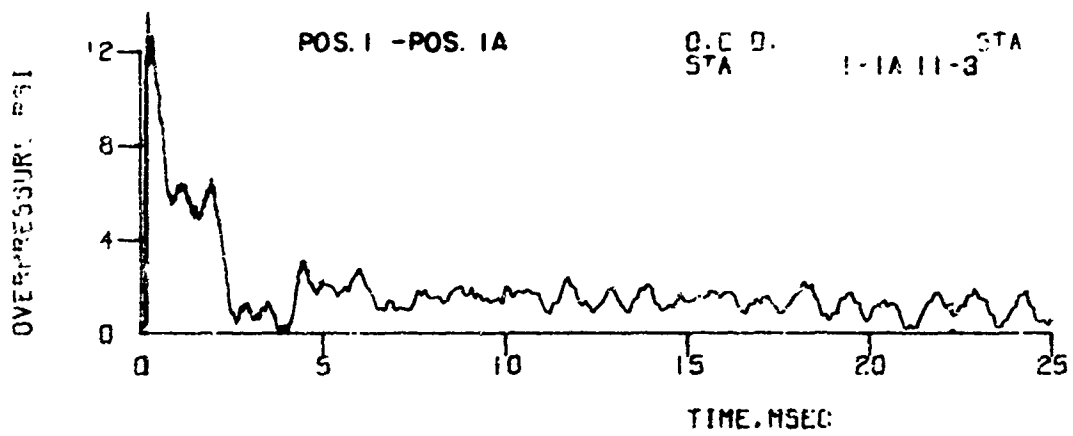
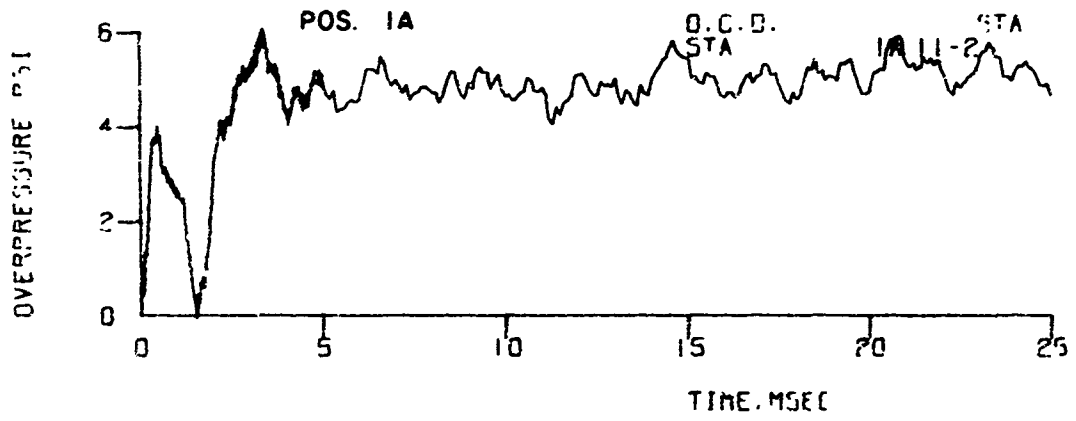
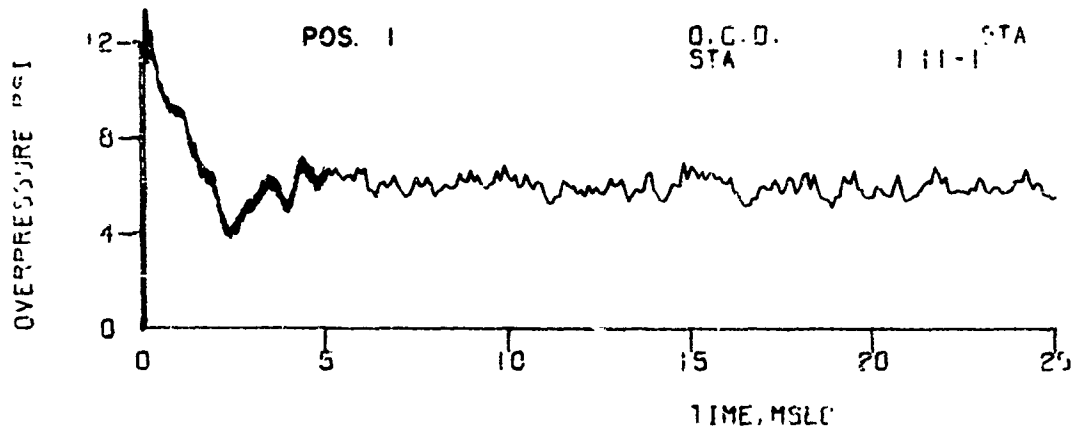


Figure A-4. Records from Model 39

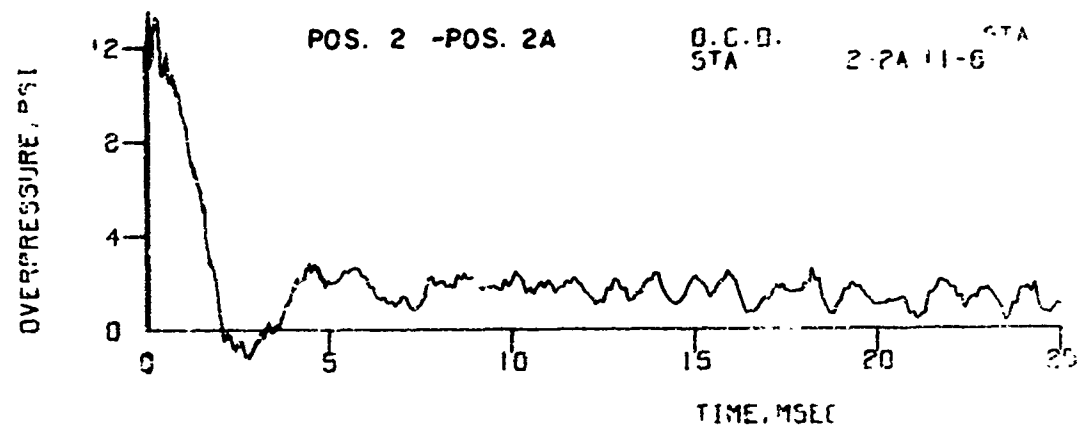
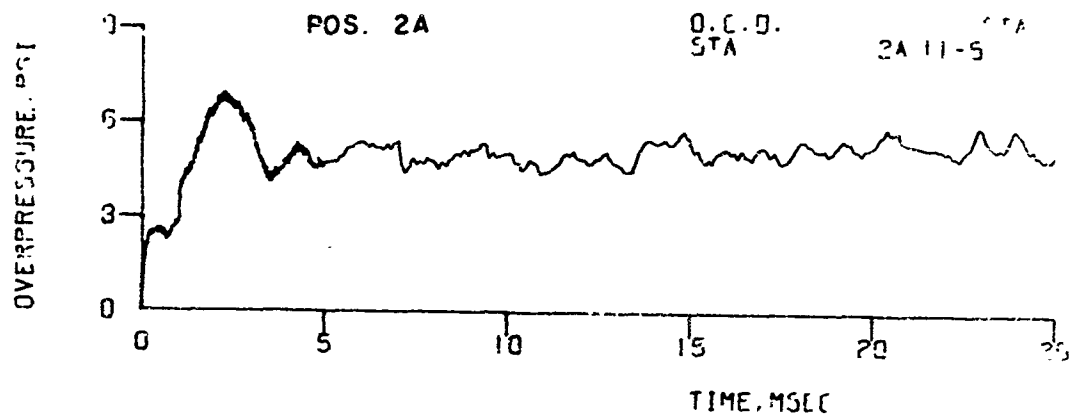
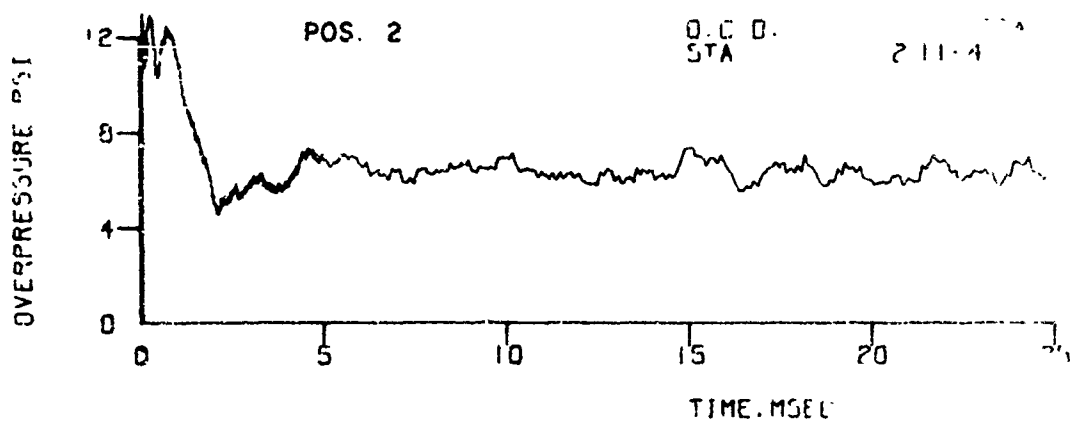


Figure A-4. Records from Model 38 (Continued)

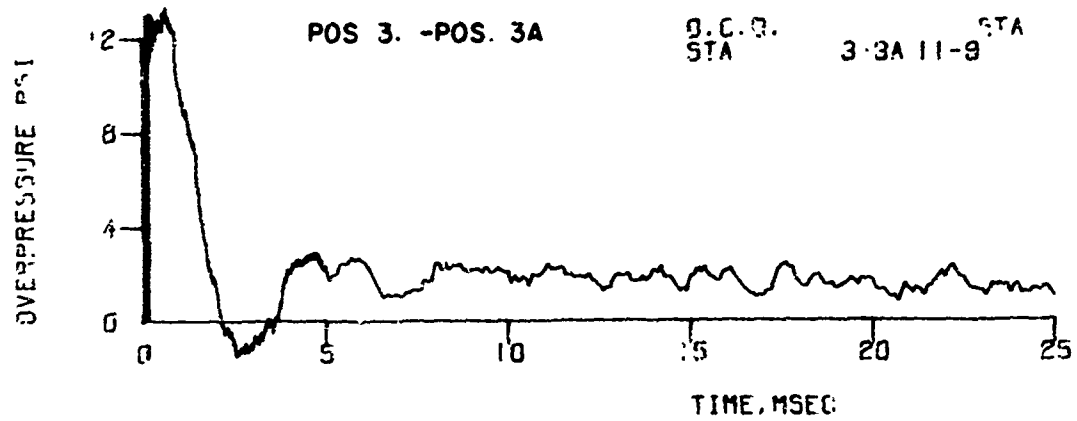
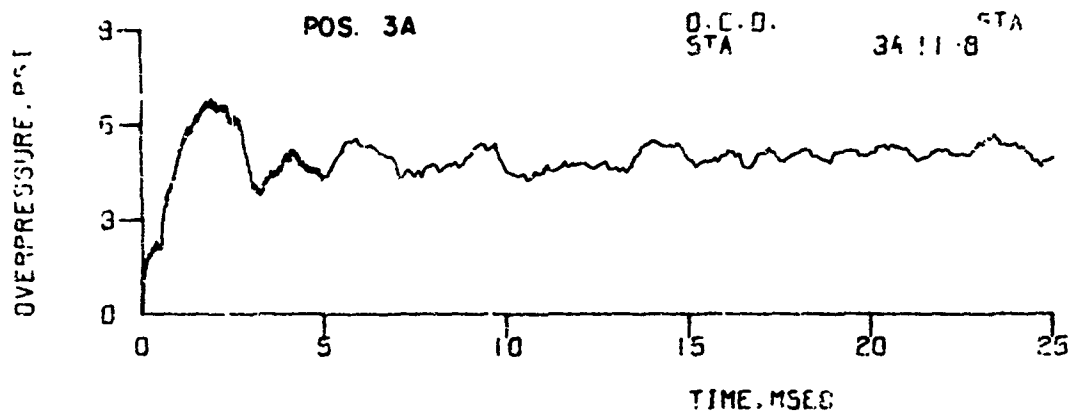
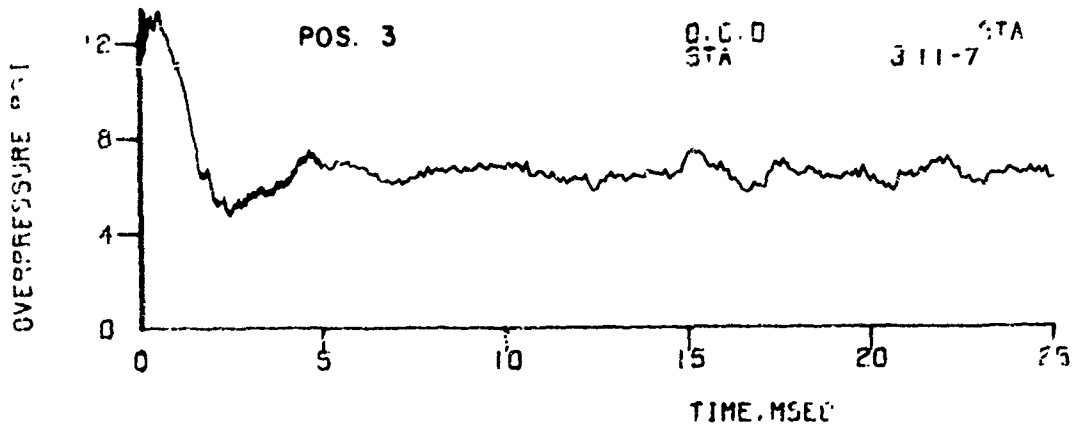


Figure A-4. Records from Model 38 (Continued)

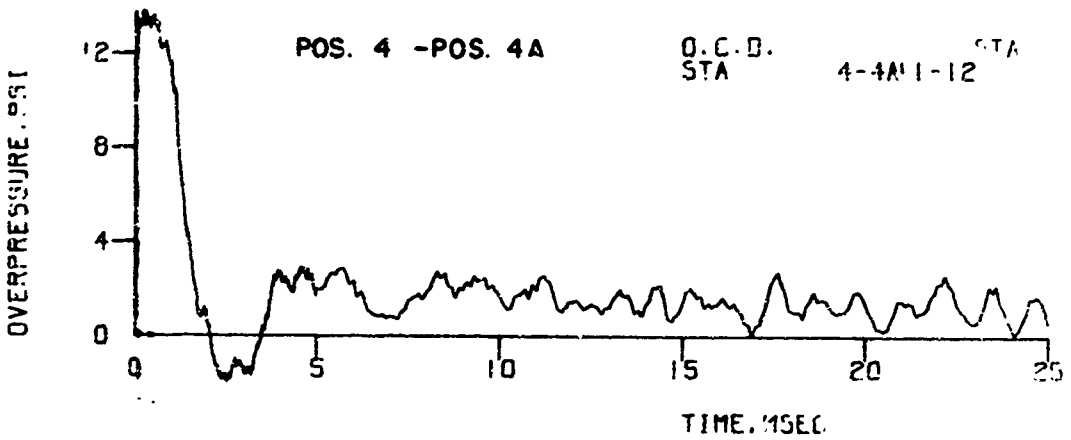
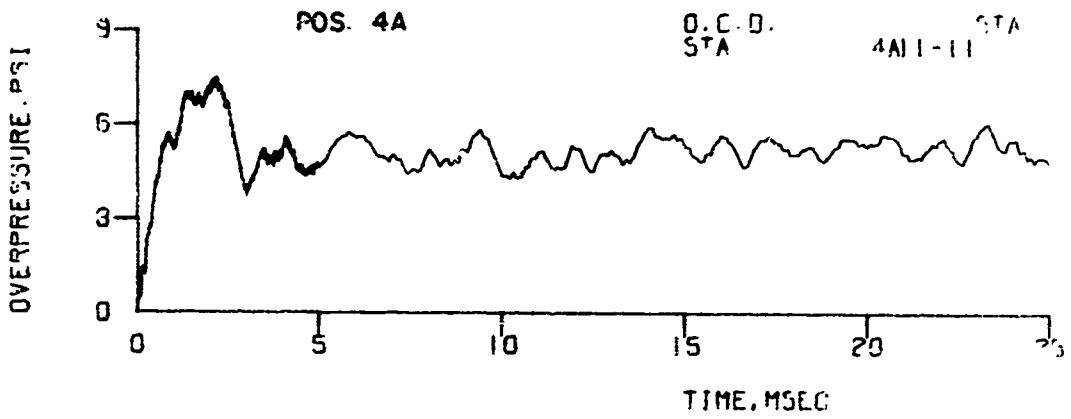
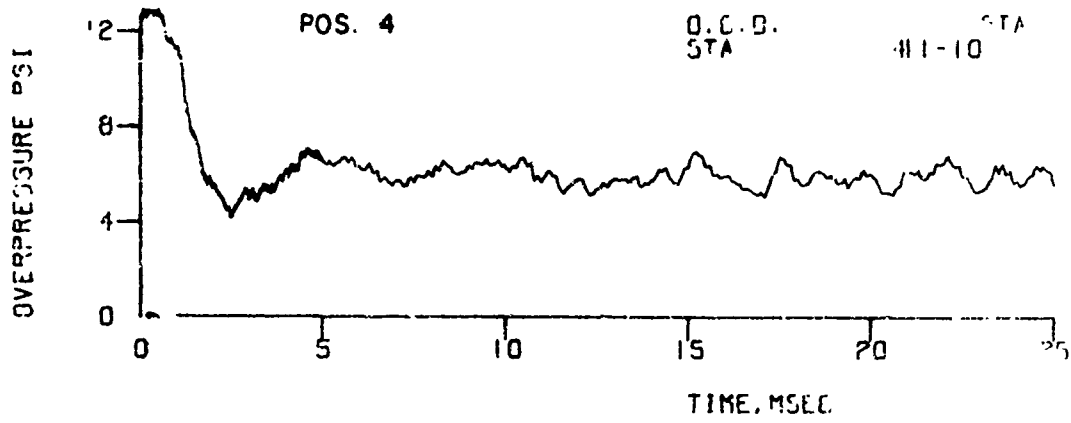


Figure A-4. Records from Model 38 (Continued)

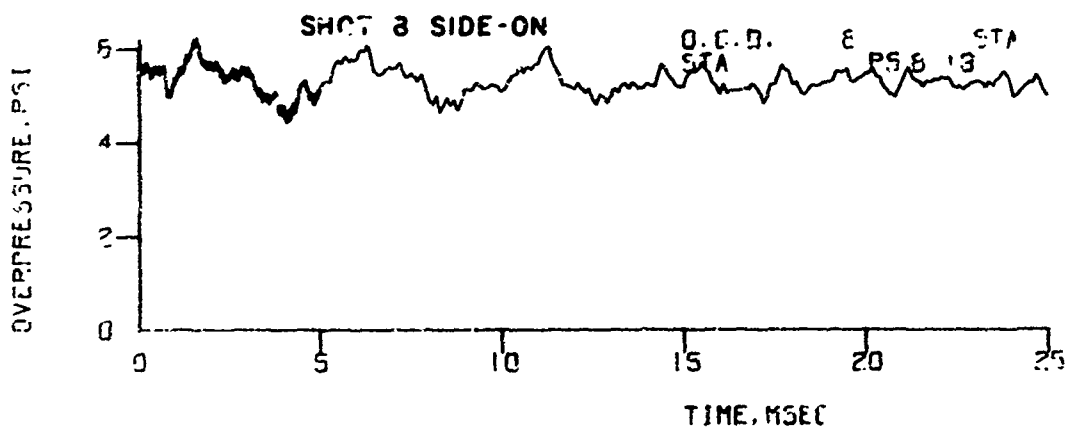
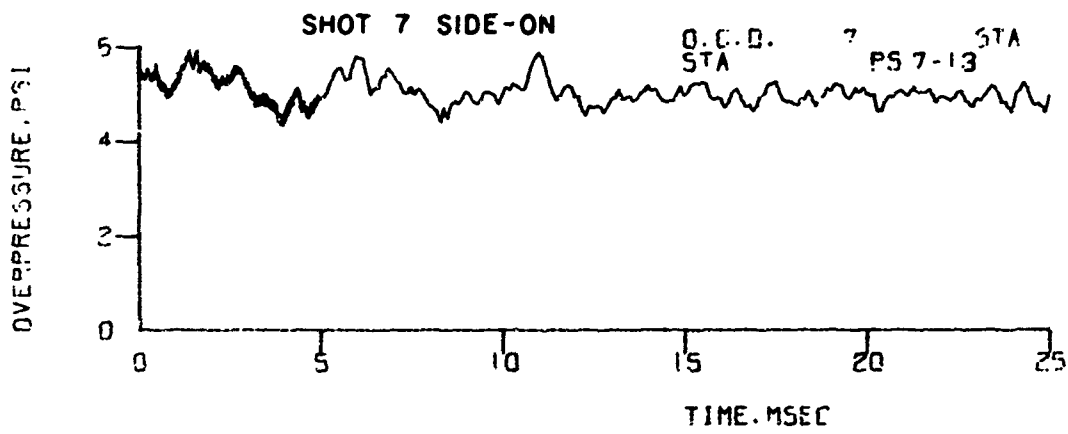
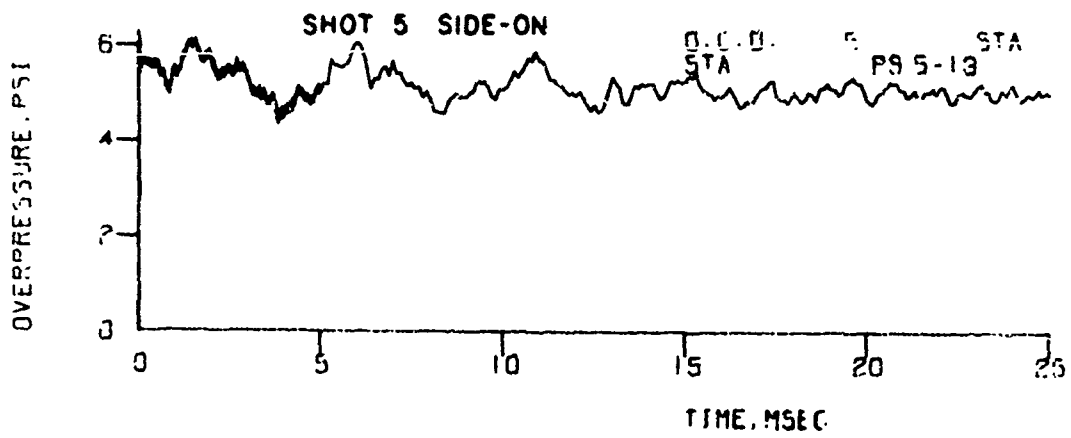


Figure A-5. Upstream Input Records

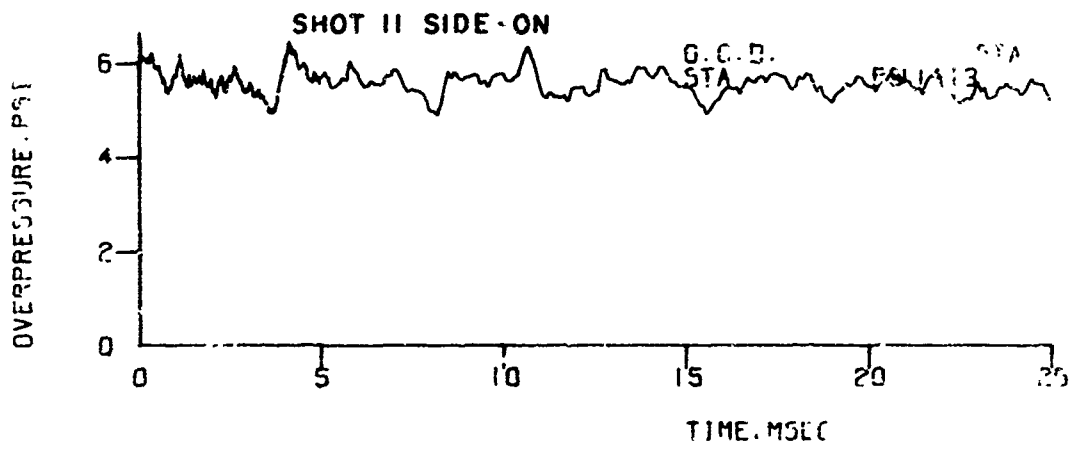
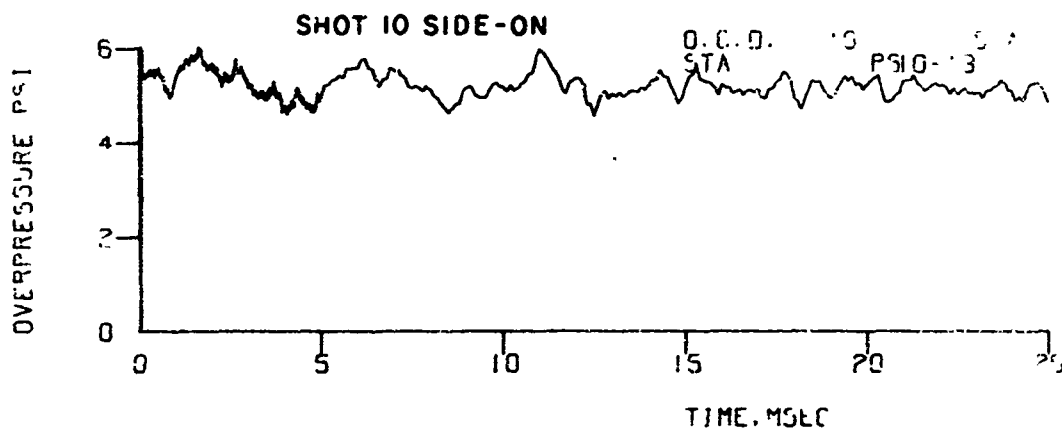
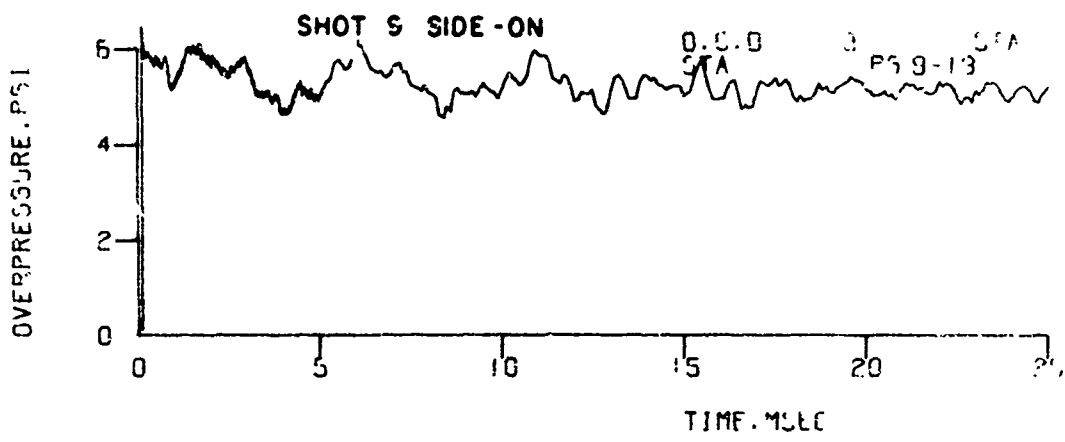


Figure A-5. Upstream Input Records (Continued)

APPENDIX B

COMPUTER PROGRAM

Preceding page blank

USE OF APPENDIX B

The computer program for predicting the outside front wall loading is written in Fortran IV with slight changes for the BRL computer.

The input data needed are listed at the end of the main program. The first line includes the width of the front (ft), the height of the front (ft), the two x-coordinates of the opening, and the two y-coordinates of the opening measured from the lower left corner of the outside of the front wall (looking at the front). The second line of input data includes the reflected shock front pressure (psig), the stagnation shock front pressure (psig), the shock front speed (ft/sec), the length of the side wall (ft), sound speed in reflected pressure region (ft/sec), and total duration of the input shock wave (sec). The third line specifies a new set of input conditions for the case in which there is no wall opening. The negative numbers (-10's) replace the coordinates for the opening. The last line has the same meaning as line two.

* TB 175 OCD LOADING OF STRUCTURES-COULTER 4911	1
* LIST(START)	A4
\$ MAXT(5)MINS.	3
\$ MAXO(8000)LINES	4
C OUTSIDE FRONT WALL - SINGLE OPENING	2
DIMENSION W(10),H(10),T(50),P(10,10,50),PT(10,10,50),FORCE(10,10,50)	5
1 FORMAT(6F12.5)	A5
2 FORMAT(1H1,1X,4HW-FT,7X,4HH-FT,7X,8HTIME-SEC,	6
13X,12HPRESSURE-PSI,5X,9HFORCE-LBS,5X,11HP-T PSI-SEC///)	7
3 FORMAT(3X,7HOPENING)	A7
4 FORMAT(2(F6.3,5X),F9.6,5X,F6.3,10X,F6.3,8X,F10.6)	8
510 READ(5,1)WD,HT,A1,A2,B1,B2	9
	10
IF(WD)500,500,520	A10
C PLACE BLANK CARD AT END JF DATA CARDS	AA10
520 READ(5,1) PREF,PSTAG,U,XL,CREF,TO	11
	12
WRITE(6,2)	13
C IF NO OPENING, PUNCH ALL NEGATIVE NUMBERS FOR A1,A2,B1,AND B2.	14
W(1)=0.0	A14
H(1)=0.0	AA14
IF(A1.LT.0.0)27,28	AAB14
27 AFRONT=WD*HT	A14
GOTO 33	15
28 AFRONT=WD*HT-(A2-A1)*(B2-B1)	A17
33 DELW=WD/20.	B17
DELA=0.01*HT*WD	18
	19
L=1	AA19
DO 300 I=1,10	A19
W(I)=W(L)+DELW	B19
DELW=WD/10.	C19
L=I	D19
M=1	20
H(1)=0.0	21
DELH=HT/20.	AA21
DO 300 J=1,10	A21
H(J)=H(M)+DELH	22
DELH=HT/10.	23
M=J	A23
T(1)=0	B23
PT(I,J,1)=0	C23
N=1	24
KK=1	25
DELT=(WD/U)/1000.	A25
DO 300 K=1,50	26
T(K)=T(N)+DELT	27
N=K	28
IF(A1.LT.0.0.AND.B1.LT.0.0)GOTO 100	29
IF(W(I).GT.A1.AND.W(I).LT.A2) 29,32	30
29 IF(H(J).GT.B1.AND.H(J).LT.B2) 31,32	31
100 IF(W(I).LE.WD/2.0.AND.W(I).LE.HT-H(J))GOTO 110	32
IF(W(I).LE.WD/2.0.AND.W(I).GT.HT-H(J))GOTO 120	33
IF(W(I).GT.WD/2.0.AND.WD-W(I).LE.HT-H(J))GOTO 130	34
IF(W(I).GT.WD/2.0.AND.WD-W(I).GT.HT-H(J))GOTO 120	
STOP	
110 C=W(I)	

Preceding page blank

	DR=AMINI(WD/2.,HT)	A34
	GOTO 50	35
120	D=HT-H(J)	36
	DR=AMINI(WD/2.,HT)	A36
	GOTO 50	37
130	D=WD-W(I)	38
	DR=AMINI(WD/2.,HT)	A38
	GOTO 50	39
32	IF(W(I).LE.A1.AND.H(J).LT.B1) GOTO 5	40
	IF(W(I).LE.A1.AND.H(J).LE.B2)GOTO 6	41
	IF(W(I).LE.A1.AND.H(J).LE.HT)GOTO 7	42
	IF(W(I).LE.A2.AND.H(J).LE.B1) GOTO 8	43
	IF(W(I).LE.A2.AND.H(J).LE.HT)GOTO 9	44
	IF(W(I).LE.WD.AND.H(J).LT.B1)GOTO 11	45
	IF(W(I).LE.WD.AND.H(J).LT.B2)GOTO 12	46
	IF(W(I).LE.WD.AND.H(J).LT.HT)GOTO 13	47
	STOP	48
5	D1=SQRT((B1-H(J))**2+(A1-W(I))**2)	49
	D=AMINI(W(I),D1)	50
	DR=A1	A50
	GOTO 50	51
6	D=AMINI(W(I),A1-W(I),HT-H(J))	52
	DR=A1/2.	A52
	GOTO 50	53
7	D1=SQRT((H(J)-B2)**2+(A1-W(I))**2)	54
	D=AMINI(W(I),D1,HT-H(J))	55
	DR=AMINI(A1,HT-B2)	A55
	GOTO 50	56
8	D=AMINI(W(I),B1-H(J),WD-W(I))	57
	DR=B1	A57
	GOTO 50	58
9	D=AMINI(W(I),HT-H(J),H(J)-B2,WD-W(I))	59
	DR=(HT-B2)/2.	A59
	GOTO 50	60
11	D1=SQRT((B1-H(J))**2+(W(I)-A2)**2)	61
	D=AMINI(B1-H(J),W(I),D1)	62
	DR=WD-A2	A62
	GOTO 50	63
12	D=AMINI(WD-W(I),W(I)-A2,HT-H(J))	64
	DR=(WD-A2)/2.	A64
	GOTO 50	65
13	D1=SQRT((H(J)-B2)**2+(W(I)-A2)**2)	66
	D=AMINI(D1,WD-W(I),HT-H(J),W(I))	67
	DR=AMINI(WD-A2,HT-B2)	A67
50	TR=D/CREF	68
	DR=AMINI(WD/2.,HT)	A68
	TC=2.5*DR/CREF	69
	IF(T(K).LE.TR)GOTO 10	70
	IF(T(K).GT. TR .AND.T(K).LE.TC)GOTO 20	71
	IF(TC.LT.T(K).AND.T(K).LE.T0)GOTO 30	72
10	P(I,J,K)=PREF	73
	GOTO 200	74
20	IF(T(K).GT.TR.AND.T(K).LT.(2.5*TR))GOTO 22	75
21	P(I,J,K)=PREF*EXP(-.36*(T(K)-2.5*TR)/(TC-2.5*TR))*70	A75
	GOTO 200	AA75
22	P(I,J,K)=PREF*EXP(-0.2320*(T(K)-TR)/TR)	B75
	GOTO 200	76
30	P(I,J,K)=PSTAG	77
200	DELPT=P(I,J,K)*DELT	78
	PT(I,J,K)=PT(I,J,KK)+DELPT	79

```

KK=K
FORCE(I,J,K)=P(I,J,K)*DELA
FORCE(I,J,K)=FORCE(I,J,K)*144.
GOTO 210
31 DELT=(XL/U)/10.
IF(K.EQ.50)GOTO 530
GOTO 300
530 WRITE(6,3)
GOTO 300
210 WRITE(6,4)W(I),H(J),T(K),P(I,J,K),FORCE(I,J,K),PT(I,J,K)
IF(K.EQ.50) WRITE(6,2)
IF(T(K).LE.(3.*WD/2.)/U)310,330
310 DELT=(WD/U)/23.
GOTO 300
330 DELT=(WD/U)/6.5
300 CONTINUE
WRITE(6,55)
320 DO 350 N=1,50
MM=0
FTOTAL=0
PTOTAL=0
DO 350 L=1,10
DO 350 M=1,10
IF(P(L,M,N).GT.0.)MM=MM+1
FTOTAL=FTOTAL+FORCE(L,M,N)
PTOTAL=PTOTAL+P(L,M,N)
IF(L.EQ.10.AND.M.EQ.10) 340,350
340 IF(MM.EQ.0)GOTO 345
PAV=PTOTAL/FLOAT(MM)
GOTO 344
345 PAV=0.
344 WRITE(6,66)T(N),FTOTAL,PAV
350 CONTINUE
GOTO 510
55 FORMAT(1H1,20X,14HFORCE ON FRONT ///,5X
18HYIME-SEC,10X,15HTOTAL FORCE-LB, 5X,20HAVERAGE PRESSURE-PSI//)
66 FORMAT(3X,F10.6,10X,F9.1,15X,F9.2)
500 END
* LIST
* DATA
1.667 1.167 0.5 1.167 0.0 .542
12.2 5.96 1292. 2.5 1232. =5
.698 .348 -10. -10. -10. -10.
11.4 5.58 1284. .25 122f. .015

```

```

A79
80
A80
81
A81
82
A82
882
83
84
A84
AA84
AAB84
AAC84
884
85
86
A86
87
A87
88
89
A89
90
A90
91
9A91
A91
AC91
AA91
92
93
94
95
96
97
98
99
100

```

APPENDIX C

HIGH SPEED PHOTOGRAPHS - MODEL 39

Preceding page blank

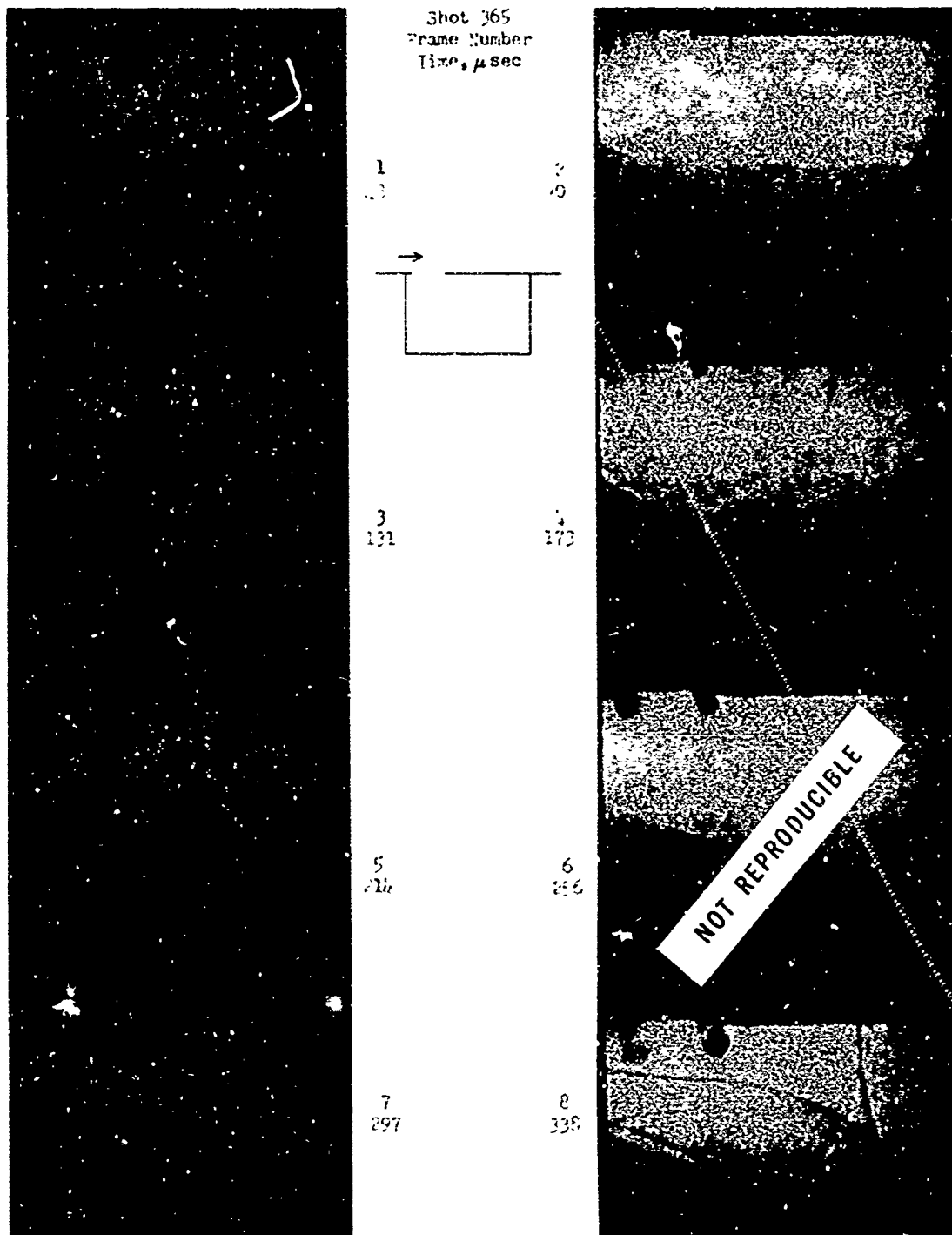


Figure C-1. Shadowgraphs of a Shock Wave Entering Model of Basement Shelter - $P_s = 5$ psi

Preceding page blank

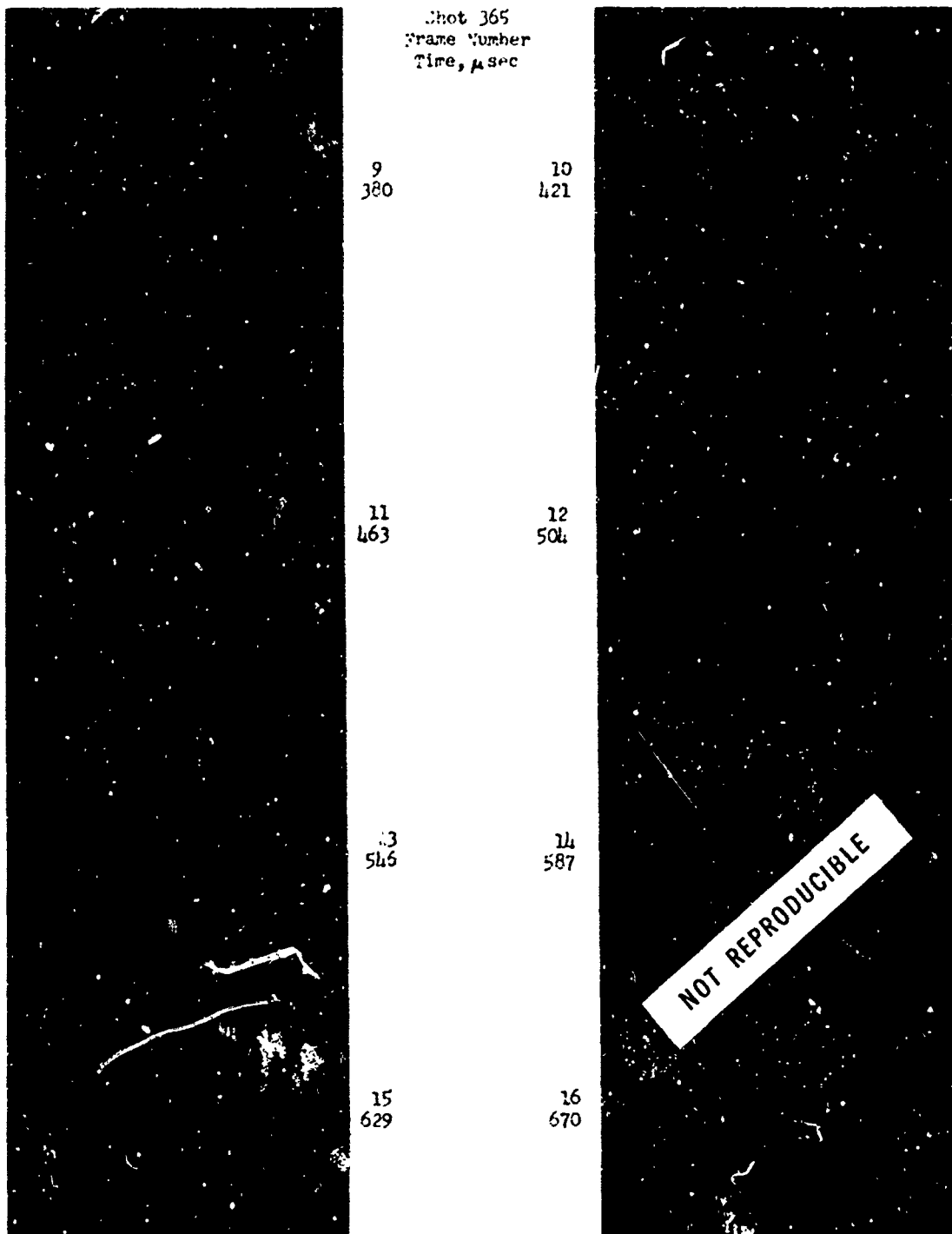


Figure C-1. Shadowgraphs of a Shock Wave Entering Model of Basement Shelter - $P_s = 5$ psi (Continued)

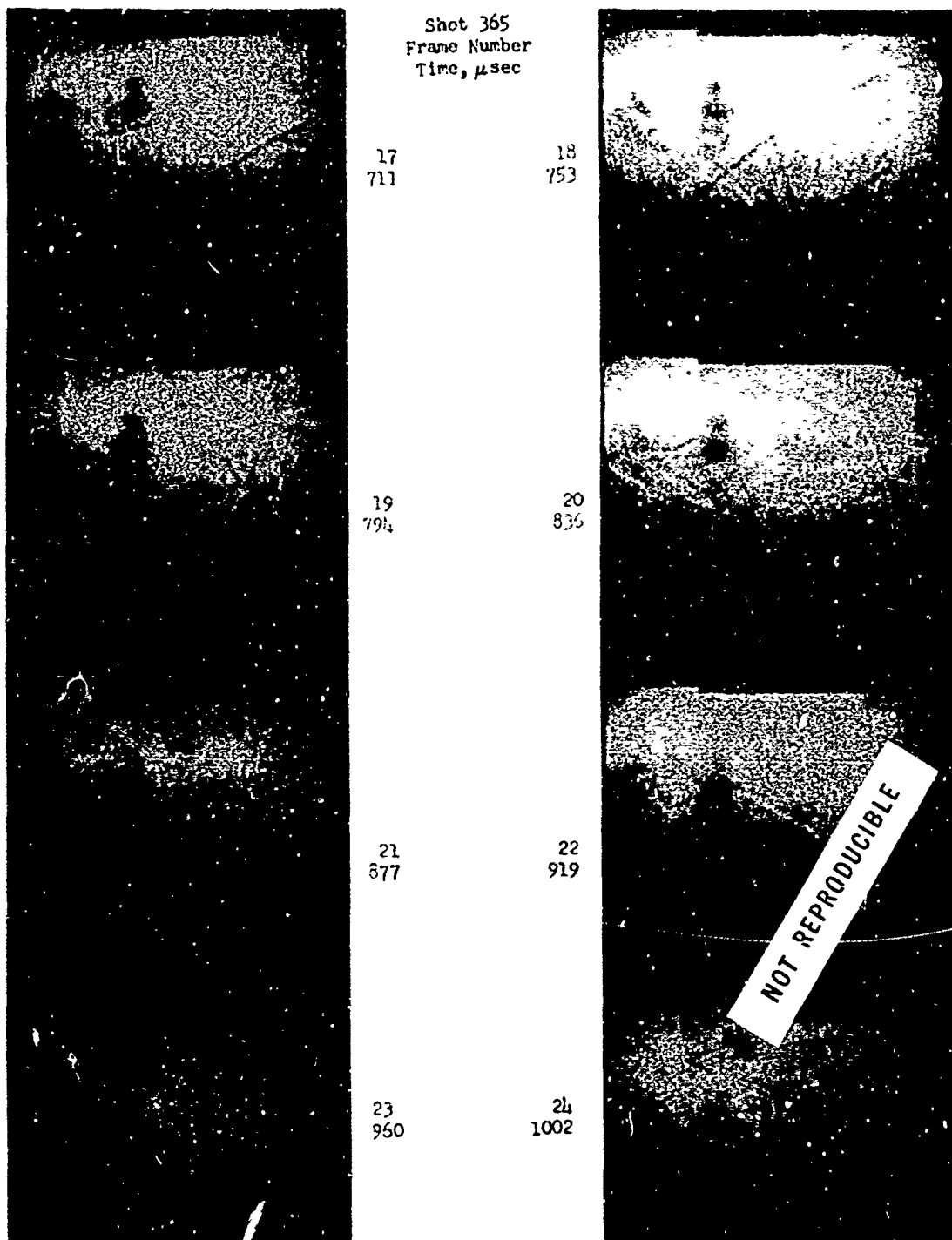


Figure C-1. Shadowgraphs of a Shock Wave Entering Model of Basement Shelter - P_s 5 psi (Continued)

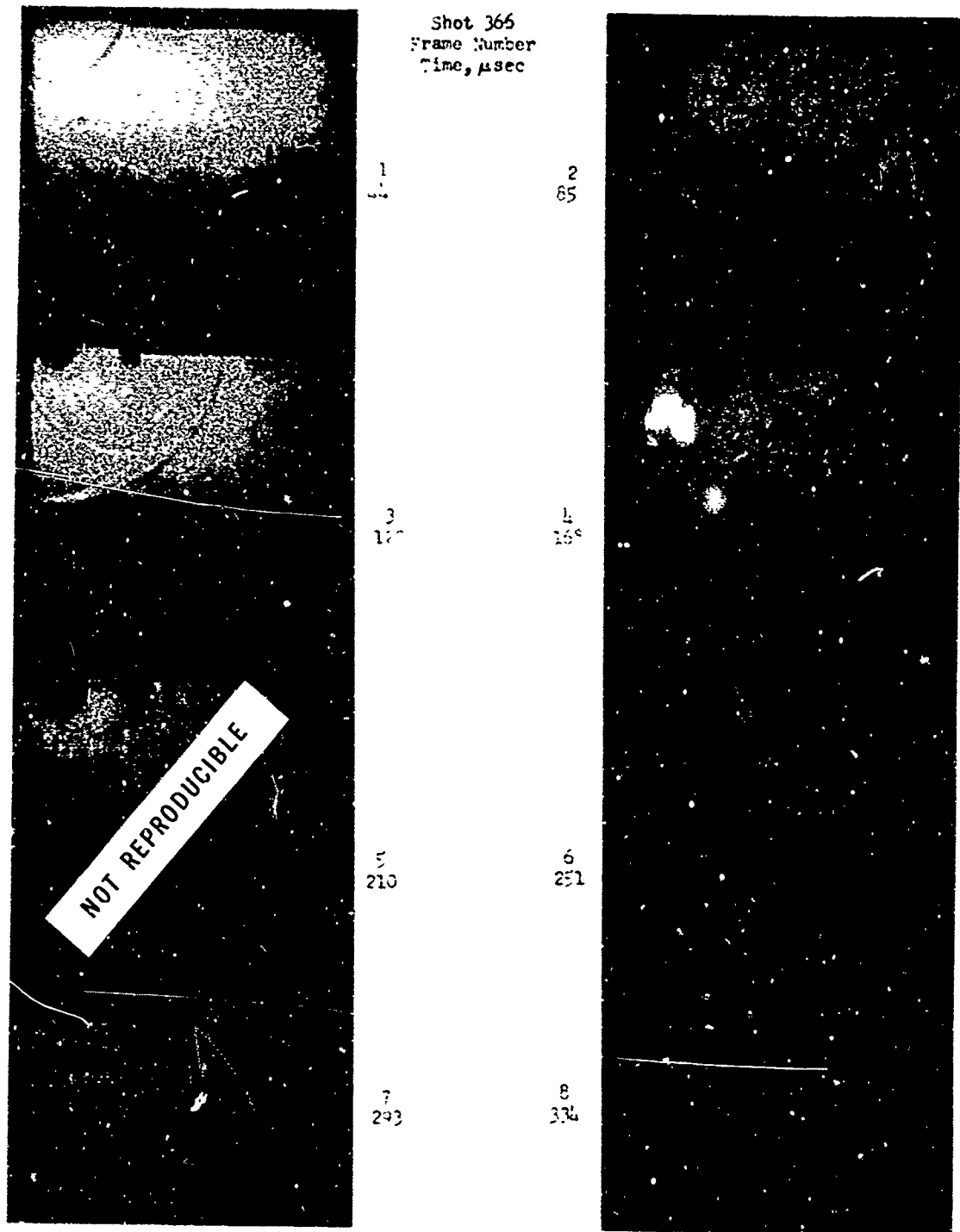


Figure C-2. Shadowgraph of a Shock Wave Entering Model of Basement Shelter - $P_s = 10$ psi

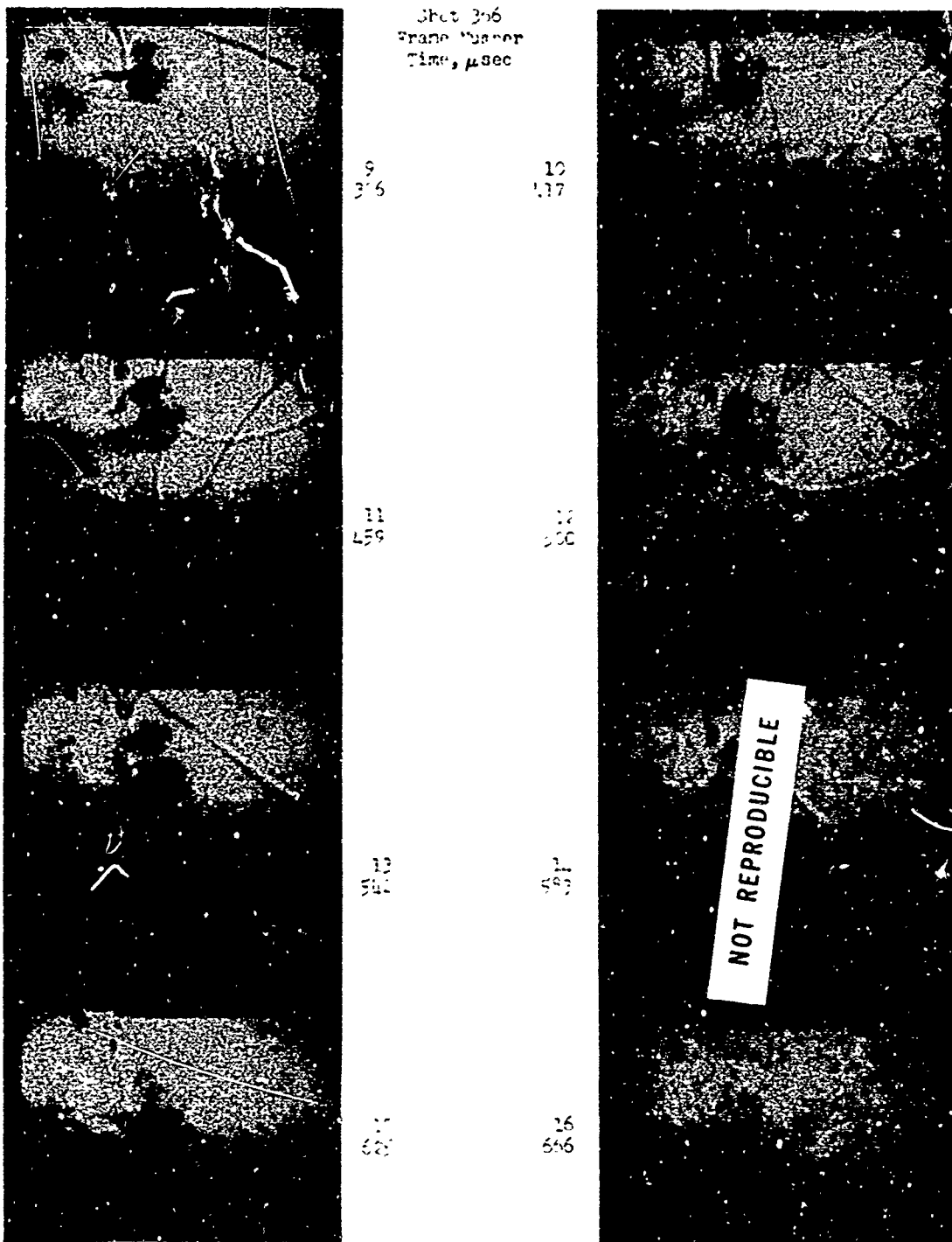


Figure C-2. Shadowgraph of a Shock Wave Entering Model of Basement Shelter - $P_s = 10$ psi (Continued)

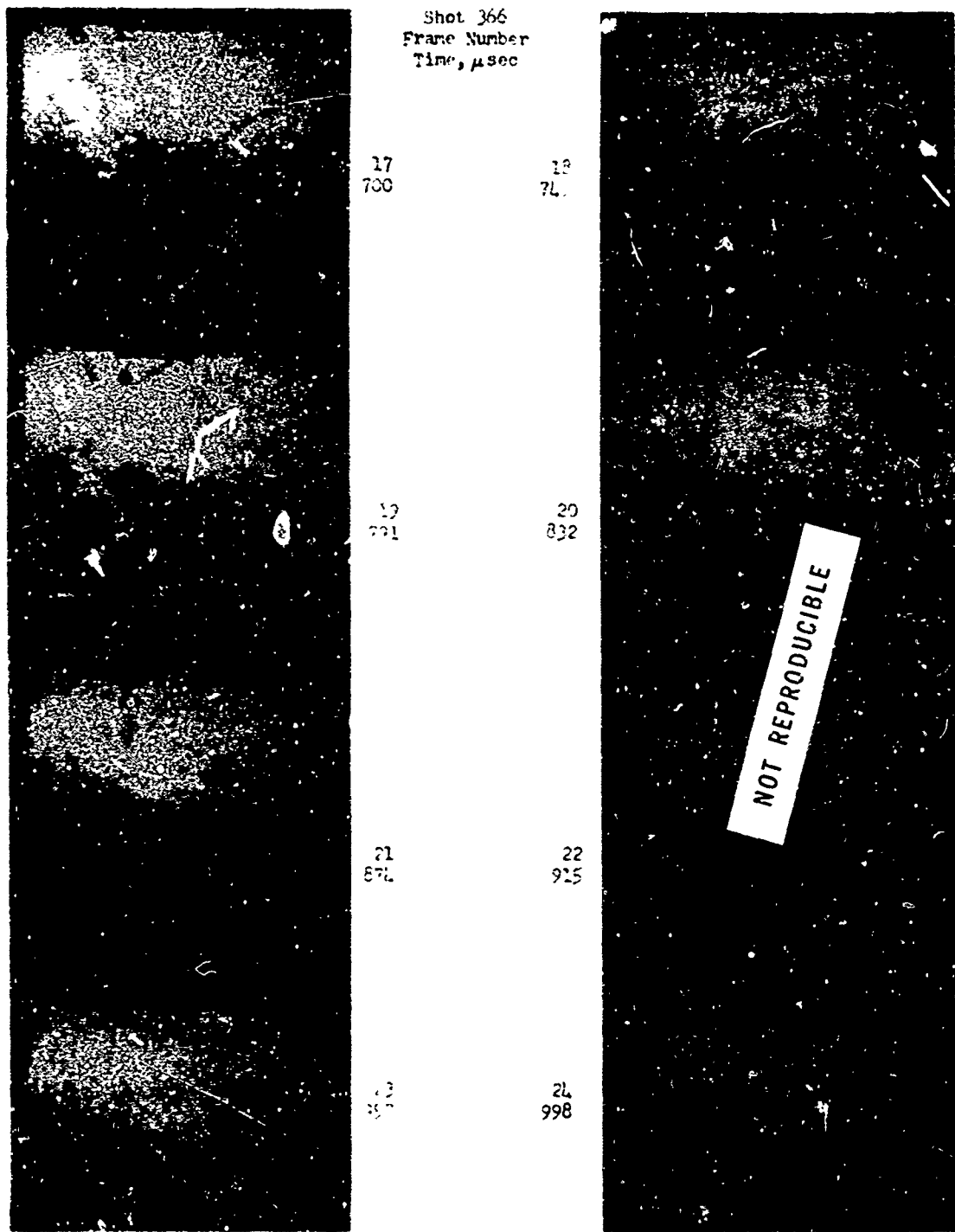


Figure C-2. Shadowgraph of a Shock Wave Entering Model of Basement Shelter - $P_s = 10$ psi (Continued)

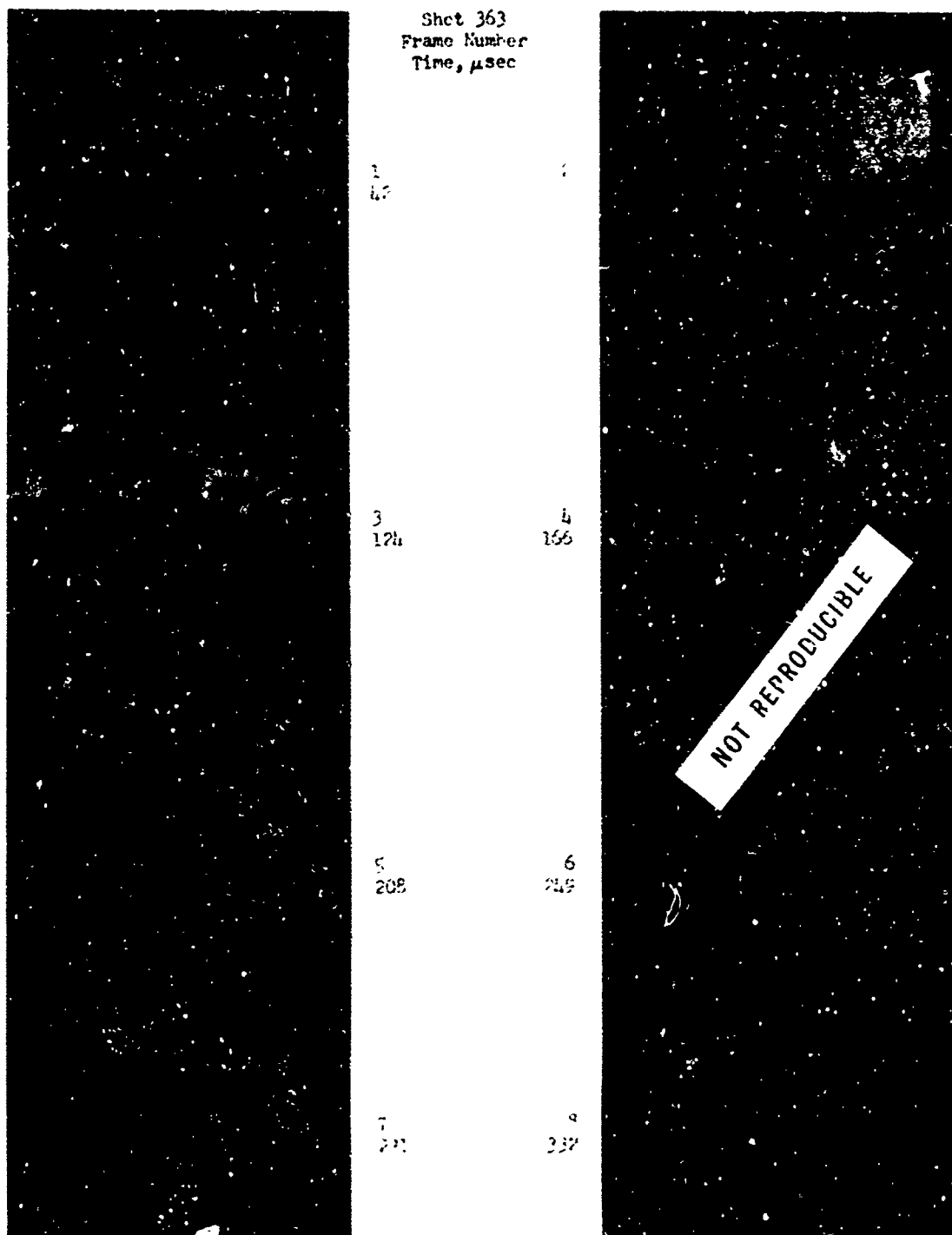


Figure C-3. Smoke Grid Flow Patterns

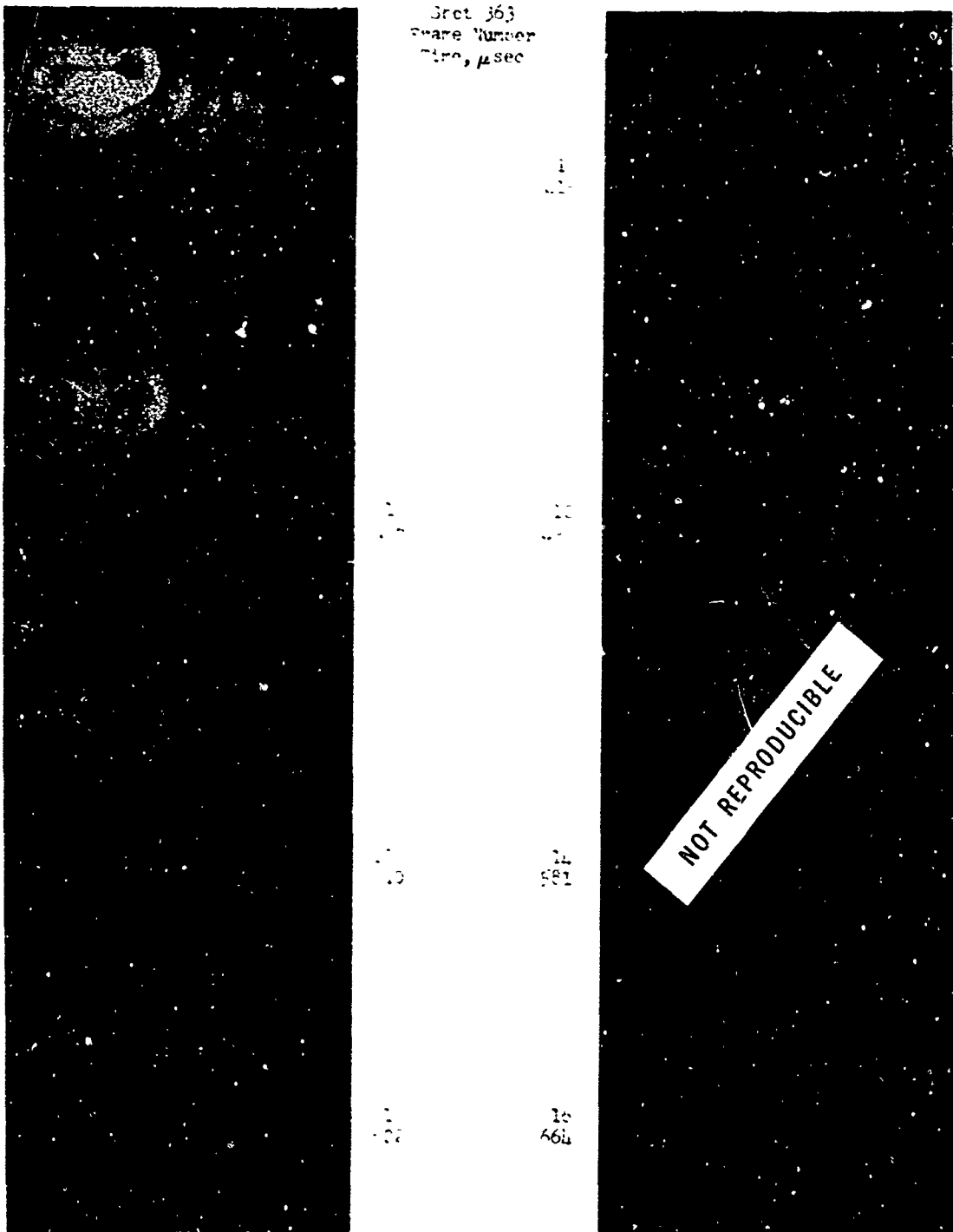


Figure C-3. Smoke Grid Flow Patterns (Continued)

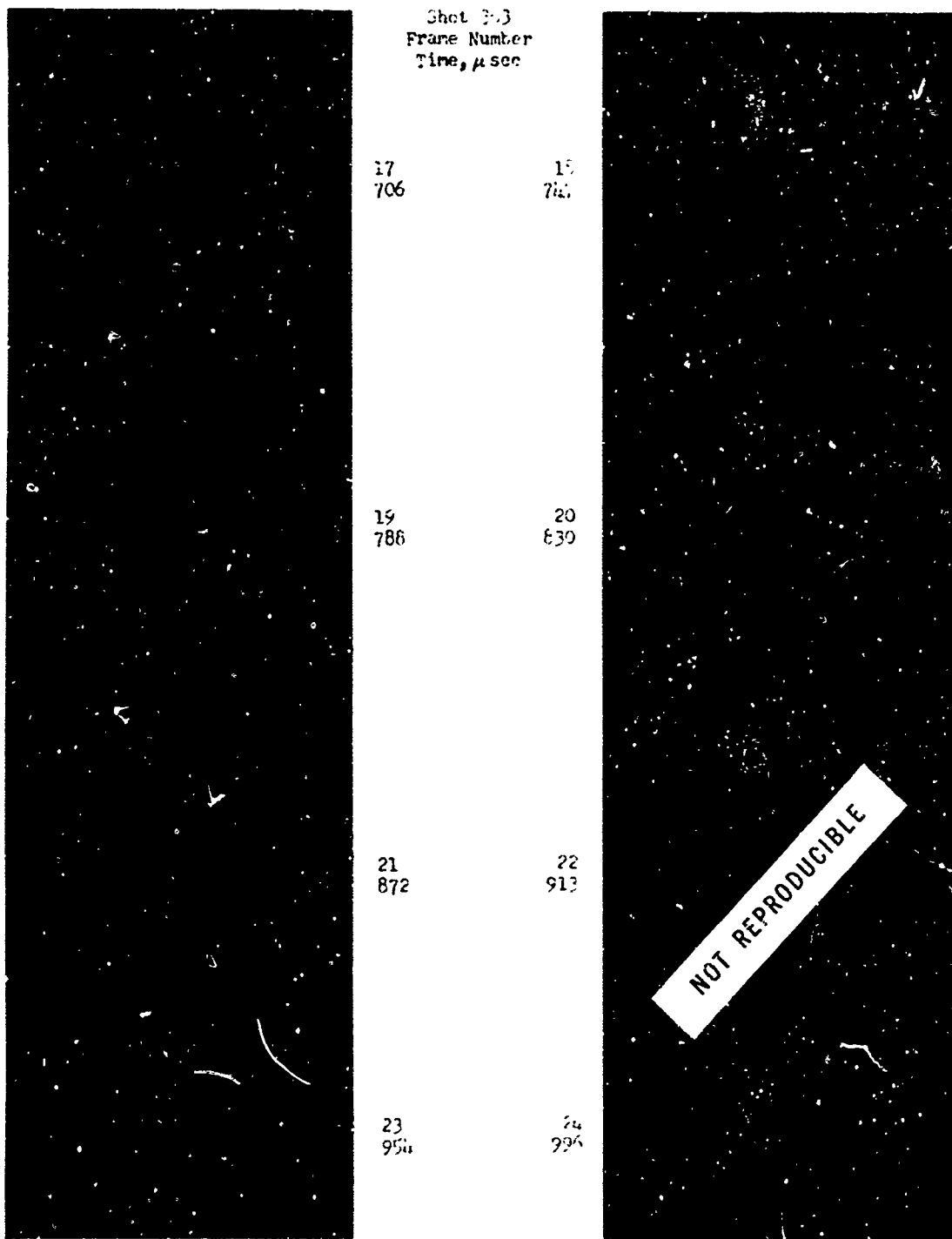


Figure C-3. Smoke Grid Flow Patterns (Continued)

APPENDIX D

AIR FLOW TABLES AND VECTOR PLOTS

Preceding page blank

USE OF APPENDIX D

Appendix D consists of two parts. The first consists of tables of the results of the calculations made from measurements from the smoke grids and the second consists of time plots of the first vertical row of grid intersections taken from the photographs of Appendix C. Additional plots of velocity vector fields computed from several grid intersections are shown for a few discrete frame times to illustrate the many directions of flow throughout the model.

The tables list the frame time in microseconds, the x-y coordinates in inches as measured from an origin at the inside, lower left bottom of the model, the average velocity of a particular smoke grid intersection (positions in frames behind and ahead of the given frame in time are used to find the average for the known camera framing speed), average angle of flow direction measured from a horizontal axis, the velocity obtained from the grid size and ambient grid area (density), and C (equal to one-half the density times the velocity squared).

The first plot of each of the figures shows the path of smoke grid intersections followed from some initial time labeled "start" to end times "T." Each path of the plot starts at a dot and ends at a time symbol, circled number. The remainder of the plots for each figure show average velocity vectors for many grid intersections for discrete times "T." The vector magnitudes are scaled at 1 in. = 200 ft/sec. The shot number is given for a reference with the photographs of Appendix C.

Table D-I. Flow Calculations - Shot 359

TIME MICROSEC	X INCHES	Y INCHES	U FT/SEC	THETA DEGREES	DENSITY SLUGS/CUFT	W LB/GRF I
41.20	0.2870	2.0537	54.2	132.3	.002115	3.10
	0.2481	1.6019	63.6	62.7	.001993	4.93
	0.2648	1.2667	40.0	43.2	.001680	1.50
	0.2648	0.8537	36.4	-36.0	.002228	1.48
	0.2648	0.0893	29.2	0.0	.002228	0.95
	0.0611	2.1907	15.0	104.0	.002057	0.23
	0.0648	1.7056	72.1	20.7	.002642	6.00
	0.7093	1.2685	37.9	144.8	.002495	1.79
	0.6593	0.9167	46.5	-41.8	.002706	2.02
	0.0944	0.0056	34.6	0.0	.002706	1.62
	1.0352	2.2537	27.4	86.2	.001582	0.59
	0.9648	1.7111	51.8	-78.4	.001957	6.55
	0.9815	1.3461	20.1	-95.2	.002045	0.41
	0.9815	0.9574	42.4	-25.5	.002122	1.01
	0.9796	0.0037	5.8	-16.4	.002122	0.04
	1.3889	2.2574	17.2	-32.0	.001957	0.29
	1.3889	1.8000	98.4	-91.1	.002045	9.90
	1.3963	1.3796	24.4	26.6	.002122	0.63
	1.3556	0.9981	30.1	104.0	.002122	0.56
	1.3967	0.0056	7.3	180.0	.001957	0.05
82.40	0.2505	2.0685	34.5	-77.5	.002155	1.28
	0.2793	1.6414	58.3	-42.4	.002323	3.95
	0.2793	1.2160	39.7	-70.7	.002141	1.69
	0.2793	0.8486	39.8	41.2	.002362	1.87
	0.2793	0.0036	30.5	-10.6	.002362	1.10
	0.6360	2.1135	230.5	-38.7	.002192	58.22
	0.6919	1.6450	141.7	-44.5	.002650	26.01
	0.6096	1.2847	56.1	25.7	.002027	3.19
	0.6739	0.8901	28.6	-11.3	.002477	1.02
	0.6739	0.0036	5.6	180.0	.002477	0.04
	1.0018	2.1982	153.6	-127.6	.001927	22.72
	0.9766	1.6793	97.8	-53.6	.002877	13.75
	0.9712	1.3171	42.3	-102.8	.002446	2.18
	1.0108	0.9504	48.7	-2.2	.002513	2.98
	1.0090	0.0036	30.0	0.0	.002513	1.13
	1.2775	2.2631	98.2	-145.1	.002877	13.87
	1.2775	1.6811	95.1	-147.9	.002446	11.06
	1.3387	1.3760	103.6	-167.5	.002513	13.49
	1.3387	1.0108	34.5	-49.4	.002513	1.50
	1.3387	0.0036	9.5	-168.7	.002877	0.13

Preceding page blank

NOT REPRODUCIBLE

Table D-I. Flow Calculations - Shot 359 (Continued)

TIME MICROSEC	X INCHES	Y INCHES	U FT/SEC	THETA DEGREES	DENSITY SLUGS/CUFT	W LB/SQFT	
123.60	0.2944	2.0204	128.7	-74.4	.001704	14.10	
	0.2907	1.5630	141.9	-102.6	.002168	21.03	
	0.2778	1.2296	47.4	-87.8	.001892	2.13	
	0.2944	0.8726	6.6	56.2	.002302	0.05	
	0.2944	0.0037	5.5	0.0	.002302	0.03	
	0.2389	2.0481	136.7	-89.2	.004160	36.25	
	0.7648	1.6074	130.7	-129.9	.004089	34.90	
	0.7593	1.2926	99.9	-51.7	.002672	13.33	
	0.6270	0.9111	35.1	-99.0	.002493	1.53	
	0.6889	0.0056	3.6	160.0	.002493	0.02	
	0.9426	2.1333	169.6	-92.5	.001915	27.55	
	1.0222	1.6333	78.4	-72.4	.003014	9.26	
	0.9722	1.3074	74.2	-62.2	.002457	6.76	
	1.0296	0.9556	62.9	-112.1	.002346	4.65	
	1.0093	0.0037	7.5	166.0	.002346	0.07	
	1.3093	2.2019	108.7	-34.8	.003014	17.80	
	1.3093	1.7500	70.9	18.0	.002457	6.17	
	1.2963	1.3574	23.7	-67.4	.002346	0.66	
	1.3776	0.9722	18.8	-60.9	.002346	0.41	
	1.3615	0.0037	9.3	11.3	.003014	0.13	
	154.80	0.2847	1.9459	219.2	-91.5	.002504	60.14
		0.2486	1.5045	181.7	-91.2	.002619	43.23
		0.2811	1.1712	118.5	-84.6	.002317	16.27
0.2829		0.8541	126.1	-130.8	.002458	19.56	
0.2647		0.0036	82.4	180.0	.002458	8.35	
0.6378		1.1784	82.3	-94.7	.002217	36.82	
0.6090		1.5459	150.6	-95.7	.002401	27.22	
0.6703		1.2072	147.1	-132.4	.002379	25.76	
0.6685		0.8559	86.3	-86.3	.002695	10.04	
0.6703		0.0036	11.4	170.5	.002695	0.17	
0.9946		2.0306	229.9	-67.0	.001857	49.09	
1.0000		1.0054	92.2	-64.2	.002675	11.38	
1.0054		1.2523	107.9	-51.3	.002503	14.58	
0.9874		0.9027	54.3	-92.0	.002433	3.59	
1.0018		0.0054	20.7	5.2	.002433	0.52	
1.3658		2.2018	146.3	-50.2	.002675	28.61	
1.3441		1.7027		-80.1	.002503		
1.3477		1.5550		-77.8	.002433		
1.3477		0.9946	38.2	-101.3	.002433	1.78	
1.3477		0.0054	13.1	0.0	.002675	0.23	

Table D-I. Flow Calculations - Shot 359 (Continued)

TIME MICROSEC	X INCHES	Y INCHES	U FT/SEC	THETA DEGREES	DENSITY SLUGS/CM ³	W LB/CM ³
206.00	0.2689	1.8037	193.2	-90.7	.001895	35.75
	0.2670	1.3633	57.2	-50.3	.003029	4.85
	0.2689	1.1130	27.6	-97.6	.002068	0.79
	0.2130	0.7952	124.7	-127.0	.002137	16.61
	0.2130	0.0037	5.6	-161.6	.002137	0.00
	0.8241	1.8685	298.9	-34.2	.003762	168.15
	0.7500	1.4593	226.6	-35.6	.003213	83.92
	0.6611	1.1652	77.7	-140.7	.002225	6.72
	0.6920	0.8259	39.4	-123.7	.002697	2.03
	0.6778	0.0074	24.0	-171.3	.002697	0.72
	1.0315	1.9241	185.9	-82.0	.001438	24.15
	1.0315	1.5426	196.2	-50.6	.002694	15.18
	1.0389	1.2241	104.6	-54.0	.005370	29.46
	1.0278	0.9739	63.0	-10.2	.002598	4.66
	1.0296	0.0056	63.8	-1.6	.002598	5.11
	1.4619	2.0907	174.6	-13.0	.002694	41.14
	1.3870	1.5000	121.6	13.0	.005370	39.87
	1.3870	0.9370	76.1	-47.0	.002508	7.27
	1.3704	0.9352	77.7	-50.7	.002508	7.37
	247.20	1.3944	0.0637	51.1	-2.0	.002694
0.2847		1.7550	127.4	-50.0	.002331	19.30
0.2773		1.4559	76.9	-67.2	.002750	8.13
0.2775		1.1441	75.0	-163.0	.002159	0.17
0.2672		0.7568	151.1	-70.4	.002524	26.60
0.2793		0.0018	50.6	-2.1	.002524	3.23
0.8108		1.7387	190.0	-70.2	.004576	90.60
0.7926		1.4144	104.4	-57.5	.002834	15.73
0.6108		1.1565	145.8	-62.4	.001979	21.02
0.6468		0.8234	110.6	-71.3	.002165	13.25
0.6468		0.0000	50.6	-2.1	.002165	2.77
0.9982		1.8468	211.1	-63.7	.001747	38.70
1.0667		1.5243	152.1	-52.0	.002343	27.19
1.0649		1.1676	134.3	-50.1	.002846	25.69
1.0649		0.2757	136.4	-44.4	.002706	29.18
1.0649		0.0036	93.7	-1.1	.002706	11.37
1.5333		2.1684	214.6	9.5	.002343	53.35
1.4613		1.7297	306.7	64.6	.002845	128.69
1.3982		1.2991	301.5	71.9	.002706	122.96
1.3964		0.9351	123.1	-26.2	.002706	29.51
1.3982	0.0036	86.2	-1.2	.002343	8.79	

NOT REPRODUCIBLE

Table D-I. Flow Calculations - Shot 359 (Continued)

TIME MICROSEC	X INCHES	Y INCHES	U FT/SEC	THETA DEGREES	DENSITY SLUGS/CUFT	W LB/SQFT	
288.40	0.2889	1.6778	147.6	-89.3	.002051	22.35	
	0.2907	1.3074	273.5	-88.1	.002405	89.94	
	0.2722	1.0407	160.6	-86.7	.001785	23.02	
	0.2630	0.6444	80.2	1.3	.002555	8.22	
	0.2630	0.0019	7.3	0.0	.002555	0.07	
	0.8907	1.6833	136.8	-87.7	.004221	39.48	
	0.8056	1.3722	110.1	-77.6	.002833	17.17	
	0.7278	1.0574	138.1	-36.4	.002109	20.12	
	0.7278	0.7222	71.6	-7.3	.002553	6.55	
	0.7278	0.0056	72.9	1.4	.002553	6.79	
	1.1241	1.7370	274.6	-46.9	.001725	65.06	
	1.1241	1.4241	167.9	-69.0	.002688	37.07	
	1.1241	1.1222	69.6	-47.1	.002667	6.47	
	1.1241	0.8074	105.9	-63.4	.002704	15.18	
	1.1222	0.0037	7.5	-166.0	.002704	0.08	
	1.6111	2.1259	194.4	-6.5	.002688	50.79	
	1.5148	1.5741	218.4	-70.5	.002667	63.63	
	1.4796	1.2204	158.5	-46.4	.002704	33.99	
	1.4796	0.8815	97.9	-45.0	.002704	12.97	
	1.4796	0.0019	67.4	0.0	.002688	6.11	
	329.60	0.2865	1.6090	121.5	-114.6	.002034	15.02
		0.2865	1.1856	28.2	-93.8	.003391	1.34
		0.2865	0.9656	64.6	-29.5	.002835	5.91
		0.2865	0.7586	88.7	45.9	.002383	9.38
		0.2865	0.0018	95.5	-1.1	.002383	10.87
		0.8162	1.6036	239.7	-134.7	.003694	106.12
		0.8162	1.3081	145.5	-124.5	.003736	39.52
		0.7207	1.0775	73.9	-59.5	.002312	6.31
0.7171		0.8144	55.7	47.7	.002623	4.07	
0.7189		0.0018	37.5	-2.9	.002623	1.84	
1.1838		1.6486	162.6	-54.8	.001782	23.57	
1.1261		1.3694	95.7	-30.6	.002772	12.70	
1.1117		1.1171	68.2	-52.8	.002569	5.97	
1.1117		0.7820	42.3	12.8	.002607	2.33	
1.0577		0.0018	43.1	-2.5	.002607	2.42	
1.7243		2.1387	157.3	0.0	.002772	34.30	
1.5333		1.5261	140.9	-23.5	.002569	25.50	
1.5063		1.1856	105.5	-16.5	.002607	14.50	
1.4649		0.8667	87.1	-25.5	.002607	9.89	
1.4649		0.0036	80.6	1.3	.002772	8.99	

Table D-I. Flow Calculations - Shot 359 (Continued)

TIME MICROSEC	X INCHES	Y INCHES	U FT/SEC	THETA DEGREES	DENSITY SLUGS/CUFT	W LB/SEC
370.80	0.2389	1.5685	146.0	-114.3	.003084	32.37
	0.2689	1.2796	6.6	-123.7	.002917	0.86
	0.3276	1.0095	23.7	22.6	.002564	0.72
	0.3241	0.7074	50.6	-59.7	.002591	3.32
	0.3574	0.0000	8.1	153.4	.002591	0.89
	0.7241	1.5148	156.9	-67.3	.002976	30.63
	0.7241	1.2537	135.6	-96.2	.002449	22.52
	0.7648	0.9944	123.2	-60.2	.002810	23.07
	0.7648	0.7030	140.5	-56.1	.002437	24.65
	0.7648	0.0037	76.6	1.4	.002437	7.14
	1.2167	1.0056	145.9	-92.1	.001656	17.62
	1.2656	1.3759	117.4	-48.1	.002515	17.34
	1.1648	1.0685	143.6	-30.5	.002585	26.71
	1.1648	0.8167	105.7	-32.3	.002491	13.90
	1.1648	0.0019	140.5	0.7	.002491	24.52
	1.7667	2.1259	177.7	-5.2	.002515	39.71
	1.6426	1.5185	109.6	-47.0	.002585	15.52
	1.5796	1.1907	97.9	-20.0	.002491	11.93
	1.5574	0.8444	107.0	-13.8	.002491	14.25
	1.5593	0.0037	134.9	-0.3	.002515	22.87
412.00	0.2270	1.4775	124.0	-66.1	.002436	19.81
	0.2829	1.1802	114.3	-71.9	.003427	22.79
	0.3081	0.9940	163.0	-91.3	.002288	30.39
	0.3117	0.7153	61.0	-90.0	.002300	4.39
	0.2793	0.0054	33.8	176.8	.002300	1.31
	0.8234	1.4486	364.3	-26.6	.003770	250.19
	0.8918	1.1748	324.6	-17.0	.003205	168.81
	0.7838	0.9676	165.6	3.5	.002172	37.46
	0.7946	0.0991	130.9	-56.1	.002681	22.97
	0.7946	0.0030	73.1	-1.5	.002681	7.16
	1.1784	1.5045	278.6	-48.3	.001527	59.24
	1.2036	1.2629	197.5	-58.6	.003084	60.18
	1.2342	1.0450	151.1	-17.3	.002855	32.57
	1.2000	0.7261	166.8	-32.6	.002693	37.45
	1.1964	0.0030	140.5	0.0	.002693	26.57
	1.8901	2.1207	190.6	-10.8	.003084	56.04
	1.6072	1.4468	231.0	18.4	.002855	76.15
	1.5910	1.1387	159.4	-29.6	.002693	34.20
	1.5676	0.8414	122.5	-23.4	.002693	20.20
	1.5982	0.0018	112.4	-1.0	.003084	19.48

Table D-I. Flow Calculations - Shot 359 (Continued)

TIME MICROSEC	X INCHES	Y INCHES	U FT/SEC	THETA DEGREES	DENSITY SLUGS/CUFT	W LB/SQFT	
453.20	0.2889	1.4556	75.1	-39.1	.002206	6.23	
	0.3241	1.1722	98.7	-85.8	.002182	10.53	
	0.3241	0.8481	114.4	-99.2	.001971	12.90	
	0.3241	0.6463	100.4	-101.5	.002424	12.22	
	0.3241	0.0019	10.9	0.0	.002424	0.14	
	1.0463	1.3537	176.8	-90.6	.006033	94.26	
	1.0296	1.1556	114.9	-48.2	.005891	38.85	
	0.9481	1.0056	126.5	-41.5	.002076	16.61	
	0.8370	0.6556	95.9	-51.2	.002383	10.96	
	0.8370	0.0019	56.5	1.8	.002383	3.21	
	1.4000	1.4000	370.8	-14.5	.002163	148.73	
	1.3074	1.2093	238.0	-37.2	.002266	64.17	
	1.3074	1.0241	117.8	-55.1	.002659	18.44	
	1.3037	0.7278	99.3	-47.2	.002918	14.38	
	1.3037	0.0019	42.1	-5.0	.002918	2.58	
	1.9519	2.0907	9.1	90.0	.002266	0.09	
	1.8593	1.5907	212.1	-13.9	.002659	59.33	
	1.7167	1.1130	158.5	-0.7	.002918	36.67	
	1.6685	0.7963	141.4	-38.2	.002918	29.19	
	1.6704	0.0019	116.7	1.8	.002266	15.42	
	494.40	0.2847	1.4306	81.9	-100.5	.002632	8.83
		0.2901	1.0829	141.0	-100.7	.002810	27.95
		0.2901	0.8829	75.8	-110.2	.001992	5.73
		0.2919	0.6180	86.3	-62.9	.002334	8.68
		0.2901	0.0054	39.4	2.7	.002334	1.31
		0.8216	1.2739	216.4	-41.1	.002611	61.11
		0.8775	1.0901	199.4	-28.0	.003388	67.36
0.8775		0.8847	148.9	-68.6	.002369	26.25	
0.8541		0.6252	12.0	-38.7	.003013	0.22	
0.8505		0.0054	28.1	0.0	.003013	1.19	
1.5333		1.4126	222.3	-29.8	.002157	53.30	
1.3910		1.1405	199.4	-25.6	.004005	79.60	
1.3009		0.9495	119.2	-30.2	.002251	15.98	
1.2667		0.6541	38.4	-43.0	.002607	1.92	
1.2378		0.0000	30.0	-3.6	.002607	1.17	
1.8991		2.1297		-178.3	.004005		
1.8108		1.3964		-179.4	.002251		
1.7477		1.1369	115.0	-30.3	.002607	17.23	
1.6775		0.7550	101.3	-19.4	.002607	13.37	
1.7135		0.0054	174.2	0.0	.004005	60.75	

Table D-I. Flow Calculations - Shot 359 (Continued)

TIME MICROSEC	X INCHES	Y INCHES	U FT/SEC	THETA DEGREES	DENSITY SLUGS/CUFT	W LR/COF 1
535.50	0.2741	1.3759		0.4	.001722	
	0.2981	1.0352	READINGS	INVALID		
	0.2981	0.7778	132.7	-98.7	.002436	21.46
	0.3630	0.5704	127.9	-35.7	.002698	22.78
	0.3630	0.0037	105.8	3.0	.002698	15.11
	1.2074	1.2130	269.4	-46.4	.007247	262.93
	1.2037	1.0630	READINGS	INVALID		
	1.0019	0.6685	171.4	-43.7	.002741	40.26
	0.8463	0.0461	59.5	-117.3	.002385	4.22
	0.8648	0.0019	33.3	170.5	.002385	1.32
	1.5907	1.2707	180.4	-88.8	.000671	10.13
	1.4852	1.1241	142.7	-61.8	.005463	55.60
	1.4093	1.9640	113.4	-43.7	.002784	17.91
	1.3315	0.7019	62.9	-22.1	.002349	4.65
	1.3333	0.0000	18.6	11.3	.002349	0.41
	0.2136	2.0389	191.4	-1.5	.005463	100.08
	0.2037	1.5741	101.9	-28.9	.002784	14.47
	1.8148	1.0356	96.0	-56.6	.002349	10.63
	1.7630	0.7630	80.3	-2.6	.002349	7.57
	1.8426	0.0019	3.1	153.4	.005463	0.16
576.80	1.7153	1.4414	43.7	-60.1	READINGS	INVALID
	NO READING		READINGS	INVALID		
	0.2703	0.7532	67.1	-149.9	.002570	5.79
	0.3946	0.5441	READINGS	INVALID		
	0.3946	0.0106	READINGS	INVALID		
	1.0054	1.0811	179.8	-69.4	READINGS	INVALID
	NO READING		READINGS	INVALID		
	1.0000	0.7670	READINGS	INVALID		
	0.8270	0.5730	READINGS	INVALID		
	0.8180	0.0106	READINGS	INVALID		
	1.5369	1.2342	194.7	-135.4	.001850	35.35
	1.4577	1.0162	244.8	-99.2	.004567	136.83
	1.3820	0.8721	383.4	-103.6	.002851	209.51
	1.3243	0.6306	READINGS	INVALID		
	1.2559	0.0036	READINGS	INVALID		
	2.0883	2.1243	READINGS	INVALID		
	1.8991	1.3477	READINGS	INVALID		
	1.8000	1.0577	READINGS	INVALID		
	1.7568	0.7514	27.8	-70.3	.002718	1.05
	1.7063	0.0090	112.4	179.0	.004567	28.84

Table D-I. Flow Calculations - Shot 359 (Continued)

TIME MICROSEC	X INCHES	Y INCHES	U FT/SEC	THETA DEGREES	DENSITY SLUGS/CUFT	W LB/SQ FT
618.00	0.2815	1.3333	READINGS	INVALID		
	0.2093	1.0259	READINGS	INVALID		
	0.2407	0.7444	READINGS	INVALID		
	NO READING		READINGS	INVALID		
	NO READING		READINGS	INVALID		
	1.2093	1.0352	76.6	-92.7	.005310	15.59
	1.2000	0.7537	READINGS	INVALID		
	NO READING		READINGS	INVALID		
	NO READING		READINGS	INVALID		
	NO READING		READINGS	INVALID		
	1.4537	1.1556	147.7	-92.1	READINGS	INVALID
	1.4463	0.8852	137.6	-11.5	READINGS	INVALID
	1.3204	0.5963	134.0	7.0	READINGS	INVALID
	NO READING		READINGS	INVALID		
	NO READING		READINGS	INVALID		
	NO READING		READINGS	INVALID		
	NO READING		READINGS	INVALID		
	NO READING		READINGS	INVALID		
	1.7722	0.7370	56.8	-47.6	READINGS	INVALID
	1.7315	0.0037	169.6	-2.5	READINGS	INVALID
659.20	NO READING		READINGS	INVALID		
	NO READING		READINGS	INVALID		
	NO READING		READINGS	INVALID		
	NO READING		READINGS	INVALID		
	NO READING		READINGS	INVALID		
	1.0018	1.0054	READINGS	INVALID		
	1.0018	0.8757	READINGS	INVALID		
	0.9856	0.7135	READINGS	INVALID		
	0.9730	0.5171	READINGS	INVALID		
	1.0018	0.0036	READINGS	INVALID		
	1.5315	1.0883	135.8	-24.4	.001039	9.57
	1.5910	0.9892	66.2	-61.3	.000766	1.68
	1.5135	0.8883	76.5	21.5	.002191	6.41
	1.3676	0.5886	READINGS	INVALID		
	1.3532	0.0018	READINGS	INVALID		
	1.9027	2.2486	READINGS	INVALID		
	2.0847	1.4396	READINGS	INVALID		
	0.1928	1.1153	READINGS	INVALID		
	1.7946	0.7089	72.3	-31.2	.002633	6.88
	1.8739	0.0018	41.2	-2.6	.000766	0.65

Table D-II. Flow Calculations - Shot 363

TIME MICROSEC	X INCHES	Y INCHES	U FT/SEC	THETA DEGREES	DENSITY SLUGS/CUFT	Q LB/SQFT	
41.50	1.2185	2.1852	41.7	-177.4	.002411	2.09	
	1.2167	1.6537	52.6	-175.8	.002565	3.55	
	1.2185	1.2074	74.6	-157.2	.002955	8.21	
	1.2185	1.1000	69.4	-172.0	.002502	6.03	
	1.2167	0.0037	67.0	-178.4	.002502	5.61	
	1.8907	2.2241	12.8	115.2	.002508	0.20	
	1.8537	1.6315	98.2	-167.6	.002604	12.55	
	1.8259	1.1444	99.6	-168.8	.002416	11.98	
	1.8241	0.9463	87.6	-166.0	.002494	9.57	
	1.8241	0.0037	83.2	-178.7	.002494	8.64	
	2.3204	2.0000	76.6	-148.2	.002593	7.61	
	2.2833	1.6093	84.6	-169.5	.002550	9.13	
	2.2278	1.1370	104.6	-170.5	.002181	11.92	
	2.2296	0.8963	103.3	-176.8	.002275	12.13	
	2.2093	0.0037	101.3	178.9	.002275	11.68	
	2.9315	1.9889	75.5	-159.1	.002550	7.27	
	2.9333	1.5944	90.9	-156.3	.002181	9.01	
	2.9315	1.1222	83.6	-174.7	.002275	7.95	
	2.9313	0.8315	84.3	-170.8	.002275	8.08	
	2.9315	0.0037	83.3	177.4	.002550	8.85	
	83.00	1.1982	2.2626	5.3	-45.0	.002264	0.03
		1.1784	1.6879	64.4	-133.8	.002359	4.90
		1.1640	1.2185	46.5	180.0	.002639	2.85
		1.1640	1.0882	46.8	173.2	.002416	2.65
1.1640		0.0000	44.7	177.6	.002416	2.41	
1.8919		2.2626	82.6	172.2	.002356	8.03	
1.8018		1.6515	44.2	165.4	.002286	2.23	
1.8018		1.1189	67.7	-164.1	.002540	5.82	
1.8018		0.9234	61.6	-174.8	.002464	4.68	
1.8018		0.6038	63.2	-178.3	.002464	4.93	
2.3027		2.0346	48.3	157.4	.002377	2.78	
2.2593		1.6266	50.7	-151.6	.002351	3.03	
2.2090		1.1074	8.3	-153.4	.002286	0.08	
2.2090		0.8890	39.2	174.6	.002296	1.77	
2.2090		0.0038	14.9	180.0	.002296	0.25	
2.9171		2.0500	47.6	128.7	.002351	2.67	
2.9189		1.6093	41.6	-153.4	.002286	1.98	
2.9189		1.1150	33.9	170.5	.002296	1.32	
2.9189		0.8315	35.9	158.7	.002296	1.48	
2.9189		0.0057	33.5	-176.8	.002351	1.32	

Table D-II. Flow Calculations - Shot 363 (Continued)

TIME MICROSEC	X INCHES	Y INCHES	U FT/SEC	THETA DEGREES	DENSITY SLUGS/CUFT	Q LB/SOFT	
124.50	1.2222	2.1815	143.7	-42.0	.002487	25.67	
	1.1722	1.6074	68.1	-52.3	.002647	6.13	
	1.1722	1.2074	68.1	-52.3	.003243	7.51	
	1.1722	1.1056	64.3	-53.8	.002573	5.33	
	1.1722	0.0056	38.2	5.8	.002573	1.88	
	1.8093	2.2352	36.1	-127.0	.002335	1.52	
	1.8111	1.6426	47.1	-2.3	.002416	2.68	
	1.7611	1.1259	26.9	90.0	.002300	0.83	
	1.7630	0.9407	140.4	89.3	.002292	22.60	
	1.7611	0.0019	2.6	-46.8	.002292	0.01	
	2.2759	2.0185	13.6	57.9	.002267	0.21	
	2.2389	1.5852	13.2	-16.9	.002716	0.24	
	2.2204	1.1333	6.0	107.4	.002271	0.04	
	2.1907	0.9000	6.8	-122.1	.002273	0.05	
	2.1944	0.0037	1.8	180.0	.002273	0.00	
	2.9019	2.0259	14.5	138.8	.002716	0.29	
	2.8963	1.5759	1.8	0.0	.002271	0.00	
	2.8981	1.1278	28.1	-33.2	.002273	0.90	
	2.8981	0.8444	31.5	-58.8	.002273	1.13	
	2.8981	0.0019	16.7	-13.3	.002716	0.38	
	166.00	1.3045	2.1668	210.4	-27.9	.002675	59.23
		1.2198	1.6342	150.8	-30.4	.002503	28.47
		1.2054	1.1648	121.7	-38.8	.004342	32.14
		1.2018	1.0335	155.9	-50.8	.002458	29.86
		1.2018	0.0038	96.8	-2.2	.002458	11.49
		1.8703	2.2339	147.7	-10.9	.002453	26.75
		1.8486	1.6496	119.7	-25.8	.002461	17.68
1.8018		1.1457	107.9	-2.0	.003396	19.77	
1.8036		1.0633	85.7	12.5	.002318	8.51	
1.8036		0.0019	83.7	1.3	.002318	8.12	
2.3099		2.0461	108.2	24.4	.002363	13.82	
2.2721		1.6227	116.0	6.4	.002312	15.56	
2.2072		1.1131	79.4	-20.6	.002116	6.68	
2.2054		0.8832	76.6	5.6	.002275	6.67	
2.2072		0.0038	74.4	-1.4	.002275	6.30	
2.9063		2.0595	53.7	14.0	.002312	3.33	
2.9207		1.6093	69.7	-9.2	.002116	5.14	
2.9423		1.0997	55.8	0.0	.002275	3.54	
2.9351		0.8047	54.0	3.6	.002275	3.32	
2.9351		0.0019	55.8	0.0	.002312	3.60	

Table D-II. Flow Calculations - Shot 363 (Continued)

TIME MICROSEC	X INCHES	Y INCHES	U FT/SEC	THETA DEGREES	DENSITY SLUGS/CUFT	Q LB/SQFT	
207.50	1.4074	2.0833	187.5	-6.5	.002660	46.77	
	1.3019	1.5315	152.2	-55.2	.002832	32.81	
	1.2667	1.1315	97.8	-39.0	.003005	14.37	
	1.2704	0.9852	213.4	-71.2	.002771	63.07	
	1.2685	0.0019	70.6	-1.6	.002771	6.90	
	1.9537	2.2074	153.8	30.8	.002321	27.45	
	1.9185	1.5907	109.7	-27.1	.002515	15.14	
	1.8685	1.1222	110.9	-39.9	.002770	17.03	
	1.8463	0.9593	250.8	-70.6	.002308	72.48	
	1.8444	0.0037	83.2	0.0	.002305	7.98	
	2.3741	2.0630	97.4	-10.2	.002298	10.90	
	2.3537	1.5981	65.6	-15.3	.002762	5.95	
	2.2944	1.1056	60.2	7.3	.002532	4.59	
	2.2667	0.9074	47.6	-29.0	.002323	2.63	
	2.2685	0.0019	39.8	-2.8	.002323	1.84	
	2.9537	2.0389	61.6	3.6	.002762	5.25	
	2.9648	1.5648	33.1	-10.0	.002532	1.38	
	2.9537	1.1278	24.2	107.4	.002323	0.68	
	2.9519	0.8481	28.9	90.0	.002323	0.97	
	2.9537	0.0019	1.8	0.0	.002762	0.00	
	249.00	1.4901	2.1458		-92.0	.002378	
		1.3063	1.5097	354.6	-80.3	.002587	162.60
		1.2811	1.1035	214.6	-64.3	.001740	40.06
		1.2703	0.6353	READINGS	INVALID		
1.2721		0.0019	READINGS	INVALID			
2.0018		2.3124	136.8	-7.7	.002314	22.30	
1.9459		1.5997	131.6	-36.4	.002705	23.44	
1.8865		1.0748	98.2	-52.7	.002287	11.02	
1.8865		0.8276	128.9	-46.2	.002984	24.78	
1.8865		0.0019	85.5	0.0	.002984	10.91	
2.4054		2.0289	128.9	-46.2	.002472	20.53	
2.3351		1.6055	72.6	-39.8	.002628	6.93	
2.2667		1.1208	58.8	-18.4	.002182	3.77	
2.2468		0.8602	81.9	-50.5	.002395	8.03	
2.2468		0.0019	50.2	0.0	.002395	3.02	
2.9676		2.0634	96.7	-22.6	.002628	12.28	
2.9532		1.6036	68.3	29.4	.002182	5.08	
2.9351		1.1227	71.0	-45.0	.002395	6.03	
2.9351		0.8334	46.8	6.8	.002395	2.62	
2.9369		0.0019	46.5	0.0	.002628	2.84	

Table D-II. Flow Calculations - Shot 363 (Continued)

TIME MICROSEC	X INCHES	Y INCHES	U FT/SEC	THETA DEGREES	DENSITY SLUGS/CUFT	Q LB/SQFT	
290.50	1.3852	1.4556	216.2	-44.7	.002952	68.99	
	1.3611	1.1833	135.8	-41.7	.003374	32.94	
	1.3593	0.9389	114.7	-62.8	READINGS	INVALID	
		NO READING		READINGS	INVALID		
		NO READING		READINGS	INVALID		
	2.0907	2.1889	174.5	-58.1	.002545	38.75	
	2.0241	1.5130	130.3	-54.3	.002812	23.86	
	1.9278	1.0444	45.6	-7.3	.002532	2.63	
	1.9352	0.8667	59.0	-41.5	.002750	4.63	
	1.9296	0.0037	43.4	0.0	.002750	2.59	
	2.4630	1.9704	82.8	-10.7	.002632	9.03	
	2.4093	1.5519	99.1	-32.9	.002618	12.86	
	2.3500	1.0870	96.6	-38.1	.002618	12.21	
	2.3125	0.8444	117.2	-35.1	.002418	16.60	
	2.3185	0.0019	94.1	2.3	.002418	10.72	
	3.0426	2.0019	73.9	-62.3	.002618	7.15	
	3.0241	1.5981	85.9	-25.2	.002618	9.67	
	3.0037	1.0778	83.6	-36.8	.002418	8.44	
	2.9981	0.8537	78.2	-49.7	.002418	7.40	
	3.0000	0.0019	48.8	0.0	.002618	3.12	
	332.00	1.6432	1.9944		56.6	.002835	
		1.4072	1.4196	227.0	58.4	.002988	77.03
		1.3333	1.0020	42.1	135.0	.001845	1.63
1.3297		0.7855	READINGS	INVALID			
1.3297		0.0038	READINGS	INVALID			
2.0937		2.1649	142.3	-17.5	.002387	24.17	
2.0216		1.4944	102.3	-1.0	.002851	14.91	
1.9315		1.0690	133.5	-12.9	.001898	16.91	
1.9297		.7893	86.5	-8.7	.002793	10.45	
1.9297		.0019	91.1	0.0	.002793	11.59	
2.4855		2.0136	115.4	2.8	.002552	17.00	
2.4180		1.5518	116.8	-9.2	.002612	17.80	
2.3423		1.0614	92.8	-32.7	.002205	9.50	
2.3423		0.7932	70.4	-12.2	.002776	6.88	
2.3405		0.0057	31.7	3.4	.002776	1.39	
3.0018		1.9982	50.7	-8.4	.002612	3.36	
3.0306		1.5672	67.0	-19.4	.002205	4.95	
3.0018		1.0729	82.3	6.5	.002776	9.41	
2.9856		0.7740	98.1	-27.1	.002776	13.36	
2.9856		0.0019	89.3	-1.2	.002612	10.40	

Table D-II. Flow Calculations - Shot 363 (Continued)

TIME MICROSEC	X INCHES	Y INCHES	U FT/SEC	THETA DEGREES	DENSITY SLUGS/CUFT	Q LB/SQFT
373,50	1,7852	2,0611	174,5	5,7	.002635	40,13
	1,4706	1,3759	204,9	8,6	.002483	52,15
	1,3296	0,9685	122,0	-15,5	READINGS	INVALID
	NO READING		READINGS	INVALID		
	NO READING		READINGS	INVALID		
	2,2259	2,1463	172,2	14,9	.002605	38,63
	2,1259	1,5111	159,2	21,3	.002758	34,94
	2,0574	1,0148	161,2	-2,7	.003151	40,93
	2,0204	0,8537	141,6	19,0	.003101	31,10
	2,0204	0,0037	148,4	0,7	.003101	34,13
	2,5778	1,9759	100,0	-5,5	.002780	13,89
	2,5241	1,5333	117,8	3,7	.002736	18,99
	2,4278	1,0370	132,2	-2,5	.002482	21,68
	2,3870	0,8296	98,6	13,5	.002373	11,54
	2,3500	0,0037	97,7	1,1	.002373	11,33
	3,0926	1,8944	106,8	33,9	.002736	15,61
	3,0870	1,5759	61,2	-12,7	.002482	4,65
	3,0852	1,0870	75,8	11,7	.002373	6,81
	3,0852	0,8093	83,8	6,6	.002373	8,33
	3,0889	0,0000	83,2	1,3	.002736	9,48
415,00	1,8162	2,0116	203,1	-49,5	.003127	64,48
	1,6090	1,4503	186,5	-14,9	.002661	47,29
	1,4505	0,9694	169,6	3,8	.002169	31,18
	1,4324	0,7932	READINGS	INVALID		
	1,4342	0,0038	READINGS	INVALID		
	2,2595	2,2090	85,0	-10,1	.002741	9,90
	2,1694	1,5518	138,4	-6,2	.002803	26,85
	2,0919	1,0614	105,8	-16,4	.002419	13,55
	2,0631	0,8353	119,9	-19,0	.003005	21,62
	2,0775	0,0038	57,9	5,5	.003005	5,04
	2,5856	2,0040	146,7	59,5	.002564	27,58
	2,5351	1,5595	81,0	-9,2	.002916	9,57
	2,4739	1,0556	95,1	-4,5	.002430	10,99
	2,4378	0,8162	72,3	-18,0	.002784	7,28
	2,4378	0,0077	78,1	0,0	.002784	8,49
	3,0901	2,0576	69,2	-30,7	.002916	6,98
	3,0901	1,5538	75,0	-29,7	.002430	6,82
	3,0757	1,0882	45,4	-35,0	.002784	2,87
	3,0685	0,7836	30,0	-29,7	.002784	1,25
	3,0685	0,0038	18,7	5,7	.002916	0,51

Table D-II. Flow Calculations - Shot 363 (Continued)

TIME MICROSEC	X INCHES	Y INCHES	U FT/SEC	THETA DEGREES	DENSITY SLUGS/CUFT	Q LB/3QFT	
456.50	1.9167	1.9074	149.4	-29.3	.003255	36.30	
	1.6611	1.3278	202.3	-47.9	.002863	58.58	
	1.4981	0.9796	80.7	-141.7	.002864	9.39	
	1.4963	0.8537	229.5	-173.3	READINGS	INVALID	
	NO READINGS		READINGS		INVALID		
	2.3093	2.1315	95.8	-27.5	.002602	11.95	
	2.2630	1.4963	104.6	-9.5	.002994	16.37	
	2.1574	0.9815	89.2	-14.9	.003249	13.12	
	2.1333	0.8148	94.8	-7.0	.003345	15.02	
	2.0778	0.0093	77.8	0.0	.003345	10.12	
	2.6519	2.1019	93.8	15.5	.002433	10.72	
	2.6037	1.5204	94.1	-1.2	.002950	13.06	
	2.5222	1.0296	47.1	-2.3	.002660	2.95	
	2.4556	0.8074	67.4	-6.6	.002516	5.94	
	2.4278	0.0037	36.4	-6.1	.002616	1.73	
	3.1519	1.9593	69.5	-33.6	.002950	7.13	
	3.1519	1.5389	64.8	38.6	.002660	5.58	
	3.1222	1.0611	57.0	-17.7	.002616	4.24	
	3.1111	0.7944	46.7	21.7	.002616	2.86	
	3.1074	0.0019	43.4	0.0	.002950	2.78	
	498.00	1.9459	1.9388	230.9	52.9	.003381	90.16
		1.7441	1.3009	237.6	-14.0	.002990	84.42
		1.3874	0.9196	248.0	-11.8	.001812	54.41
1.2054		0.7663	READINGS INVALID				
1.2054		0.0038	READINGS INVALID				
2.3441		2.1649	92.6	10.4	.002808	12.04	
2.2721		1.5346	106.2	4.0	.003014	17.01	
2.1784		1.0384	104.3	3.1	.002698	14.67	
2.1568		0.8238	83.1	10.3	.003343	11.56	
2.1550		0.0038	102.7	-5.2	.003343	17.62	
2.6757		2.0289	136.5	-52.2	.002918	27.18	
2.6288		1.5576	102.3	0.0	.002852	14.91	
2.5207		1.0537	100.7	-4.2	.002601	13.18	
2.5045		0.8085	126.6	2.8	.002797	22.40	
2.4739		0.0038	122.7	0.9	.002797	21.06	
3.1477		2.0193	194.6	65.4	.002852	54.13	
3.1405		1.5940	75.3	15.8	.002601	7.38	
3.1297		1.0710	70.8	29.9	.002797	7.01	
3.1117		0.8008	78.9	45.0	.002797	8.70	
3.1117		0.0038	54.0	2.0	.002852	4.15	

Table D-II. Flow Calculations - Shot 363 (Continued)

TIME MICROSEC	X INCHES	Y INCHES	U FT/SEC	THETA DEGREES	DENSITY SLUGS/CUFT	Q LB/SQFT	
539.50	2.0556	2.0907		-95.4	.003091		
	1.8907	1.2704	64.6	-63.4	.003812	7.94	
	1.7370	0.9296	227.3	-5.8	READINGS	INVALID	
	NO READING		READINGS	INVALID			
	NO READING		READINGS	INVALID			
	2.4000	2.1481	51.4	69.4	.002848	3.76	
	2.3685	1.5037	62.0	-7.1	.002963	5.73	
	2.2611	0.9870	90.8	-4.9	.003228	13.30	
	2.2148	0.8296	93.8	-15.5	.003000	13.21	
	2.1796	0.0000	92.3	-1.2	.003000	12.77	
	2.7352	1.9944	34.4	0.0	.002426	1.43	
	2.7056	1.5204	41.0	22.1	.003189	2.68	
	2.6222	1.0222	65.4	-5.1	.003158	6.75	
	2.5815	0.8130	56.1	0.0	.002821	4.44	
	2.5500	0.0056	83.2	0.0	.002821	9.77	
	3.2296	2.1370	39.1	62.4	.003189	2.43	
	3.2241	1.5593	23.0	-19.5	.003158	0.84	
	3.1833	1.0963	37.7	54.8	.002821	2.00	
	3.1667	0.8500	36.2	3.0	.002821	1.85	
	3.1611	0.0037	36.2	-3.0	.003189	2.09	
	581.00	1.9207	1.6745	159.9	123.1	.003641	46.53
		1.7730	1.2434	52.4	-6.1	.003206	4.39
		1.6126	0.8966	226.3	-28.5	READINGS	INVALID
NO READING			READINGS	INVALID			
NO READING			READINGS	INVALID			
2.3622		2.2128	89.6	131.6	.002749	11.02	
2.3333		1.5269	20.8	63.4	.003181	0.69	
2.2685		1.0307	24.5	-98.7	.002893	0.87	
2.2468		0.7989	71.8	-53.4	.003628	9.34	
2.2468		0.0019	READINGS	INVALID			
2.7099		2.0289	9.3	180.0	.002931	0.13	
2.6667		1.5729	37.4	95.7	.003564	2.14	
2.5856		1.0480	46.6	94.6	.002630	2.86	
2.5604		0.8085	26.8	33.7	.002948	1.06	
2.5568		0.0038	10.0	-21.8	.002948	0.15	
3.1658		2.0538	104.1	-108.8	.003064	16.59	
3.1622		1.5863	28.4	-168.7	.002630	1.06	
3.1514	1.1016	9.5	101.3	.002948	0.13		
3.1477	0.8027	16.6	-26.6	.002948	0.41		
3.1477	0.0019	22.7	0.0	.003064	0.76		

Table D-II. Flow Calculations - Shot 363 (Continued)

TIME MICROSEC	X INCHES	Y INCHES	U FT/SEC	THETA DEGREES	DENSITY SLUGS/CUFT	Q LB/SQFT	
622.50	1.9685	2.2241	READINGS	INVALID			
	1.9426	1.2648	64.0	28.8	.004217	8.63	
	1.9352	0.8222	87.0	-136.7	READINGS	INVALID	
	NO READING		READINGS	INVALID			
	NO READING		READINGS	INVALID			
	2.3407	2.2148	127.7	153.1	.002710	22.11	
	2.3778	1.5222	58.1	133.2	.003022	5.10	
	2.2574	0.9630	87.2	-167.3	.002827	10.74	
	2.2574	0.7722	92.5	-168.0	READINGS	INVALID	
	NO READING		READINGS	INVALID			
	2.7259	1.9944	89.2	-173.8	.002891	11.49	
	2.7019	1.5574	71.0	173.8	.003305	8.32	
	2.6185	1.0685	76.0	178.5	.002839	8.20	
	2.6037	0.8278	87.4	-173.7	.002788	10.64	
	2.5593	0.0019	119.5	177.2	.002788	19.92	
	3.1963	2.0389	78.2	-174.4	.003305	10.10	
	3.1963	1.5537	75.1	-171.2	.002839	8.00	
	3.1815	1.1056	64.4	-162.6	.002788	5.79	
	3.1815	0.8426	60.2	172.7	.002788	5.05	
	3.1833	0.0037	72.4	180.0	.003305	8.65	
	664.00	NO READING		READINGS	INVALID		
		1.8288	1.2740	41.3	-82.2	.003280	2.79
		1.5495	0.8372	93.4	121.2	.002665	11.63
1.2360		0.7625	READINGS	INVALID			
NO READING			READINGS	INVALID			
2.2486		2.2703	READINGS	INVALID			
2.2937		1.5691		93.3	.003089		
2.1838		1.0116		76.9	.002789		
2.1568		0.7798	234.0	75.7	.003458	94.70	
2.0847		0.0019	READINGS	INVALID			
2.6216		2.0193	84.8	105.3	.002948	10.60	
2.5964		1.5806	7.7	104.0	.002982	0.09	
2.5099		1.0499	50.6	-72.9	.002614	3.34	
2.4739		0.7989	35.5	-96.0	.002788	1.76	
2.4378		0.0096	41.1	5.2	.002788	2.35	
3.0883		2.0461	64.7	-18.4	.002982	6.24	
3.0883		1.5748	18.4	135.0	.002614	0.44	
3.0901		1.0825	20.8	-79.7	.002788	0.60	
3.0883		0.8104	32.5	-103.2	.002788	1.47	
3.0757		0.0019	9.5	-168.7	.002982	0.13	

Table D-II. Flow Calculations - Shot 363 (Continued)

TIME MICROSEC	X INCHES	Y INCHES	U FT/SEC	THETA DEGREES	DENSITY SLUGS/CUFT	Q LB/SQFT	
705.50	1.8204	2.2667	READINGS	INVALID			
	1.9481	1.2241	134.8	14.9	.003366	30.57	
	1.8870	0.9019		10.0	READINGS	INVALID	
	NO READING		READINGS	INVALID			
	NO READING		READINGS	INVALID			
	NO READING		READINGS	INVALID			
	2.3370	2.2241	74.1	48.8	.002799	7.69	
	2.3944	1.5500	83.2	1.3	.001741	6.03	
	2.3148	0.9981	54.8	-8.1	READINGS	INVALID	
	NO READING		READINGS	INVALID			
	2.7037	2.0759	131.3	85.3	.002562	22.07	
	2.7000	1.5640	54.2	48.1	.003086	4.54	
	2.6335	1.0204	89.0	5.0	.002902	11.49	
	2.5000	0.7920	86.1	9.0	.003043	11.28	
	2.6000	0.0056	123.1	-2.7	.003043	23.09	
	3.2574	2.0185	36.0	25.3	.003086	2.00	
	3.1833	1.5667	54.7	16.3	.002902	4.34	
	3.1852	1.0852	52.0	12.8	.003043	4.11	
	3.1741	0.8111	40.9	-44.9	.003043	2.54	
	3.1741	0.0019	41.7	2.6	.003086	2.63	
	747.00	NO READING		READINGS	INVALID		
		1.9586	1.3085	14.5	39.8	.004434	0.47
		1.9495	0.9081	69.7	170.8	.005033	12.22
1.9359		0.7683	READINGS	INVALID			
NO READING			READINGS	INVALID			
2.1694		2.3450	READINGS	INVALID			
2.3423		1.6246		-85.6	.002372		
2.2667		1.0135		-96.9	.002655		
2.2158		0.7721	161.0	-96.6	.003257	42.20	
2.2036		0.0019	READINGS	INVALID			
2.6324		2.1496	84.9	-118.8	.002585	9.31	
2.6324		1.6208	51.3	133.5	.002933	3.86	
2.5982		1.0576	44.9	114.4	.002656	2.68	
2.5586		0.8123	35.5	84.0	.003153	1.99	
2.5604		0.0038	5.3	-45.0	.003153	0.04	
3.1207		2.0615	96.0	-158.4	.002933	13.51	
3.1405		1.5902	5.9	71.6	.002656	0.05	
3.1405		1.0940	45.9	148.2	.003153	3.32	
3.1171		0.7817	31.2	162.6	.003153	1.53	
3.1171		0.0038	33.5	175.8	.002933	1.65	

Table D-II. Flow Calculations - Shot 363 (Continued)

TIME MICROSEC	X INCHES	Y INCHES	U FT/SEC	THETA DEGREES	DENSITY SLUGS/CUFT	Q LB/SQFT	
788.50	1.6074	2.2833	READINGS INVALID				
	1.9593	1.2333	125.7	60.7	.004018	31.75	
	1.8185	0.9130	READINGS INVALID				
	1.7315	0.7667	READINGS INVALID				
	NO READING		READINGS INVALID				
	2.2704	2.2333	55.8	-151.1	.003256	5.06	
	2.3852	1.6037	96.2	88.9	.003341	15.46	
	2.3315	1.0315	65.5	24.3	.003414	7.32	
	2.2963	0.8389	172.8	41.1	.003697	55.16	
	2.3204	0.0056	94.1	2.3	.003697	16.38	
	2.6630	2.0019	26.7	152.0	.003092	1.27	
	2.6648	1.6019	46.7	81.1	.003097	3.38	
	2.6148	1.0611	19.7	23.0	.002912	0.56	
	2.6037	0.8278	52.8	6.3	.003150	4.39	
	2.6037	0.0019	30.8	0.0	.003150	1.49	
	3.1685	1.9833	50.8	-127.3	.003097	3.99	
	3.1852	1.5722	51.4	110.6	.002912	3.84	
	3.1463	1.1097	32.8	93.2	.003150	1.69	
	3.1444	0.8204	26.6	70.1	.003150	1.11	
	3.1407	0.0037	9.2	-12.0	.003097	0.13	
	830.00	1.6468	2.3105	96.7	178.9	.002579	12.06
		2.0198	1.4177	259.9	56.1	READINGS INVALID	
		NO READING		READINGS INVALID			
		NO READING		READINGS INVALID			
		NO READING		READINGS INVALID			
		2.1207	2.3182	134.8	155.6	.002699	24.52
		2.3441	1.7204	110.3	84.2	.002772	16.85
2.3261		1.0403	84.0	24.9	.003804	13.43	
2.3405		0.8851	169.0	24.9	.003775	53.30	
2.2973		0.0057	89.3	-1.2	.003775	15.04	
2.6072		2.1630	55.9	68.6	.003066	4.80	
2.6396		1.6668	77.7	69.0	.002917	5.50	
2.6162		1.0682	104.1	41.4	.002772	15.01	
2.6108		0.8181	115.0	39.1	.003279	21.68	
2.6010		0.0038	72.6	2.9	.003279	8.64	
3.1201		2.0212	74.6	94.3	.002917	8.11	
3.1225		1.6381	71.0	84.0	.002772	7.00	
3.1387		1.1265	61.9	41.3	.003279	6.29	
3.1261		0.8066	69.7	46.1	.003279	7.93	
3.1261		0.0019	52.1	0.0	.002917	3.95	

Table D-II. Flow Calculations - Shot 363 (Continued)

TIME MICROSEC	X INCHES	Y INCHES	U FT/SEC	THETA DEGREES	DENSITY SLUGS/CUFT	W LB/SOFT	
871.50	1.5111	2.2852	99.8	-175.6	.002304	11.47	
	2.1037	1.4481	40.9	57.9	.003743	3.13	
	1.9759	0.9278	READINGS	INVALID			
	1.9037	0.8481	READINGS	INVALID			
	NO READING		READINGS	INVALID			
	2.1481	2.2889	152.0	-74.1	.002990	34.54	
	2.3963	1.7130	114.9	99.1	.003008	19.86	
	2.4074	1.0667	92.6	54.1	.004133	17.71	
	2.4481	0.9093	34.1	57.9	.003935	2.28	
	2.4093	0.0037	60.0	-5.5	.003935	7.08	
	2.6833	2.0537	25.0	-136.3	.003307	1.04	
	2.6926	1.6741	50.1	85.9	.003147	3.96	
	2.6926	1.1296	121.0	72.6	.003199	23.40	
	2.6926	0.9000	68.9	49.0	.003114	7.38	
	2.6759	0.0056	48.8	0.0	.003114	3.71	
	3.1630	2.0574	106.0	74.1	.003147	17.67	
	3.1926	1.6426	64.6	63.4	.003199	6.67	
	3.1926	1.1500	38.3	58.7	.003114	2.28	
	3.1926	0.8704	73.3	56.7	.003114	8.36	
	3.1926	0.0037	30.8	3.6	.003147	1.49	
	913.00	1.5477	2.3029	148.4	-142.1	.002872	31.62
		2.0414	1.4522	221.3	79.4	READINGS	INVALID
		NO READING		READINGS	INVALID		
NO READING		READINGS	INVALID				
NO READING		READINGS	INVALID				
2.1622		2.1726	26.3	-171.9	.004006	1.38	
2.3261		1.8335	46.6	85.4	.002831	3.08	
2.3802		1.1150	106.5	44.3	.002943	16.69	
2.3586		0.9139	47.4	-41.8	.003505	3.94	
2.3568		0.0000	74.4	0.0	.003505	9.69	
2.5892		2.1458	39.2	174.6	.002904	2.23	
2.6472		1.7166	37.9	11.3	.003001	2.16	
2.6523		1.1802	66.6	-35.9	.002720	6.03	
2.6559		0.3698	54.0	-2.0	.003162	4.60	
2.6396		0.0038	70.7	-1.5	.003162	7.90	
3.1189		2.1228	39.4	-98.1	.003001	2.33	
3.1514		1.6955	16.7	-90.0	.002720	0.38	
3.1586		1.1591	40.1	13.4	.003162	2.55	
3.1550		0.8706	53.2	12.1	.003162	4.48	
3.1568		0.0038	52.1	0.0	.003001	4.07	

Table D-II. Flow Calculations - Shot 363 (Continued)

TIME MICR SEC	X INCHES	Y INCHES	U FT/SEC	THETA DEGREES	DENSITY SLUGS/CUFT	Q LB/FOOT
954.50	1.3944	2.1944	367.7	-169.8	.002887	195.13
	2.1444	1.6648	359.8	111.5	.003434	222.28
	2.0963	0.9463	READINGS	INVALID		
	2.0222	0.7833	READINGS	INVALID		
		NO READING	READINGS	INVALID		
	2.1222	2.2852	301.2	140.8	.003293	149.39
	2.4000	1.7593	126.9	-176.5	.002960	23.82
	2.4833	1.1407	READINGS	INVALID		
	2.4833	0.8778	68.8	116.5	.003894	9.22
	2.4833	0.0037	52.8	173.7	.003894	5.42
	2.6444	2.9574	115.7	-162.6	.003479	23.27
	2.7296	1.6815	78.9	160.0	.003253	10.13
	2.7463	1.0907	85.2	162.9	.003517	12.75
	2.7463	0.8981	57.6	160.5	.003159	5.24
	2.7463	0.0037	67.0	-178.4	.003159	7.08
	3.1574	2.0185	92.3	-178.8	.003253	13.85
	3.1926	1.6259	110.5	-144.9	.003517	21.47
	3.2315	1.1593	102.3	154.4	.003159	16.54
	3.2444	0.8815	88.7	178.8	.003159	12.42
	3.2444	0.0037	67.0	-178.4	.003253	7.29
996.00	1.1874	2.2377	208.2	-156.9	.002994	64.93
	1.9099	1.7556	237.3	147.8	READINGS	INVALID
	1.9495	1.0786	92.5	59.8	READINGS	INVALID
	1.9153	0.7893	82.8	9.0	READINGS	INVALID
		NO READING	READINGS	INVALID		
	1.9297	2.3623	122.7	180.0	.003046	22.93
	2.2000	1.8258	100.2	130.5	READINGS	INVALID
		NO READING	READINGS	INVALID		
	2.3279	0.9752	100.6	70.6	.003581	18.10
	2.3048	0.0057	7.4	0.0	.003581	0.10
	2.4793	2.1113	31.6	-118.2	.002928	1.46
	2.5694	1.7434	78.9	136.9	.003420	10.65
	2.5712	1.2051	100.5	92.1	.002637	13.31
	2.6018	0.8890	41.6	79.7	.003226	2.79
	2.5730	0.0019	7.4	0.0	.003226	0.09
	3.0270	2.1209	48.3	105.0	.003420	3.98
	3.0613	1.6323	29.8	93.6	.002637	1.17
	3.0667	1.2032	50.1	58.7	.003226	4.04
	3.0667	0.8755	12.5	-26.6	.003226	0.25
	3.0901	0.0019	5.3	45.0	.003420	0.05

MODEL 39

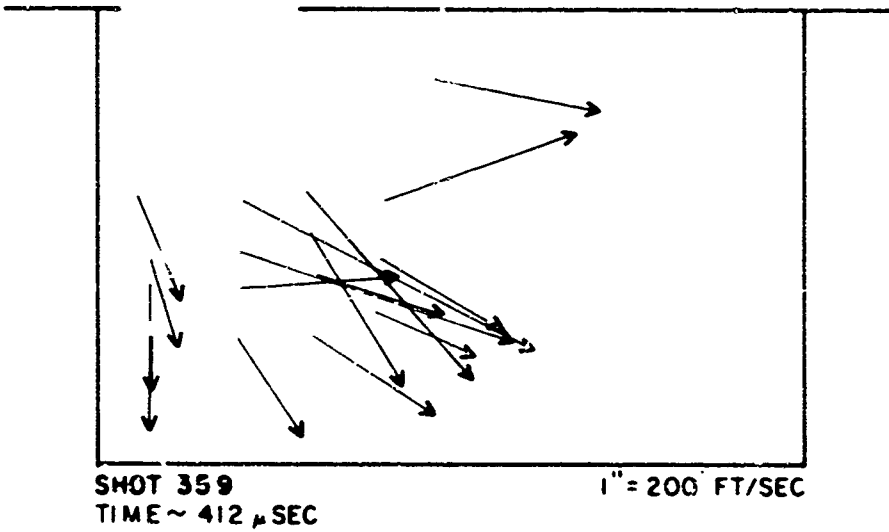
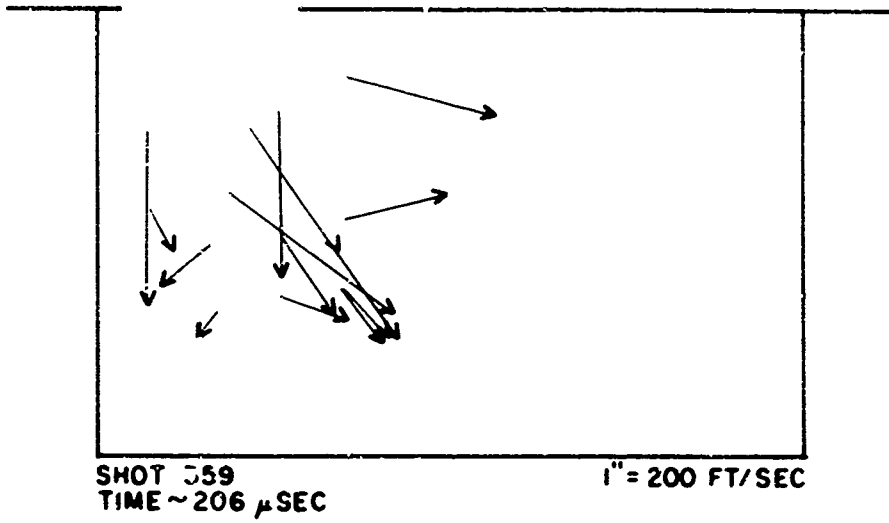
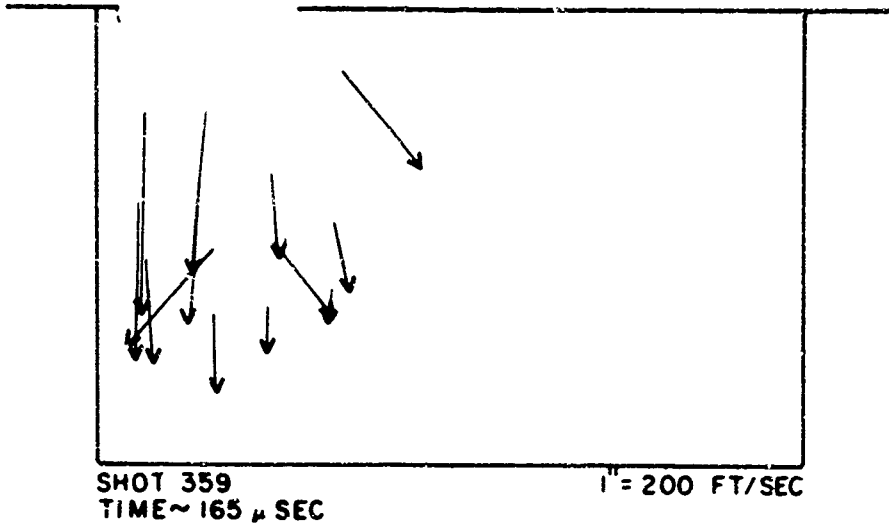
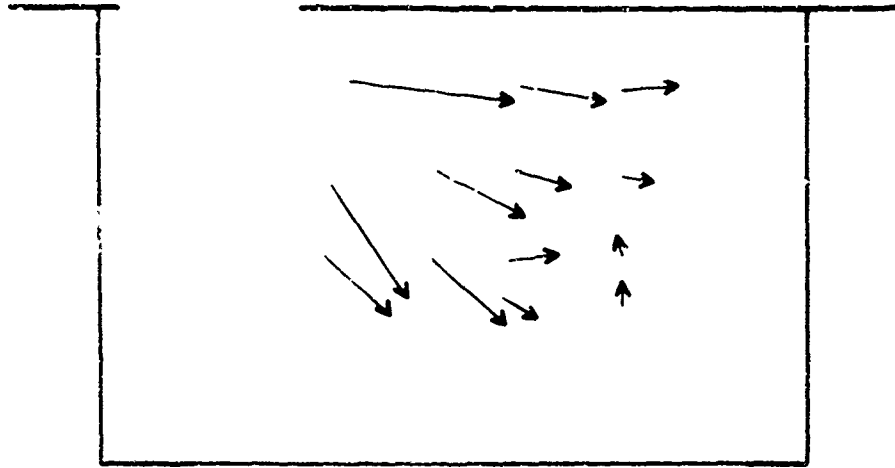


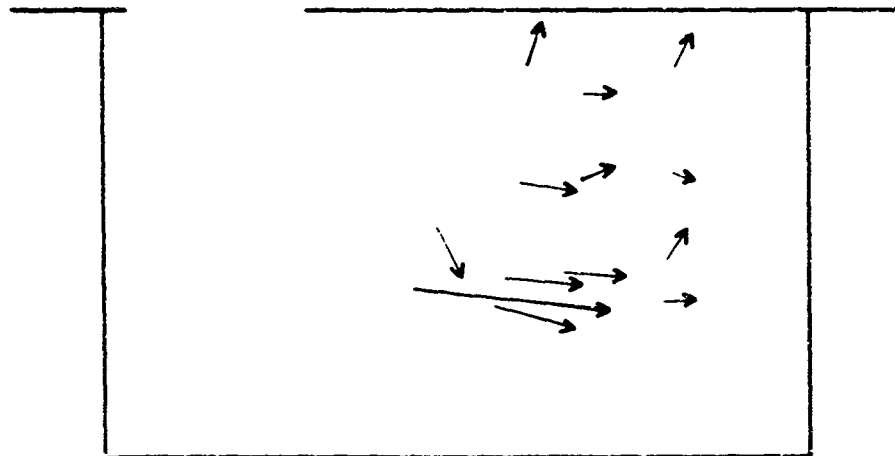
Figure D-1. Flow Vectors from Model 39 - Shot 359

MODEL 39



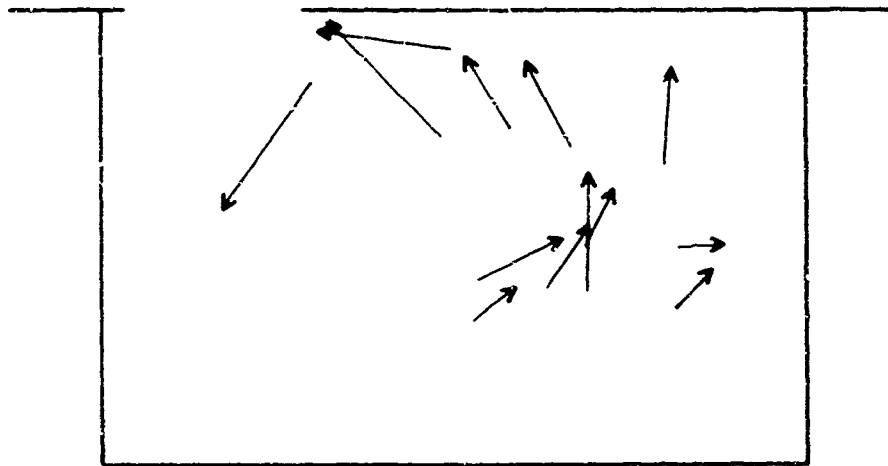
SHOT 363
TIME ~ 208 μ SEC

$I'' = 200$ FT/SEC



SHOT 363
TIME ~ 540 μ SEC

$I'' = 200$ FT/SEC



SHOT 363
TIME ~ 1038 μ SEC

$I'' = 200$ FT/SEC

Figure D-2. Flow Vectors from Model 39 - Shot 363

APPENDIX E

APPLICATION TO A FULL-SIZE ROOM

The conclusions reached from the study of the air shock loading of the front wall of Model 37 may be applied to a full-size room with the help of the following example.

Assume a full-size room with twelve times larger linear dimensions than the model and compare positions on the front wall similar to model Positions 4, 4A, and their difference. Figure E-1 illustrates such a scaled up full-size room. Figures E-2 and E-3 are the corresponding pressure-time records for the model and those predicted for the full-size room. Times are scaled by the linear dimension factor of twelve.

To understand this better, consider first the loading on the outside of the front wall. This loading may be divided into three types: (1) reflected pressure, (2) rarefaction decay, and (3) stagnation pressure. For example, as the input shock wave of 5.3 psi reflects from the front wall, the pressure rises to a reflected value of 12.2 psi. The reflected pressure remains until a rarefaction reaches the gage location from a distance, $D = 2.5$ ft, the nearest relieving edge. The first rarefaction arrival time, T_R , may be calculated from Equation E-1.

$$T_R = D/CREF \quad , \quad (E-1)$$

where CREF is the sound speed, 1232 ft/sec, in the reflected pressure region.

The reflected pressure decays by a series of rarefaction waves which arrive from the other more distant relieving edges. After a clearing time, T_C , the pressure falls to the stagnation value, P_{STAG} , of about 6 psi. The clearing time may be calculated from Equation E-2.*

$$T_C = 2.5 DR/CREF \quad , \quad (E-2)$$

*Variations of this equation may be found elsewhere, such as in "The Effects of Nuclear Weapons," Department of the Army Pamphlet No. 39-3, Hq., Department of the Army, April 1962.

where DR is the smaller of the front wall height of 14 ft, or one-half of its width, 10 ft. A more complicated method of calculating DR by means of weighting the various parts of the front wall for clearing ability may be used but is probably not needed.

The pressure-time loading on the inside of the front wall is complicated by the many internal reflections of the entering shock wave. However, to understand something of the inside loading, the reflections may be grouped according to their origin at the interior side walls, or at the interior rear wall.

No loading occurs inside, of course until the shock wave arrives at the gage position at a time, TAI, which may be calculated from Equation E-3.

$$TAI = TH/U + DI/UI \quad , \quad (E-3)$$

where TH is the thickness of the front wall, 2.5 ft, U is the speed of the input shock wave, 1293 ft/sec, DI is the distance measured from the edge of the entrance to the gage position, 2.5 ft, and UI is the speed, 1178 ft/sec, for the transmitted shock wave pressure of about 1.5 psi calculated for the position.

The first of the group of reflections, 3 psi, returns from the near, side wall at a time calculated from Equation E-4.

$$TW = 2 DREF/UI \quad , \quad (E-4)$$

where DREF is the distance to the near side wall, 1 ft away. The reflections in this group repeat with a period proportional to the width of the room. Equation E-5 gives this relationship.

$$PERIOD = WDI/C1 \quad , \quad (E-5)$$

where WDI is the interior room width of 15 ft and C1 is the ambient sound speed, 1130 ft/sec.

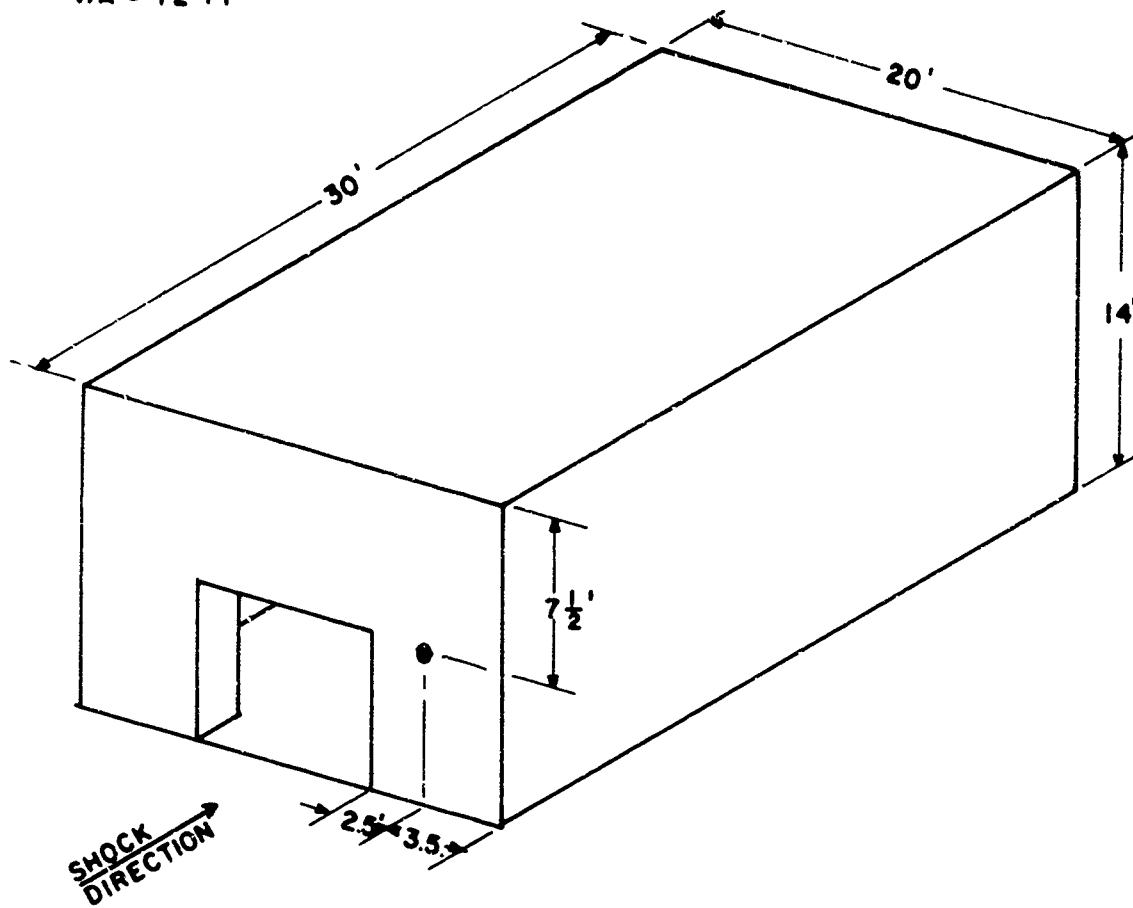
The last group of reflections returns from the back interior wall at a time equal to one round trip of the length of the room, is given by Equation E-6.

$$TB = (XLI/\bar{U}) + (XLI/C1) \quad , \quad (E-6)$$

where XLI is the length of the room and \bar{U} is an average speed $(U + C1)/2$, of the speed of the input shock wave and the speed of the shock wave (assumed to be C1) when it reaches the side wall. These reflections occur with about the same period as those from the side wall. They decrease in pressure amplitude until, at about three round trips of the room, stagnation pressure is reached.

The pressure difference curve between the outside and inside loading of the front wall will follow times as calculated above.

$A = 52 \text{ FT}^2$
 $V = 3750 \text{ FT}^3$
 $V/A = 72 \text{ FT}$



ENTRANCE - 8' x 6 1/2'

INTERIOR - 10' x 15' x 25'
ALL WALLS - 2 1/2' THICK
● - GAGE POSITION

Figure E-1. Full-Size Room

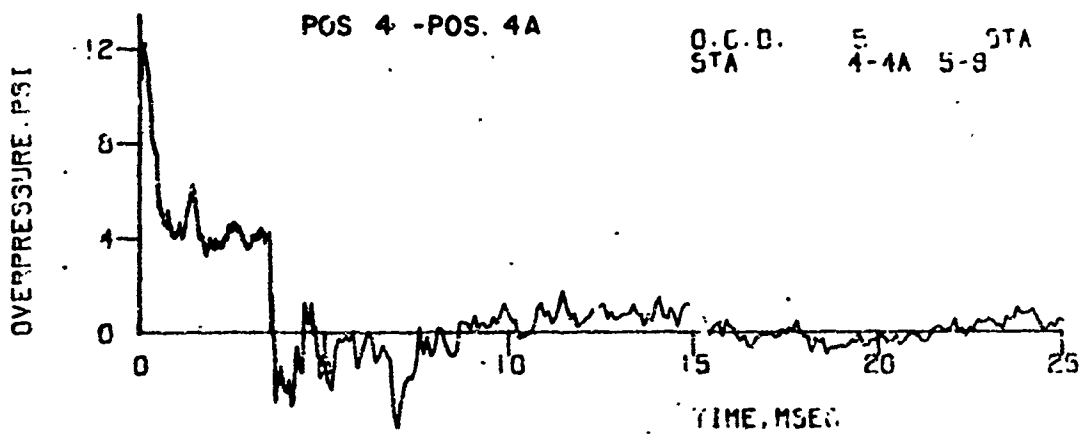
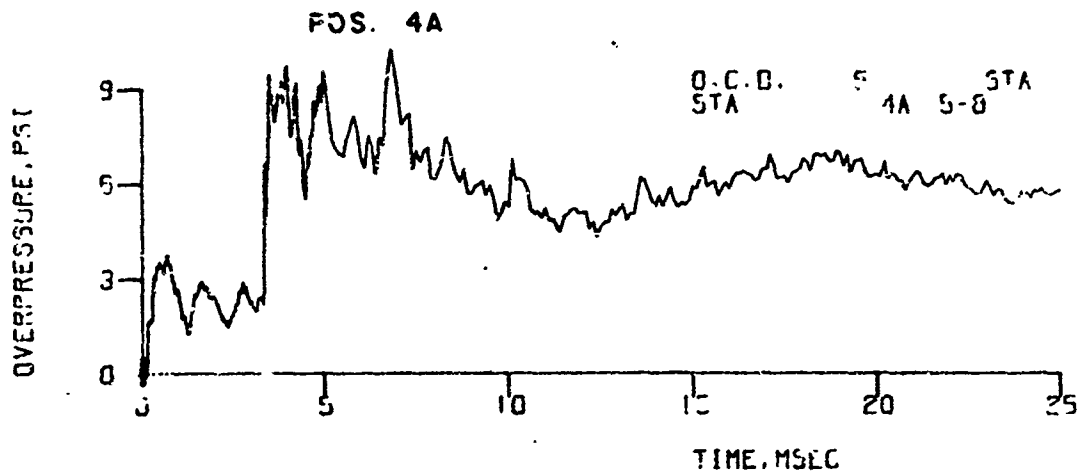
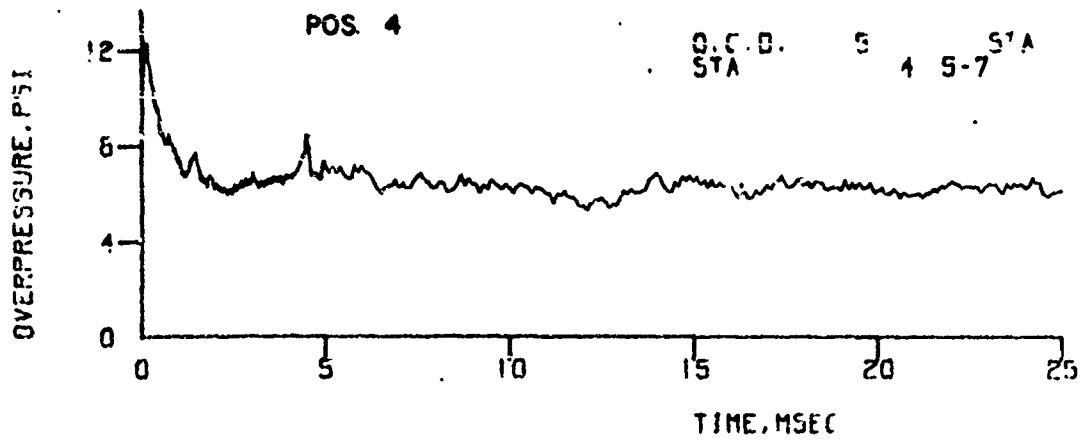


Figure E-2. Records from Model 37

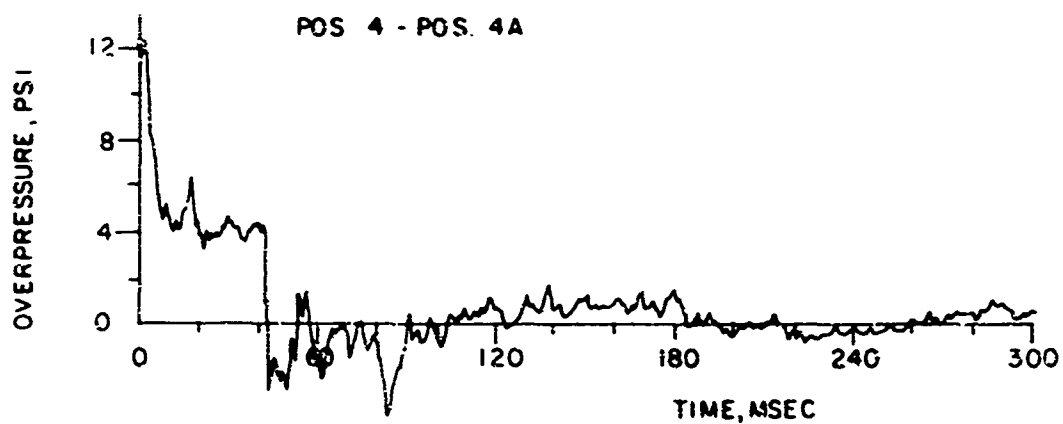
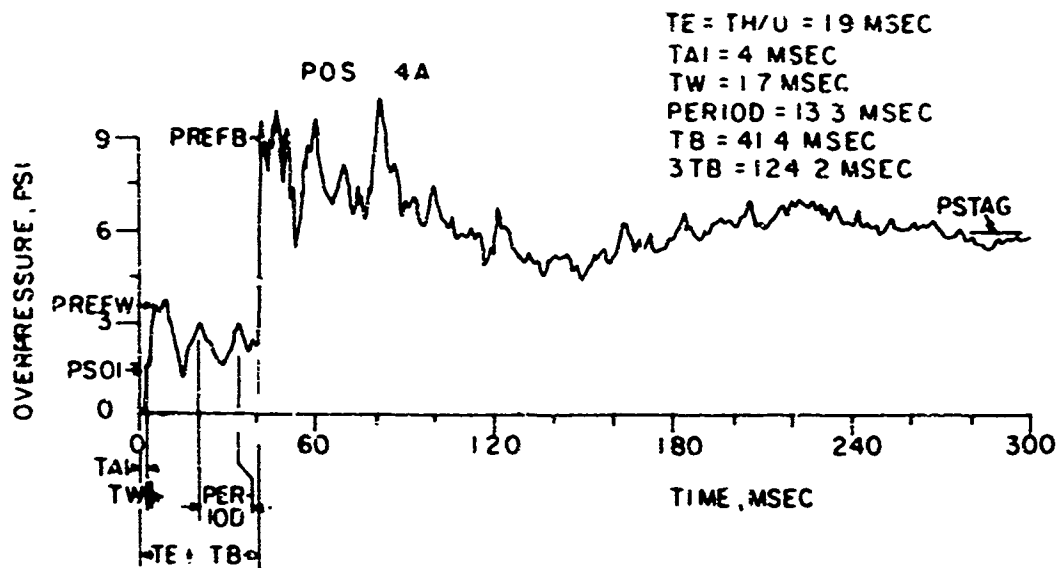
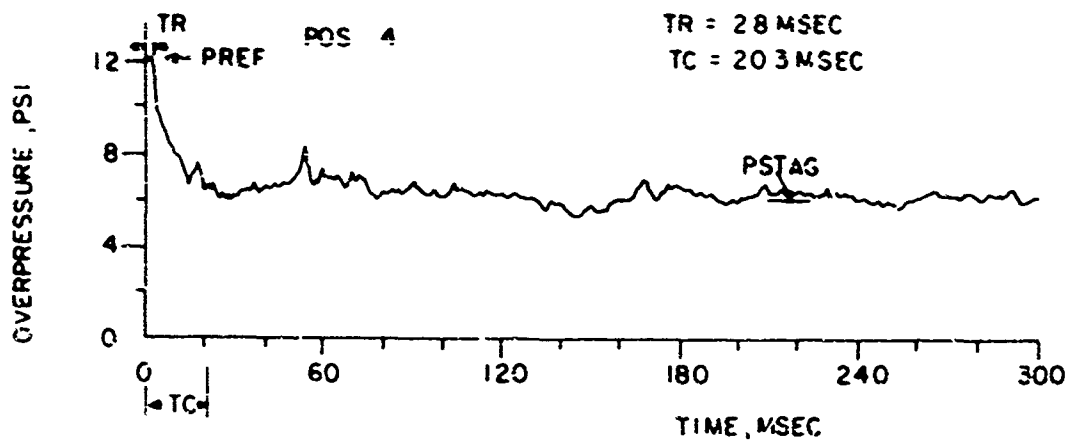


Figure E-3. Records for Model 37 Scaled to a Full Size Room